GEOSTATISTICAL ESTIMATION OF A PALEOPLACER DEPOSIT WITH HARD GEOLOGICAL BOUNDARY: CASE STUDY AT TARKWA GOLD MINE, GHANA

by © Solomon Kwabena Ansah

A thesis submitted

to the School of Graduate Studies in partial fulfillment of the

requirements for the degree of

Master of Engineering

Faculty of Engineering and Applied Science

Memorial University of Newfoundland

August 2018

St. John’s Newfoundland and Labrador

ABSTRACT

Geostatistical estimation requires the definition of geological domains by using geologic variables or structural information. The misclassification of the estimation domains may have a significant effect on the resource estimate such as dilution, oversmoothing, undersmoothing of gold grades.

In this project, detailed geological modelling coupled with statistical analysis is carried out to aid in the definition of 3 geological domains with hard boundaries. A hard boundary is characterized by an abrupt variation of grade along the boundary between two lithological contacts. The A1 reef in Akontasi east of the Tarkwa Gold mine concession was investigated out of the 7 stratified reefs. The drillhole data considered were obtained by reverse circulation and diamond drilling with ordinary kriging being the preferred estimator for the deposit.

Semi-variograms were generated for all 3 domains and estimation within the domains were cross validated and results showed a high Correlation Coefficient. An alternative case was also analyzed, where all three domains were combined and showed a low Correlation Coefficient. Results indicate that the division of the orebody into separate homogenous domains produce accurate results with a high level of confidence.

ACKNOWLEDGEMENTS

Firstly, I thank almighty God for giving me the zeal to complete my masters program successfully.

Special thanks go to my Supervisor, Dr. Stephen Butt for his enormous support and tutorship. This project couldn't have been a success without your input.

To my former manager in Goldfields Ghana Limited (Mineral resources department) for his guidance and advice throughout the project.

I would like to thank all Drilling Technology Laboratory members at Memorial University Of Newfoundland especially Igor Kyzym, David Onalo and Sunday Olarere Oloruntobi. You guys are awesome.

Finally, a big thank you to my beautiful wife Louisa, and adorable son Solomon Jr. Love you forever.

Table of Contents

List of Tables

List of Figures

Nomenclature

JORC	Joint Ore Reserve Committee
RC	Reverse Circulation
DD	Diamond Drilling
SMU	Selective Mining Unit
CV	Coefficient of Variation
OK	Ordinary Kriging
IDW	Inverse Distance Weighting
KNA	Kriging Neighborhood Analysis
KE	Kriging Efficiency
BV	Block Variance
KV	Kriging Variance
R	Regression
DTM	Digital Terrain Model
P-value	Probability value
Q_Q	Quantile-quantile
TCu	Total copper
Z(u)	Regionalized Variable
°	Degrees (angle)
+/-	plus or minus
g (h)	Variance at a lag h
(Ho)	Null hypothesis

(H1)	Alternative hypothesis
N	Number of samples
μ	Lagrange multiplier
s	Standard deviation
s^2	Variance
a	Range (metres)
A	Area
Au	Gold
C	Covariance
Co	Maximum covariance
Co+C	Sill
Co	Nugget variance
E{Z}	expected value of Z
g/t	Grams of gold per tonne of rock
h	lag (metres)
km	kilometre
m	Metre
tonne	One thousand kilograms
LTK46	RC drill rig model number
BQ	Core diameter 36.5 mm
V	Volume
Z*	Estimator

List of Appendices

CHAPTER 1

1.0. Introduction

This chapter deliberates on the study background, definition of the problem statement, specific objectives of this work, the methods used to achieve aim of study and how the thesis is organized. This work reflects the detailed analysis and investigation done by the candidate.

1.1. Background of study

It is generally a normal procedure to estimate a paleoplacer deposit without dividing mineralized zones into homogenous domains because the gold grades have little variance with a good correlation after estimation [1]. However, this tends to be quite misleading as the process of domaining is critical and must be adopted as a significant methodology when dealing with paleoplacer deposits. Current practices of using single domain produces large errors between the orebody model and recovered ore grade. The project area is characterized by two overlapping faults that have displaced the orebody. The displacement caused by the fault has partitioned the orebody into three different domains. This work started when the candidate was the Mine Geologist in Goldfields Ghana Ltd. and has continued into this thesis investigation.

The ore grade data and the licensed orebody modelling software (Surpac software) that was used for conducting this research was provided under the auspices of the Mineral Resource Department of Goldfields Ghana limited. The approach used in this research hopes to

address the problems identified in the misclassification of domains for the current mine deposit and to present a model methodology for future deposits for this and other mines.

1.2. Statement of the problem

An accurate recoverable resource estimation and grade control practices are the main driving tools to ascertain the feasibility of a successful mining operation. In an industry characterized with data abundance, extra effort is put in place to achieve robust local estimates. In addition, the quality of an estimate is fully dependent on the quality of data, and a detailed statistical analysis of the drillhole data will reveal any patterns or correlations between them. Goldfields Tarkwa Mine currently practices select mining for its paleoplacer deposit with stratified lithologies and employs the Ordinary Kriging (OK) method for grade control estimation. Statistical analysis helps to ascertain the nature of the data that will be fitted into the model for a precise resource or reserve estimate.

Domaining is a common practice in mineral resource estimation, which consists of partitioning the orebody into several zones. Within each domain, the statistical parameters, kriging variance and spatial dependency between geological variables are analyzed.

It has been found that the misclassification of geological boundaries has implication on resource estimation such as dilution, over or under estimation, tonnage, ore loss or mixture of populations [1]. This poses a big threat to recoverable resources if a stepwise approach is not adopted to evaluate the consequences of defining inadequate estimation domains. In light of this, a concept must be adopted to deconstruct the problem by describing and modelling the relationship between each geological variable to ascertain and justify the geological domains that will be used for geostatistical analysis.

This investigation seeks to assess and evaluate the importance of domaining in mineral resource estimation.

1.3. Objectives of research work

The objectives of this thesis are to:

- Review the current resource/reserve estimation methods used at Gold Fields Ghana Limited, Tarkwa Mine.
- Observe and run a statistical analysis on a sample drillhole gold data
- Highlight and know the importance of statistical analysis before any grade interpolation method. (OK)
- Investigate and analyse the effects of geological domains on mineral resource estimates.
- Successful outcomes can be incorporated into future domaining and resource estimation procedures at the Tarkwa Mine and similar mines worldwide.
- Provide necessary recommendations and observations.

1.4. Methods used

The method to be adopted to achieve the objective includes:

- The collection and processing of geological data (diamond drill, reverse circulation and survey data).
- Extraction of drillhole cross sections and digitizing of ore zones within the deposit to create wireframes.
- Analysis of drillhole data using Minitab, Excel, Surpac modelling software

- Definition of domains and boundary analysis
- Estimate resource using OK
- Compare mineral resource estimates of different types of estimation domains

1.5. Thesis organization

This thesis is organized into six chapters.

Chapter 1 deliberates on the statement of the problem, objectives and methodology employed in meeting the objectives, scope of work and the order of the presentation.

Chapter 2 gives a summary of company profile, location, climate and vegetation, regional geology and local geology of the concession.

Chapter 3 elaborates on the review of literature associated to the area of research

Chapter 4 deliberates on the methodology used for mineral resource estimation and domaining of the deposit reefs.

Chapter 5 talks about processes involved in sample evaluation using research data. This includes data processing, data validation and digitization of ore zones, statistical analysis, definition of estimation domains and semi-variogram analysis, wireframing and Blockmodelling.

Chapter 6 concentrates on the results obtained from estimates of domains, semi-variogram analysis, grade interpolation and resource estimation.

Chapter 7 enumerates the findings, draws conclusions and give recommendations on future work to be done.

CHAPTER 2

DEPOSIT GEOLOGY

2.1. Location of the Tarkwa Mine

Goldfields Ghana Limited's Tarkwa surface mine is in the Western region of Ghana and has been in operation since 1993. Gold Fields Tarkwa Mine forms part of the 176 km² Tarkwa concessions. It is in the south-western part of Ghana on latitude 5°15'N and longitude 2°00'W [2]. The location of the Mine is shown as red dot in Figure 2.1.

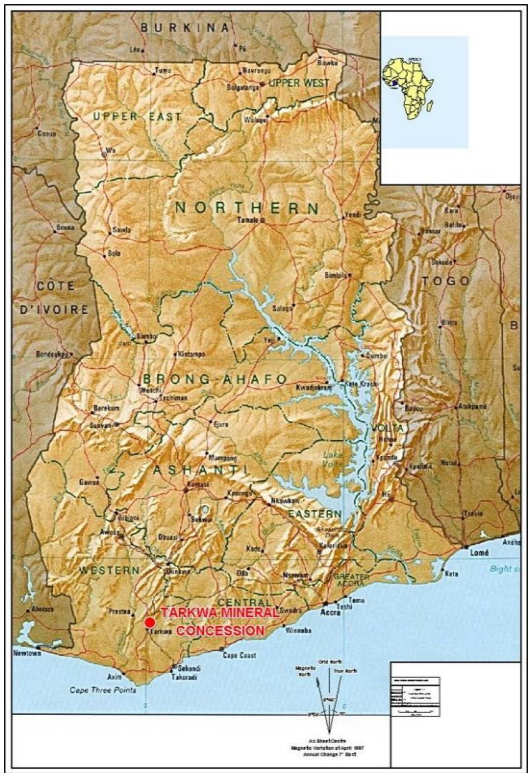

Figure 2.1. The location of the Tarkwa Mine concession of Goldfields Ghana Limited [3]

2.2. Regional physiographic features

This aspect of the project highlights an introduction to the physiographical environment of Tarkwa and its vicinity within which the Goldfields Ghana Limited concession is located.

2.2.1. Topography

The topography of the Tarkwa concession of Goldfields Ghana Limited consists of a series of ridges and valleys parallel to one another and to the strike of the underlying geology. This reflects the fold structures present in the Banket Series and Tarkwa Phyllite beds. The transverse valleys and gap ridges are determined by faulting and jointing, the long ridges formed by them easily distinguish the thicker beds of phyllite in the sandstone [4].

The whole area is highly dissected and of moderate relief, which varies between 30 m and 335 m above mean sea level and generally slopes to the south. The elevations of areas underlain by Huni Sandstones vary between 50 m and 90 m, while the areas underlain by Kawere formation vary from 60 m to 120 m.

2.2.2. Climate and rainfall

Annual rainfall in Tarkwa and its surroundings averages 2030 mm, but annual and seasonal fluctuations are becoming increasingly pronounced. The central and northern parts of the districts record an annual rainfall capacity between 1500-1750 mm.

2.2.3. Vegetation

The primary forest occurring in the concession area has been severely disturbed and largely replaced by secondary forest and early successional vegetation because of a long-standing history of human activity in the area, which includes small scale mining, timber exploitation, firewood collection, charcoal production and various farming activities.

2.3. Regional geology

The Tarkwa ore bodies are located within the Tarkwaian system and forms part of the Ashanti belt in southwest Ghana. The Ashanti belt strikes in the north-eastern direction with a broad synclinal structure made up of Lower Proterozoic sediments and volcanics underlain by the meta-volcanics and meta-sediments of the Birimian System. The contact between the Birimian and the Tarkwaian is commonly marked by zones of intense shearing and is host to a number of significant shear hosted gold deposits. The Tarkwaian is a folded syncline with a total thickness varying between 2000-2500 m. The age of the Tarkwaian is between 2132 ± 3 Ma [5].

There exists an unconformity between the Birimian and the Tarkwaian, the latter is characterized by lower intensity metamorphism and the predominance of coarse grained, immature sedimentary units. The oldest to youngest of these lithologies [6] as shown in Fig. 2.2. are presented in the subsections below.

2.3.1. Kawere Conglomerate

Kawere Series (250 – 70 m) – poorly sorted, polymictic conglomerates and quartzites with no significant mineralization. The coarse units include clasts of quartz, mafic volcanics, phyllites and minor red chert and porphyry [4]. The pebbles consist predominantly of mafic lava together with granitoids, felsic lavas, pyroclastics and minor quartz, very different from those of the Banket [7, 8].

2.3.2. Banket Series

The conglomerate zone is described as the thickest in the south [4] where it is up to about 76 m (250 ft.) thick and includes several coarse units, but further north it thins to about 30 m- 45 m (199 -150 ft.). Gold grains are usually between 1-10 microns in diameter and mostly located around the periphery of the pebbles [9].

Gold in the Tarkwaian is largely associated with the conglomerate of the Banket Series. The Banket Series is composed of a succession of flat dipping amalgamated tabular units, consisting dominantly of quartz pebble, which are nearly always barren, cemented together by quartzite, which may or may not be gold bearing and in many cases contains varying quantities of black magnetite and hematite grains [7, 8].

The conglomerates are relatively well sorted, oligomictic to polymictic supported, cross-bedded and are horizontally stratified. Approximately ten such separate economic units occur in the concession area within a sedimentary package that is between 40 m and 110 m thick with low grade to barren quartzite units inter-layered with the Au-reefs [6].

2.3.3. Tarkwa phyllite

Tarkwa Phyllite with thickness between (120 m– 140 m) is fine grained chloritic siltstones, mudstones and schists with no significant mineralization [6]. The Tarkwa phyllites show wave, current ripples and mud cracks. Basal contact with Banket either sharp or gradational, top contact gradational.

2.3.4 Huni Sandstone

Huni Series (1370 m) is fine grained massive meta-arenites with no significant mineralization [6]. Fine grained cross bedded to massive feldspathic quartzite. Probably a down-basin flowing distal fluvial system.

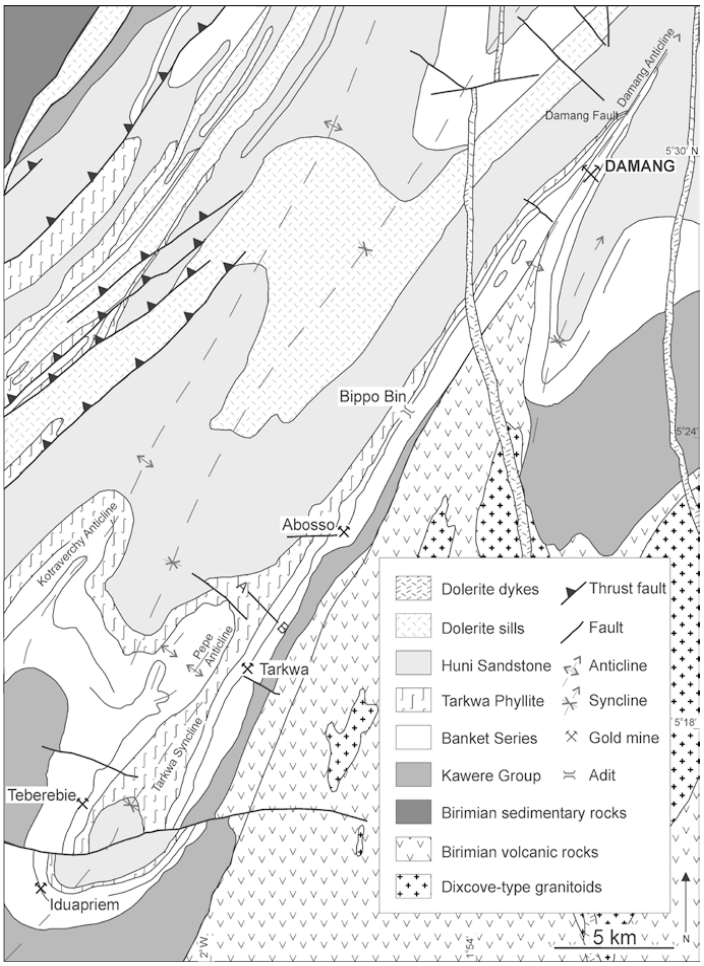

Figure 2.2. The Geology of the Tarkwa gold deposit. The line A-B represents the location of the cross section in Figure 2.2. The dashed line within the Banket Series is the conglomerate horizon [6].

2.4. Geology of project area

Due to copyright and data confidentiality, geological data for only A1 Reef was provided for this research. The A1 Reef is well developed and strikes between 12º - 18º with a true thickness of at most 7 m.

The geology of the project area is disrupted by thrust fault that has partitioned the orebody into several geological zones as shown in Fig. 2.3. The fault (green dyke) has displayed the reefs into separate zones. The identifiable mineralized zones are separated from each other and the dyke lithologies are about 10 m in width [9, 10]. The frequency of faulting/jointing is related to the extent of folding (deformation). This area was selected due to complexity of the orebody and the problems encountered during geostatistical modelling and estimation.

The local geology at Akontasi central pit concession is dominated by the Banket Series, which can be further sub-divided into a footwall and hanging wall barren quartzite, separated by a sequence of mineralized conglomerates and pebbly quartzites. The stratigraphy of the individual quartzite units is well established with auriferous reefs inter-bedded with barren immature quartzites. The major gold bearing horizons [11] are described below and Fig. 2.4. shows the various lithogies located in the six open pits of Goldfields Ghana Ltd. Operation.

(i) AFc

The AFc reef is up to 3 m thick, only occurs in the west and subcrops against the A1in the east. It is well sorted with rounded clasts of quartzite and visible gold.

(ii) A1 (this study**)**

The A1 reef is between 2 m - 7 m thick, moderately to poorly sorted conglomerate and thin quartzites with occasional visible gold.

(iii) A3

The A3 up to 7 m thick, moderately sorted thin discontinuous conglomerate lenses within a package of cross stratified quartzites, visible gold is rare.

(iv) CDE

CDE reef is up to 8 m thick and can be subdivided into the lower C reef and upper E reef, both of which are conglomeratic and are separated by the D reef quartzite;

(v) F2

The F2 reef is a variably developed polymictic gravel up to 2 m thick, essentially a marker horizon, except in the east where it carries low grades; and

(vi) G

G reef varies from a 2 m – 6 m thick poorly sorted conglomerate with clasts of quartzite and phyllite.

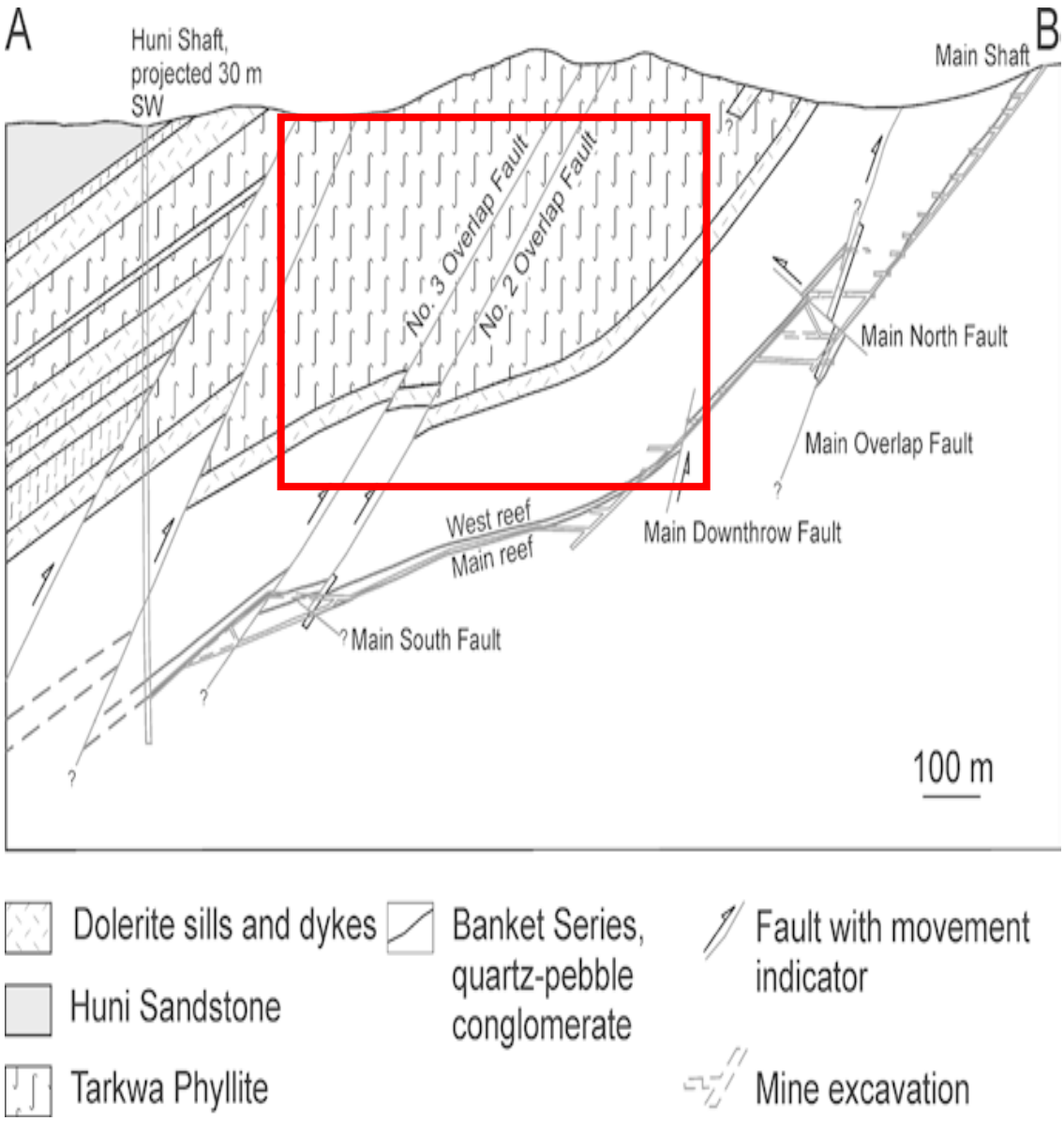

Figure 2.3. Cross section through the Tarkwa Mine workings, showing the lithology and the main structures mostly gentle dips, open folds and brittle faults. The project has been highlighted in red showing the reef displacement due to the overlap faults [6, 10].

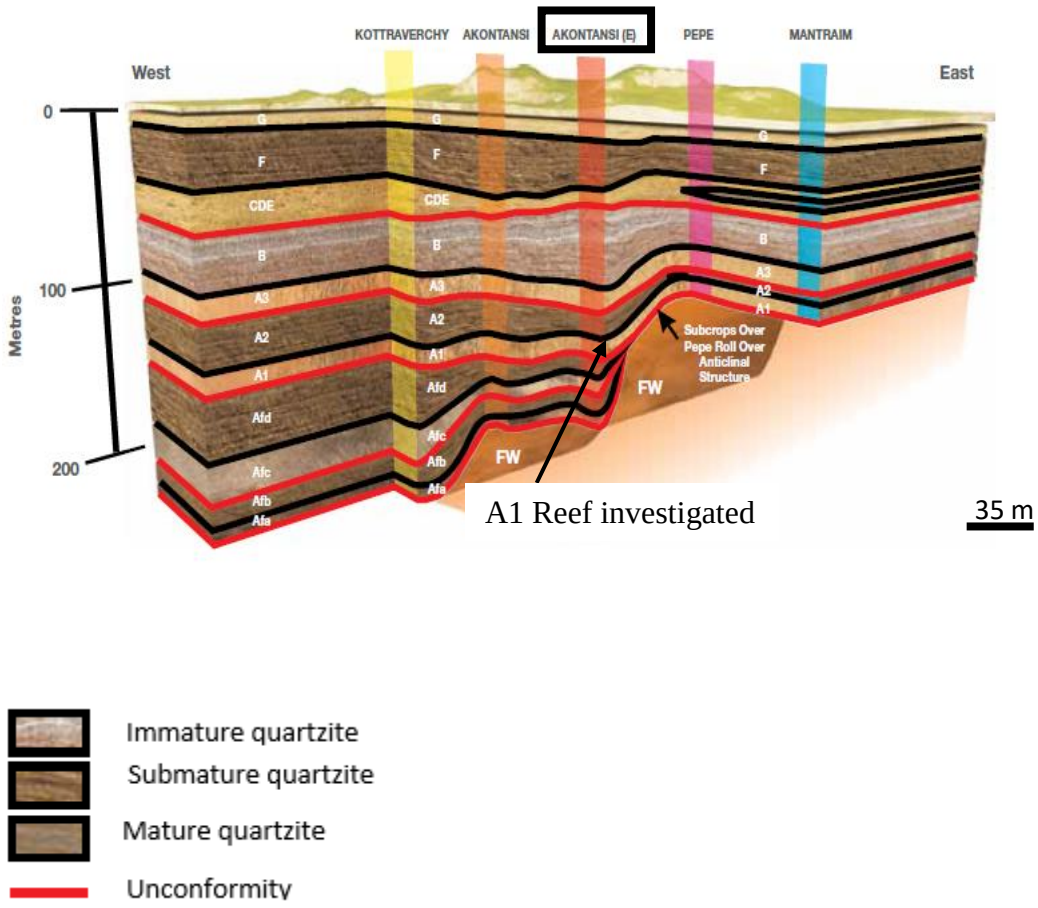

Figure 2.4. A Schematic sedimentological profile through the Tarkwa orebody, showing the various stratigraphic units in the six different open pits of Tarkwa Mine operations [4].

CHAPTER 3

LITERATURE REVIEW

3.1. Introduction

This chapter presents the literature on geostatistical ore reserve estimation, with domaining being the underlining process in the estimation process. This literature expands to cover other research done on other deposits with similar methodologies employed in the definition of domaining.

3.2. Geostatistical theory

Geostatistics is the statistics of Regionalized Variables (RV) where samples are independent from each other beyond a characteristic separation distance and direction called the range. For separation distance less than the range, the statistical relationship depends on the semi variogram. Numerous tests are used for geostatistics theory [1, 12, 13, 14] and this deliberates more on the modelling, random function concept and prediction of uncertainty associated with RV.

The random function concept implies that RV (grade) within a geographical location or space is considered stationary (constant mean). The objectives of geostatistics is to estimate error and provide a measure of confidence for each block estimate [15].

3.3. Geostatistical resource estimation techniques

3.3.1. Kriging

Kriging is a method of calculating weights that are combined through a linear equation to give the best estimate. The choice of applying any kriging method depends basically on

the local or stationary mean. With satisfactory weighting coefficients, the variance for the general unbiased linear estimator is obtained as:

$$\sigma_e^2 = \sigma_z^2 - 2\sum a_i \sigma_{zxi} + \sum_i \sum_j a_i a_j \sigma_{x_i x_j} \tag{3.1}$$

This can be modified using the Lagrange principles as:

$$\sigma_e^2 = \sigma_z^2 - (\sum a_i \sigma_{zxi} + \mu) \tag{3.2}$$

where

σ_e^2 is the estimation variance

σ_z^2 is the grade of blocks

$\sigma_{x_i x_j}$ is covariance of grades of samples x_i and x_j

μ = Lagrange parameter

To find the weights a_i which minimize the estimation variance σ_e^2 such that $\sum a_i = 1$, the derivatives of the function $F = \sigma_e^2 + 2\mu (\sum a_i - 1)$ with respect to all the unknowns (a_i) are equated to zero [14]. The resulting linear equations, which are solved for a_i, are:

(3.3)

$$\begin{cases} \sum a_i \sigma_{ij} + \mu = \sigma_{vi} \\ \sum a_i = 1 \end{cases}$$

This can be put in matrix form as:

$$[C][A] = [D] \tag{3.4}$$

where

$$[C] = \begin{vmatrix} \sigma 11 & \sigma 12 & \cdot & \cdot & \cdot & \sigma 1n & 1 \\ \sigma 21 & \sigma 22 & \cdot & \cdot & \cdot & \sigma 2n & 1 \\ . & . & . & . & . & . & . \\ . & . & . & . & . & . & . \\ . & . & . & . & . & . & . \\ \sigma n1 & \sigma n2 & \cdot & \cdot & \cdot & \sigma nn & 1 \\ 1 & 1 & . & . & . & 1 & 0 \end{vmatrix}, [A] = \begin{vmatrix} a1 \\ a2 \\ . \\ . \\ . \\ an \\ \mu \end{vmatrix}, [D] = \begin{vmatrix} \sigma vi \\ \sigma vg_2 \\ . \\ . \\ . \\ \sigma vg_n \\ 1 \end{vmatrix} \tag{3.5}$$

σ_{ij} stands for the covariance of the sample i and j, σ_{vgi} = the covariance of the block v and the sample i, σ_v^2 = the variance of the grade of blocks, μ = the Lagrange multiplier.

The solution of the above matrix for the weighting coefficients a_i is given by:

$$[A] = [C]^{-1}[D] \tag{3.6}$$

All the σ 's are derived from the semi-variogram, for weight calculation.

3.3.2. Block kriging

The modification of kriging equations to estimate an average value $Z_{(A)}$ of the variable z over a block of area A is illustrated in Fig. 3.1.

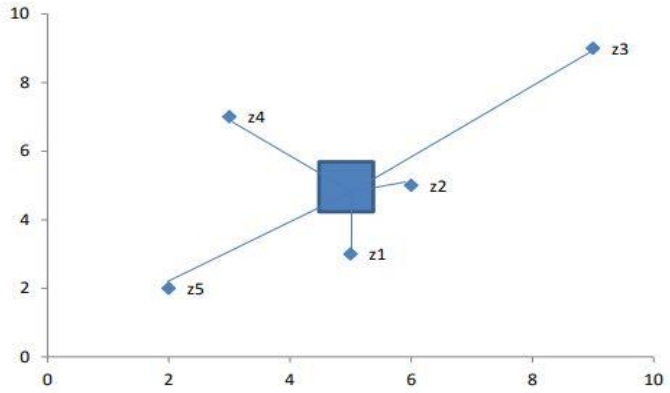

Figure 3.1. Block estimation using neighboring samples [19]

In many occasions, we are interested in estimating the value in a block (cell) rather than that at a single point. The block kriging system is like that of the OK of the form:

$$C \quad w = D$$

$$\begin{bmatrix} C_{11} & 1 \\ C_{n1} & 1 \\ 1 & \end{bmatrix} \cdot \begin{bmatrix} W_1 \\ W_2 \\ W_n \end{bmatrix} = \begin{bmatrix} C_{1A} \\ C_{nA} \\ 1 \end{bmatrix} \tag{3.7}$$

where

$$C_{iA} = \frac{1}{A} \sum_{j \epsilon A} C_{ij} \tag{3.8}$$

i.e., the covariogram between block *A* and sample point *i* is the average of the covariograms between the points locating within *A* and *i*.

The block kriging variance is

$$\sigma^2{}_{OK} = C_{AA} - w'D \tag{3.9}$$

where

$$C_{AA} = \frac{1}{A^2} \sum_{i \epsilon A} \sum_{j \epsilon A} C_{ij} \tag{3.10}$$

The true values of the RV represent a certain volume of support. Therefore, estimating the mean grade of a block must represent and honor the change in support. This leads to regularization (point grades integrated or regularized to represent a sample volume) of the samples where the average value of Z_A over the block A is given by:

$$Z_A = \int_A^n . \frac{z(x) \partial x}{area A} \tag{3.11}$$

From the equation the average value of Z_A is calculated by integrating the covariance of the entire block over the entire block area.

3.3.3. Ordinary Kriging

In OK, the local mean of the samples is implicitly re-estimated as a constant within each search neighborhood. OK is a common technique used to obtain interim estimates and has proven to be the best linear unbiased estimator. The first step in OK is to construct a variogram from the scatter point set to be interpolated. Once the experimental variogram is computed, the next step is to define a model variogram in Fig. 3.2.

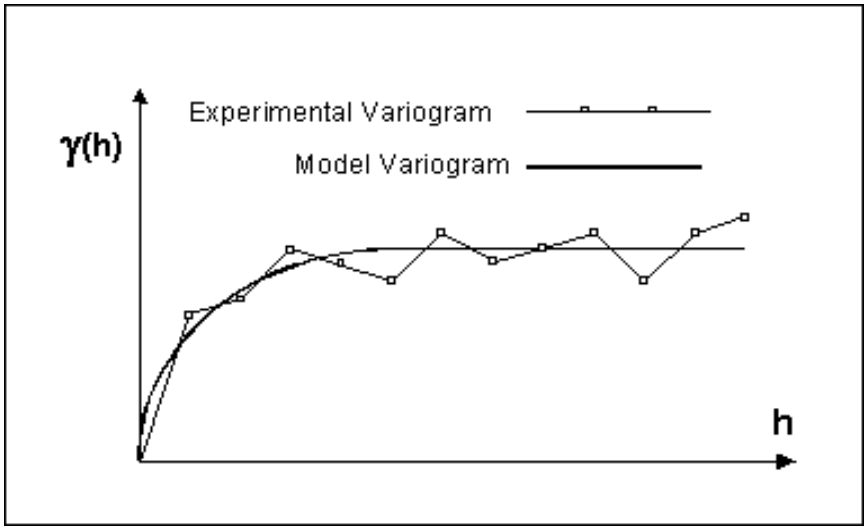

Figure 3.2. Experimental and Model Variogram Used in OK [19]

Once the model variogram is constructed, it is used to compute the weights used in kriging.

The basic equation used in OK is as follows:

$$Z = \sum_{i=1}^{n} W_i Z_1 \qquad (3.12)$$

Where

n is the number of scatter points in the set,

Z*i* is the values of the scatter points,

w*i* is the weights assigned to each scatter point.

3.4. Semi-variogram

To calculate the standard deviation and variance of data pairs, mathematically it is given as:

Standard deviation $= s = \sqrt{s^2}\sqrt{\frac{1}{n-1}\sum_{i=1}^{n}\sum_{j\geq i}^{n}\left(Z(x_i) - Z\left(x_j\right)\right)^2}$ (3.13)

Variance $= \frac{1}{n-1}\sum_{i=1}^{n}(Z(x_i) - \bar{Z})^2$ (3.14)

where

n is the number of samples

Z_{Xi} is the value of regionalised variable at sample location

Matheron [16], through the application of geostatistics defined the semi-variogram through his seminal work "The theory of regionalized variables". With the same concept, a variogram was defined which deals with RV. A variogram is a graph which compares differences between samples against distance. Thus, semi variogram in simple terms means half the variance (i.e. half the expression in equation 3.2), for geological data pairs leading to the mathematical expression:

Variance $= \frac{1}{n}\sum_{1=1}^{n}(Z_{Xi} - Z_{(Xi+h)})^2$ (3.15)

where

$Z(x_i)$ =the value of the regionalized variable at point x_i

$Z(x_i + h)$ the grade of another point at a distance h from the point x_i

n= the number of sample pairs

Different theoretical models exist that may be fitted to the experimental points. The different types of theoretical semi-variograms that are likely to be encountered in nature are shown in Table 3.1. A schematic spherical model in Fig. 3.3. Shows clearly that at a zero-separation distance, two variables (grade) have a maximum covariance *Co* (nugget). The nugget is a product of assaying, sampling errors and measurement errors. Nugget effect can also be described as the nonzero variance at the origin of the semi-variograms. In addition, the nugget is considered as random noise and may represent a short scale variability, measurement error and sample rate.

In Fig. 3.1, the Range (a), signifies the distance at which the overall population variance is recorded/reached. At this distance, samples are not auto correlated or there is no spatial correlation between data pairs.

Sill (*Co* + *C*), represent the maximum variance between data pairs and is displayed as the flat portion of the graph.

The spherical model is characterized as:

$$\gamma(h) = \mathrm{C_o} + \mathrm{C}\left[1.5\left(\frac{h}{a}\right) - 0.5\left(\frac{h}{a}\right)^3\right], h < a \qquad (3.16)$$

Where

N is number of pairs at lag (*h*);

Co is nugget variance;

C is regionalized variance;

(*Co* + *C*) is sill and '*a'* is geostatistical range.

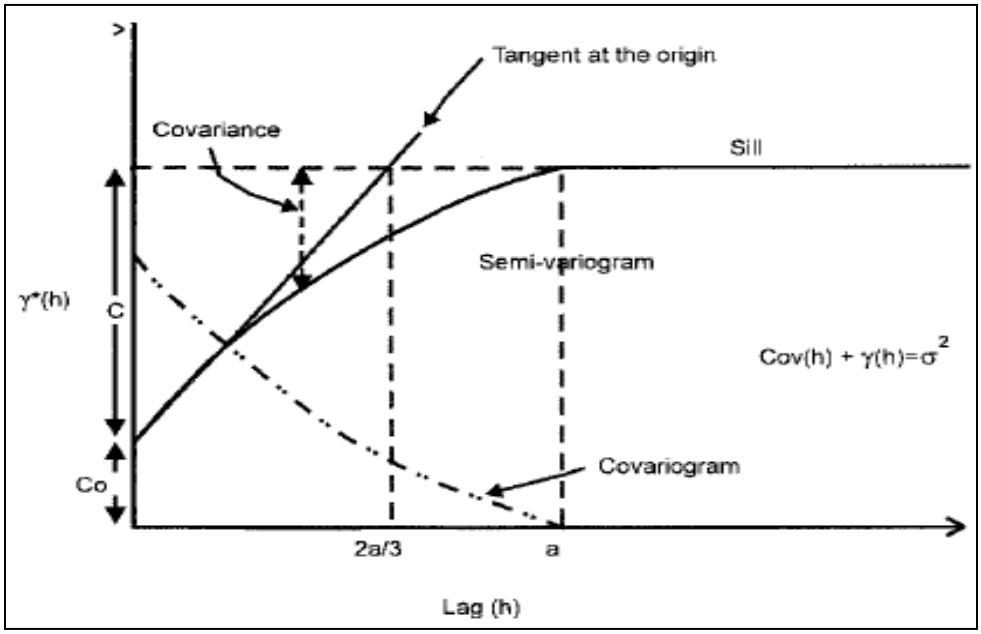

Figure 3.3. A Spherical model with its main components [17]

Table 3.1. Types of Semi-variogram models with respective equations [1, 12]

MODEL TYPE	**EQUATION**	**COMMENT**
Spherical	$\gamma(h) = C_o + C\left[1.5\left(\frac{h}{a}\right) - 0.5\left(\frac{h}{a}\right)^3\right], h < a$ $\gamma(h) = C_o + C, h \geq a$	This is the most frequent model type encountered in mining practice. It is often accompanied by a nugget effect.
Exponential	$\gamma(h) = C_0 + C\left[1 - exp^{\left(-\frac{h}{a}\right)}\right]$	Almost similar to the spherical model except that it reaches its sill asymptotically and much slower than the spherical model.

3.4.1. Cross validation of semi -variogram

Estimation of unsampled locations depends heavily on the semi-variogram model as the representation of the true spatial structure for that measurement. The optimality of the kriged estimates also depends on robust and a well modelled semi-variogram. There have

been numerous studies by scholars to evaluate the confidence of the semi-variogram model [18]. The semi variogram still remains the best spatial variability modelling tool, thus iterative process should be put in place to check its validity. Since it cannot be justified too strongly that inappropriate semi-variogram model will lead to inappropriate and potentially misleading estimates, kriging only gives the "best" answers if our model is correct.

One of the suggested methods for checking the validity of the semi variogram model is cross validation. Cross validation is a series of mathematical processes that try to see whether the estimates produced by the kriging process resemble those which really exist within the specified confidence intervals. The operating principle behind this method is that, at each sample location, a sample is removed from the data set and the value at this point re-estimated using the other surrounding (n-1) sample values within a specified search volume. This is repeated for all samples and the remaining samples produces an estimator, z^*, and its associated standard error, σ. The standard deviation is calculated as:

$$\sigma = \sqrt{\frac{1}{N-1}} \sum (z_i - z_i^*)^2 \qquad (3.17)$$

Where

N is the number of samples

Z_i is value of grade

Z_i^* is the estimated grade

3.5. Non-geostatistical estimation methods.

3.5.1. Inverse Distance Weighting (IDW) method

IDW method is a technique that applies a weighting factor that is based on an exponential distance function of each sample within a defined search neighborhood, at about the central point of the area to be estimated [20].

Theoretically, all samples can be used in the estimation of a block; but practically it is sufficient to limit the choice of samples to those close to the block. The distant samples will have little weighting effect because of their distance to the block and the degree of continuity (or variability) of the variable in the mineralization.

The selection of a close sample is done through a 'search neighborhood' centered on the block. This is illustrated Fig. 3.4. Sample values captured within the neighborhood are weighted by the inverse of the distance of the sample from this point raised to a power 'n'.

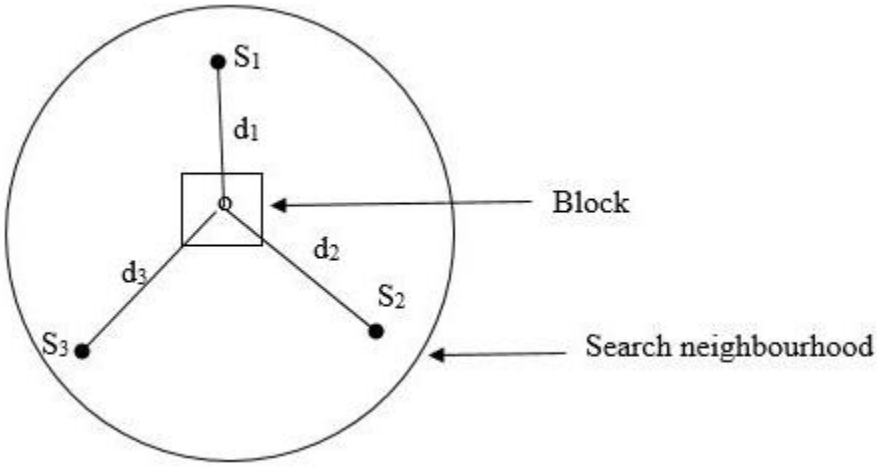

Figure 3.4. Search neighbourhood [20]

For a two-dimensional isotropic case the block grade, assuming constant support, is given by

$$Z = \sum_{i=1}^{n} \frac{Z_{i\frac{1}{d_1{}^n}}}{Z_{i\frac{1}{d_1{}^n}}} \qquad (3.18)$$

Where:

$Z_B{}^*$ is the estimated variable of the block (of grade, thickness, accumulation etc.)

Z_i is the value of the sample at location i

d_i is the separation distance from point i, to the point of reference.

n is the power index.

The weighting power for the inverse of the distance may vary between 1 and 5. The most common weighting power is n = 2, however the choice of the weighting power is arbitrary and is often based on experience of the evaluator and not on any explicit model of any intrinsic geologic characteristic [20, 21].

The IDW has been widely used in the estimation of many deposits where it has given acceptable results that compare well with those produced by Kriging [21]. According to Royle [21], the IDW is not seriously biased when the nugget effect is small, but the bias increases when the nugget effect increases. Thus, this method is questionable until more is known about the nugget effect of the orebody.

3.5.2. Search strategy

The purpose of sample selection is to provide a subset of the data that is representative of the region around the block. The sample must be selected from geologic domains similar to that of the block and the maximum radius that should be at least equal to the distance between samples to prevent discontinuities in the weighted average. Three composites are usually the maximum, required from a single drillhole. More than three provides redundant data and may cause strange weights [20, 21].

3.6. Review of domaining and Geostatistical estimation literature

For paleoplacer deposits little literature can be found with emphasis on domaining. The papers reviewed made extensive deliberations on geostatistical estimation of ore deposit with soft boundaries (no change in grade level at the boundary which is significantly related to the importance of this research.

A critical step in the definition of domains is the logging and mapping of lithological units [22]. In Billitons Escondida Mine case study [22], describes in detail how four estimation domains were created. The geologic variables considered were lithology, mineralization types and alteration. These variables were coded and integrated into a complete Escondida geological database system for simplified modelling and definition of estimation domains. The domains and open pit design as modelled by production geologists is shown in Fig. 3.5. The fifth domain located at the flanks of the deposit is unmineralized.

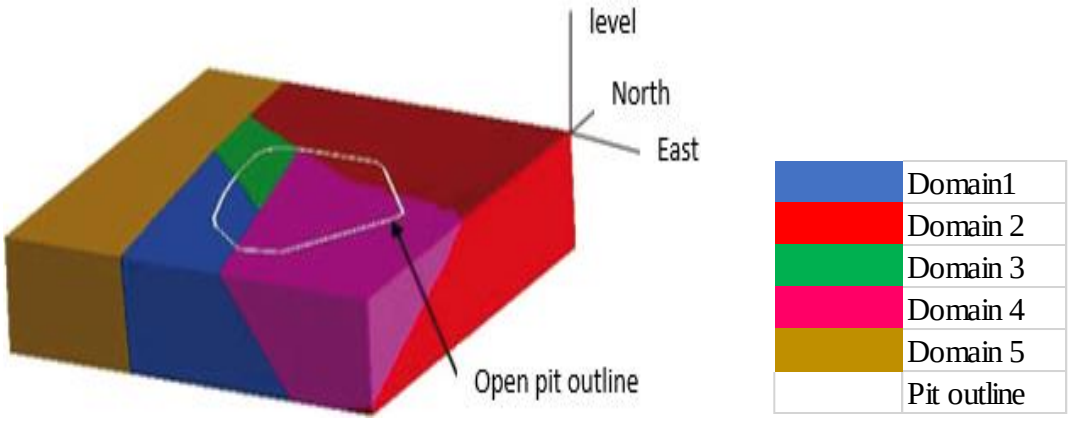

Figure 3.5. Four structural domains within the pit projection outline [22]. Domain 5 is non-mineralized and outside the area of interest for this paper. For scale, the projection of the pit to the surface has an approximate dimension of 3 × 3 km, and no vertical exaggeration.

A new method of estimating mineral resources was proposed by estimating the probabilities for the unsampled locations to belong to each grade domain and performing a cokriging of the coregionalization and stochastic modelling of the grade domains. This helps minimize conditional bias and kriging variance [23].

Ortiz [24], through a case study on a Porphyry Copper Mine in Chile used several geostatistical methodologies to handle soft boundaries. The use of regression analysis and basic statistics are some of the tools used in this project. In his project, five different scenarios are presented where he used: i) OK for estimating geological domains; ii) OK omitting the boundaries; iii) traditional cokriging; iv) ordinary cokriging of the other domains and finally v) the OK using dilated domains to ease the difficulty in representing the spatial correlation of the grades within and across the geological domains. Results indicated that the dilated domains yielded better results with minimal mean absolute error

in Table 3.2. The scatter plot for the dilated domain also recorded a high correlation with correlation coefficient of 67% between true and estimated grades.

Table 3.2. Performance comparison among the five geological domains for 12973 blast holes and 2248 blastholes along the soft boundary [24].

		CASE 1 **Hard boundary**	**CASE 2** **without hard boundary**	**CASE 3** **traditional OCK**	**CASE 4** **Standard OCK**	**CASE 5** **dilated domains**
validation set 12 793 BH	correlation True-estimated	0.655	0.665	0.657	0.662	0.67
	Mean error	-0.049	-0.042	-0.05	-0.054	0.044
	mean absolute error	0.324	0.320	0.323	0.320	0.317
	Mean squared error	0.225	0.219	0.224	0.220	0.215
validation subset 2 248 BH near boundary	correlation True-estimated	0.485	0.56	0.500	0.543	0.563
	Mean error	-0.103	-0.081	-0.102	-0.11	-0.079
	mean absolute error	0.379	0.351	0.377	0.355	0.348
	Mean squared error	0.287	0.246	0.281	0.257	0.242

Mostly, paleoplacer deposits have short ranges because the orebody is more continuous and the relationship between variances of data pairs with their corresponding lags are not autocorrelated after a shorter distance. This is evident from some semi-variograms models of some paleoplacer deposits [25].

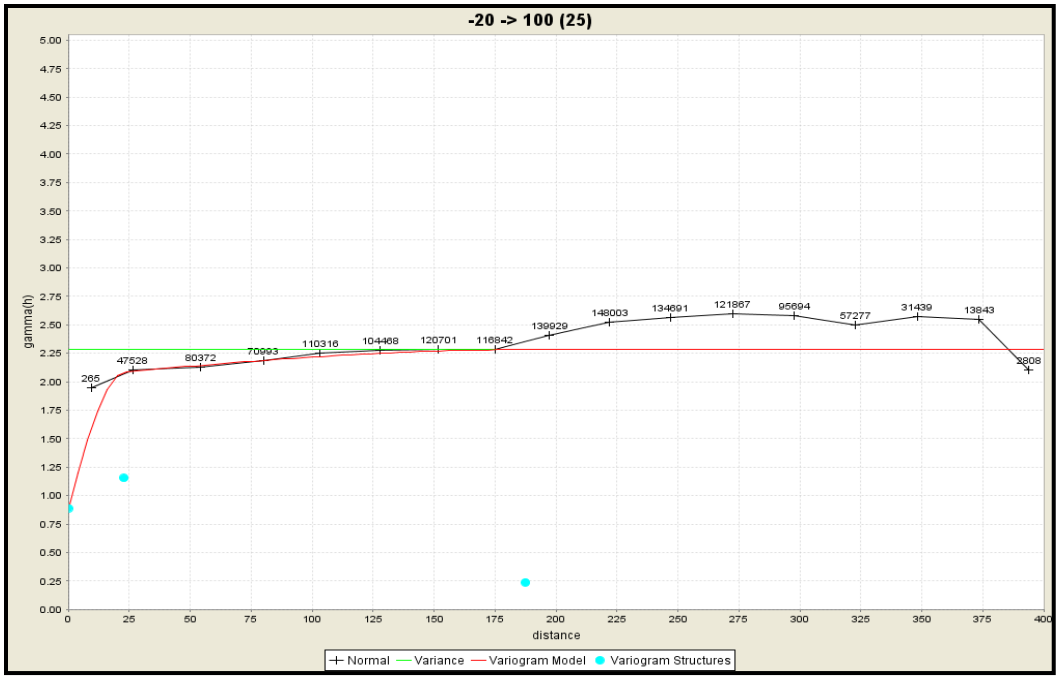

Figure 3.6. A Semi-variogram along 100^{o} direction in Teberebie Pit, Goldfields concession [25]

Owusu [25], used OK to estimate the paleoplacer deposit in Teberebie pit of Goldfields concession. In his work he compared OK estimates to IDW as a way of validating OK block estimates. Ore grade data was positively skewed and was later normalized before grade interpolation. A generated Blockmodel report displaying mean grade for OK and IDW was plotted as shown in Fig. 3.8. The main aim of the project was to investigate if IDW could be used as an alternative technique for the Tarkwa Goldmine paleoplacer deposit when the need arises. In addition, the IDW estimates were used as a validation tool for OK estimates.

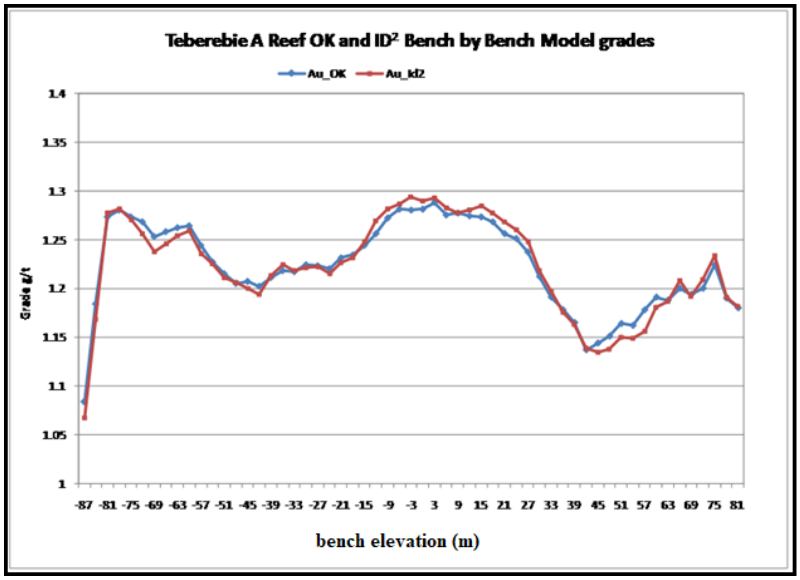

Figure 3.7. A Reef OK model grades compared with ID^2 model grade from -87m to 81m elevation above sea level [25]

The comparison of OK estimates with IDW estimates also showed a correlation of at least 90% in Fig. 3.9. The IDW estimates were carried out using an exponent of 2, thus ID^2. The only limitation was a failure to partition the geological data into estimation domain prior to grade interpolation. This project intends to highlight the importance of geological domaining in one of the Goldfields open pit with a complex geology.

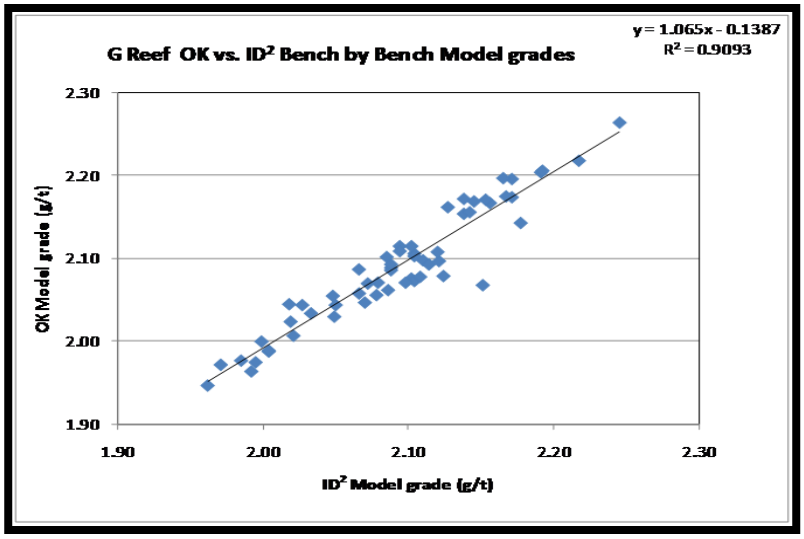

Figure 3.8. Scatter plot of actual on kriged values [25]

In this project, all procedures which are important in the definition of domains such as statistical analysis, mapping of lithological units are employed. Other statistical tests such as the t-test, removal of outliers, special data treatments (grade cutting, grade capping) and probability plots are also used to help in the creation of geological domains.

CHAPTER 4

METHODOLOGY

4.1. Domaining

Domaining is a very critical step in mineral resource estimation and extra care must be taken in its definition. However, few references can be found in this literature and little work has been done with respect to paleoplacer deposit. Domain, as described earlier, represents an area or volume within which the characteristics of mineralization are more similar than outside the domain [26]. The definition of domains is mostly accompanied by lithological interpretation and the delineation of ore bodies with the same structural and geological features.

Stationarity is based on the concept of carefully treated statistically homogenous distributions and is formally defined by [27].

In most cases, geological units are the same as mineralogical domains, such as iron ore deposits, metasedimentary deposits or metal sulphide syngenetic paleo placer deposit in Tarkwa goldmine in Ghana [26].

4.1.1. Types of geological domains

All deposits being syngenetic or epigenetic will show some variation from ore to non -ore. If the concentration of metals in rock is below the cutoff grade, the rock is classified as waste and cannot be mined for profit. The Selective Mining Unit (SMU) representing the standard volume of rock material where mining decisions are taken should honor the

geological domains if possible. The two types of domains are hard and soft boundary, and both will be described in detail in the subsequent pages.

(i) Hard boundary

Since geological domains are representative of a stationary randomized homogenous variable, the definition of hard boundaries is based on five processes as described by [28]. The decision of stationarity is a five-step process:

1. Choose the number and type of domains
2. Model the domain boundaries
3. Determine the nature of transitions across domain boundaries
4. Quantify large-scale trends within domains
5. Predict with a trend model

Hard boundaries show an abrupt change across the boundaries which is demonstrated by other paleoplacer deposits [26]. Also, the grades measured at either side of the boundary are independent, with evidence of no spatial correlation across the boundaries. Contact plots may highlight several domains that can be analyzed statistically to ascertain the boundaries present within the deposit. There is a drop in average value of the variable of interest from one domain to the other as shown in Fig. 4.1. They greatly facilitate resource estimation and selecting a natural cut off does not cause over or under smoothing of grades. Issues of grade misclassification barely occur and there is no over estimation or underestimation of metal concentrations.

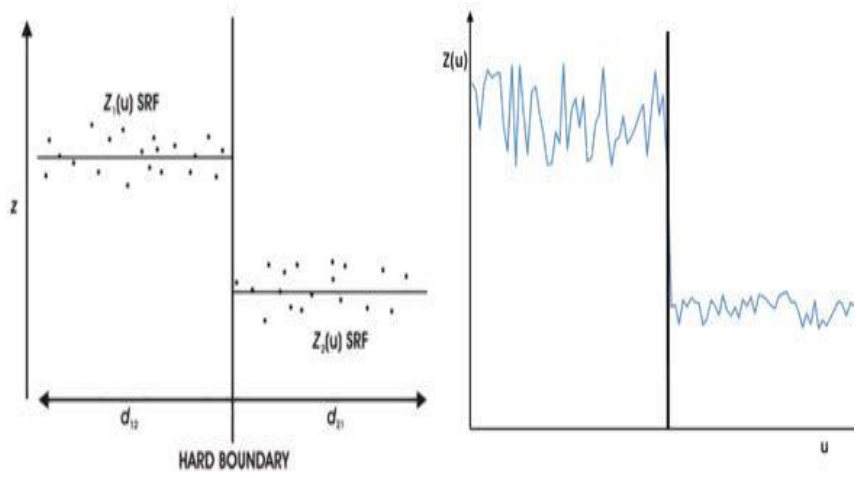

Figure 4.1. A contact plot showing abrupt changes in Z across hard boundaries [28]

The distance between samples and Z represents the grade or any variable being investigated. In paleoplacer deposits, hard boundaries are sometimes characterized as a region of non-deposition or unconformity obeying the principle of lateral continuity.

In addition, the boundaries defined are clearly differentiated because of the style of deposition and mineralization. Hard domains do not allow the interpolation and simulation of grades across boundaries. A statistical contact plot analysis, displaying the distribution of samples across the boundary, will show a clear drop in trend line across boundaries [24, 29] and log probability plot will show a deviation of scatter points away from the diagonal line.

(ii) Soft boundary

A soft boundary is present when the grade in at least one domain shows a significant trend, but there is no significant change in grade level at the boundary. A soft boundary also shows a transition zone between two domains [30] making it difficult to define the exact layout of the threshold as shown in Fig. 4.2.

It allows grades from the other side of the boundary to be used in estimating both domains to varying degrees. The way of ensuring an accurate geostatistical technique is to prevent the use of a high-grade domain to estimate an adjacent low-grade domain [26].

Boundaries are mostly defined by a change in local mean grade where grades within the domain show no spatial dependency across the boundary. In order to preserve the natural variability and reduction of artificial variance the boundaries are extended.

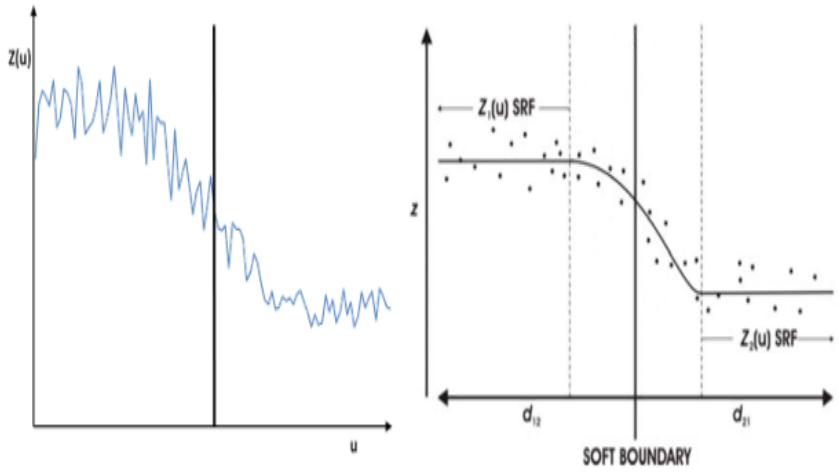

Figure 4.2. A contact plot showing gradational change in Z (u) across soft boundaries [28]

4.2. Definition of domains

Delineating the domains must be done carefully accounting for the geological knowledge of the deposit and how it was formed. Other petrophysical properties of rocks help in the determination and definition of domains. Some of these are:

I. Specific gravity and the strength of the rocks

II. Structural control of grades such as faulting, unconformity etc.

III. Thickness of reefs or mineralised rocks and its corresponding accumulation.

In most instances, geological or mining practitioners misconstrue the differences between estimation and geological domains [22]. Geological domains in this sense are mostly described as a single geologic variable whilst estimation domains place more emphasis and analysis on the controls of mineralization. Mostly, estimation domain contains a set of unique variables (alteration, lithology, mineralization types etc.) and its definition is facilitated with the combination of one or geologic variables.

Since geostatistical simulation makes strong assumptions of stationarity in the mean and variance of the domains created a new technique is designed to account for stationary variables within rock types [31].

4.2.1. Dependency between grade domains

It is always prudent to ascertain the dependency between domains caused by the spatial continuity of the deposit. In geostatistics, which deals with the study of RV, the samples collected must show some sort of continuity in a direction and the creation of domains may influence this spatial continuity due to the formation of geological or statistical boundaries. The process of estimating grades within domains separately means that they are considered as independent entities [23]. This creates a boundary that does not exist geologically and contradicts the assumption of spatial continuity in grade distribution.

4.2.2. Data distribution analysis

The initial step is to plot and observe the nature of assay data using statistical tools. Statistical tools help to improve the understanding of the data, ensure data quality and assess the confidence of predictions**.**

The first step is the production of histograms and frequency distribution curves to ascertain the overall impression of assay distribution. For a normal population, the arithmetic mean or the median, is regarded as good estimator of grade. For a perfect normal distribution, a normal probability plot shows points lying on a straight line [32].

The histogram plot can be used to identify a bimodal distribution and outliers. Bimodalism indicates the use of data with mixed population and should be statistically separated to help produce the best grade and tonnage estimates within a deposit.

Outliers are values different from the rest of the sample and raise the suspicion that they may be from a different population. Usually the effect of outliers on variograms is a very erratic curve which is difficult to interpret [33]. Outliers are mostly treated by capping or cutting of grades and must be accepted as a real member of the complete population [21].

(i) Normal (Gaussian) distribution

The normal distribution is widely used to describe a discrete data set. It is represented by a bell-shaped curve, symmetric about the mean, the mode and the median of the distribution (Fig. 4.3). Normal curves can be fitted to an unbiased histogram to demonstrate the likelihood that the variable in question is normally distributed [34].

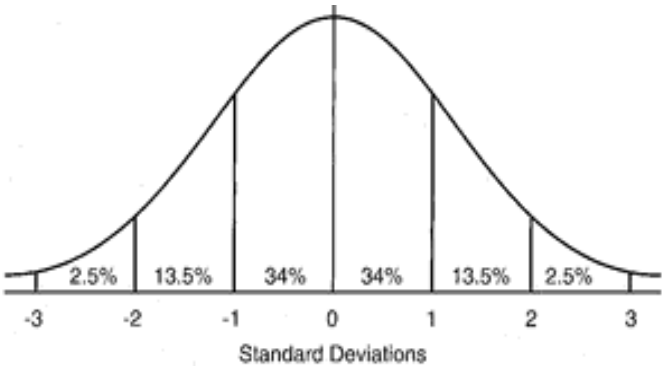

Figure 4.3. A normal distribution curve [34]

(ii) Lognormal distribution

A distribution of variable x is said to be lognormal if the log transform [t = ln(x)] of the variable has a normal distribution. It has been established [35] that in most geological formations, assay values do not conform to normal distribution but rather their logarithms tend to be normally distributed. The true mean of a log-normal population is derived from the relation [14]

$$\mu = e^{(\alpha + \frac{\beta^2}{2})} \qquad (4.1)$$

Where α = mean of logarithms of raw data,

β^2 = variance of logarithms of raw data.

If a plot of the cumulative frequency on log-probability paper results in a curve that deviates from a straight line this may constitute evidence of skew under lognormal conditions. In such a case, a third parameter called an additive constant k may be added to the raw data values as shown in Fig. 4.4.

$$t = \ln (x + k) \quad (4.2)$$

whose distribution may be lognormal [1] as shown in Fig. 3.4.

Where 1n(x) = logarithm of raw data,

k= constant,

t = normally-distributed random quantity

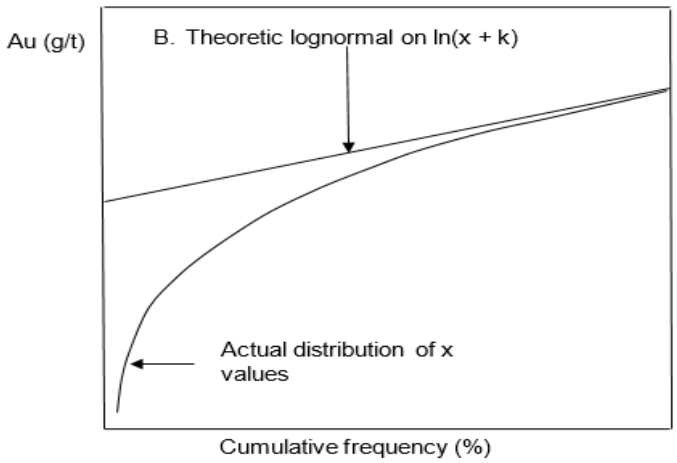

Figure 4.4. A 3-Parameter lognormal plot as a log probability plot [34]

(iii) Skewness

The coefficient of skewness is a measure of asymmetry of the histogram. In a normal distribution, where the distribution is symmetric, the skewness is zero. The skewness is negative for distributions tailing to the left and positive for distributions tailing to the right. These are illustrated in Fig. 4.5. It is an indication of whether a distribution is better described as normal or lognormal. The general equation is,

$$\text{Skewness} = \sum \frac{\left(g_i - \bar{g}\right)^3}{ns^3} \quad , \tag{4.3}$$

Where

s is the standard deviation

g_i is the value of the variable g

$\bar{g}$ is the mean of the variable g

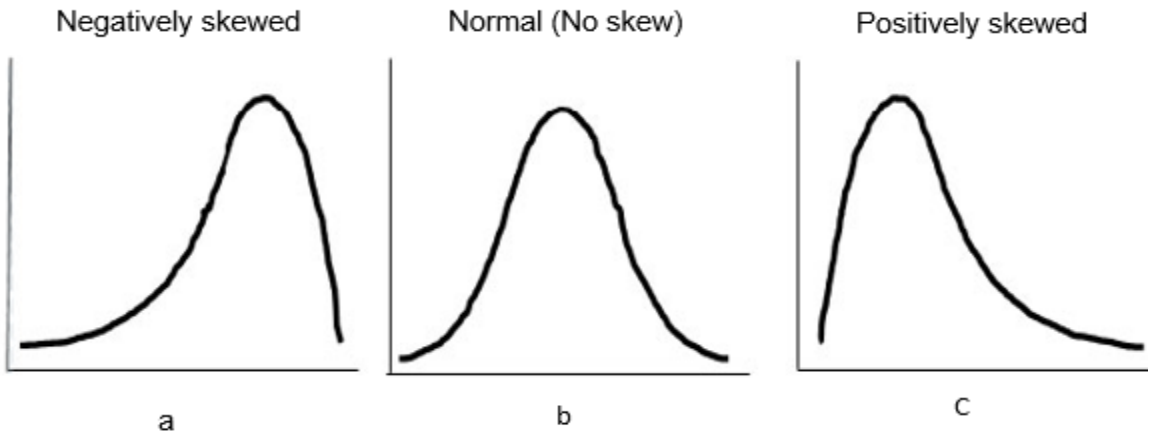

Figure 4.5. Types of frequency distribution curves (a) Negatively skewed distribution (b) Normal (no skew) distribution (c) Positively skewed distribution.

(iv) Coefficient of Variation (CV)

The Coefficient of Variation (CV) is a measure of the relative variation of the data and is calculated by dividing the standard deviation by the mean. It provides a very useful guide

to the variability of the data and their subsequent suitability for use in geostatistics. Table 4.1. shows some important characteristics of CV.

Table 4.1. Characteristics of CV Value [36]

CV	INTERPRETATION
0 % - 25 %	Simply symmetrical grade distribution. Resource estimation is easy.
25 % - 100 %	Skewed distribution with moderate difficulty in resource estimation
100 % - 200 %	Highly skewed distribution with a large grade range. Difficulty in estimating local grades
Above 200 %	Highly erratic, skewed data or multiple populations. Local grades are difficult or impossible to estimate.

4.3. Orebody modelling

Exploration holes drilled to intersect mineralized rocks are carefully modelled in 3D to define the shape, size, structure and extents of the orebody. After detailed geological interpretation, variables of interest are carefully grouped and working sections with (hand) drawn interpretations allow for a dynamic understanding of geologic controls, and better management of future data gathering campaigns.

According to Glacken [37], the orebody being modelled, complexity of the geology deposits and requirement of accuracy are some of the factors that affects the choice of

orebody models to be used. A sound geological model is the foundation for robust resource estimation, efficient mine planning and effective near-mine exploration. The main objective of orebody modelling is to estimate and predict the tonnage and grade of the ore body. The two types of orebody modelling are explicit and implicit geological modelling with the latter evolving over the past few years.

Explicit modelling (traditional) creates sections which are targets of explicit modelling workflow. The workflow consists of digitizing geological features on a section and then joining this interpretation to create a pseudo- 3D model as shown in Fig. 4.6. Geological features on sections are represented by polygons and polylines. All features are stored in a single file called geo strings. This makes modelling at times a herculean task and inflexible as it is difficult to update the model when more data becomes available.

Implicit modelling eliminates the laborious work by using algorithms to generate the pseudo 3D-model from the data (Fig. 4.7.). A mathematical constraint is built that can be used to visualize different aspects of the data in 3D. Extra care must be taken not to skip a validating test in this scenario to minimize mining risk. 3D surfaces and volumes are generated directly from the point data by intersecting boreholes or representation of polylines. Most implicit models are dynamic, thus any changes to the geological parameters that gets applied automatically updates the 3D model. It therefore provides greater flexibility, efficiency and smooth idealized isosurfaces.

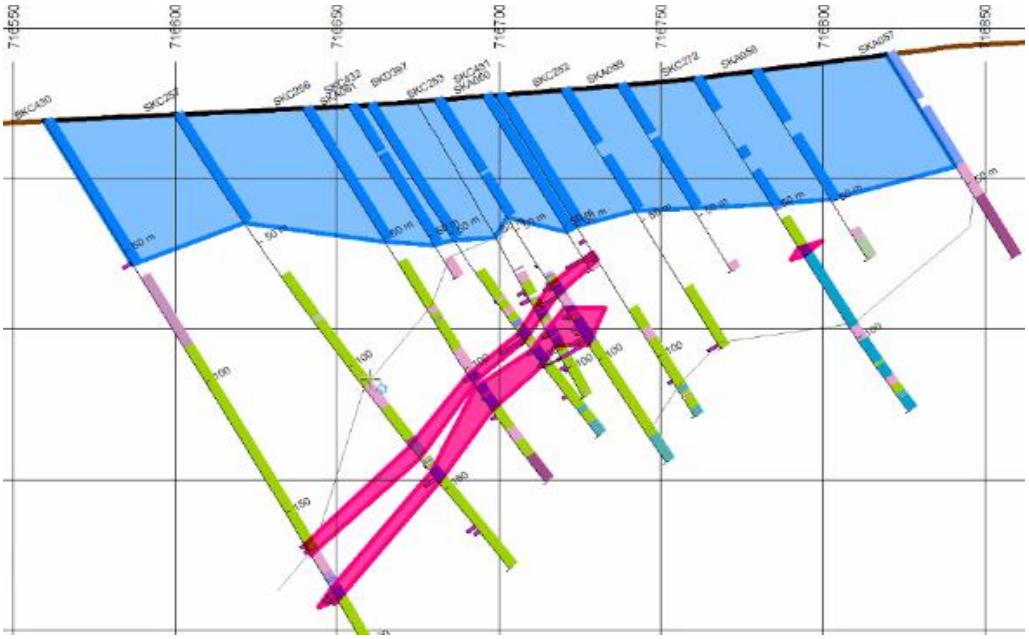

Figure 4.6. Digitizing of polylines in a drillhole section to create a wireframe model

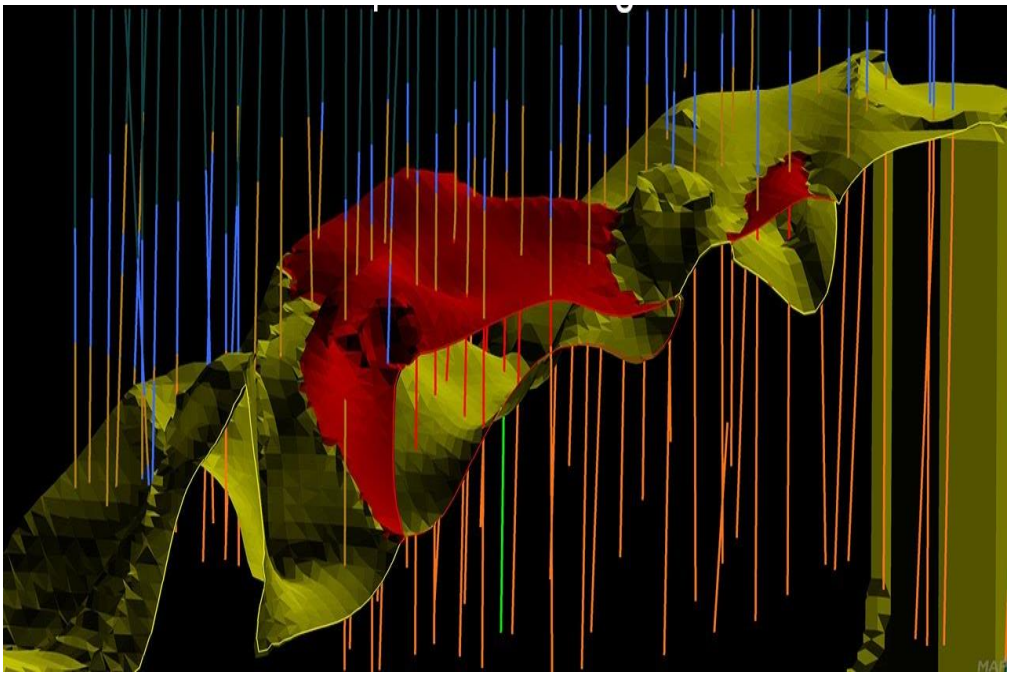

Figure 4.7. A pseudo -3D implicit model modelled in Surpac

Finally, its ability to create and visually interrogate several models simultaneously based on different interpolations parameters is another key capability of the modelling method. Ore body models are later reconstructed to form Blockmodels that are spatially georeferenced and divided into fixed size blocks (Fig. 4.8). The Blockmodels are filled with geological attributes and serves as a model for grade interpolation. The geometry of the Blockmodel depends on the characteristics of the deposit, the geological features being modeled, and mine planning requirements, such as equipment size and type to be used by the operation. Block size and geometry is an important decision in resource modelling. Blockmodels contain sub-blocks which depends on the model extents and resolution. Division of the main blocks into sub-blocks is to gain a perfect resolution when dealing with areas along the periphery of the geological contacts.

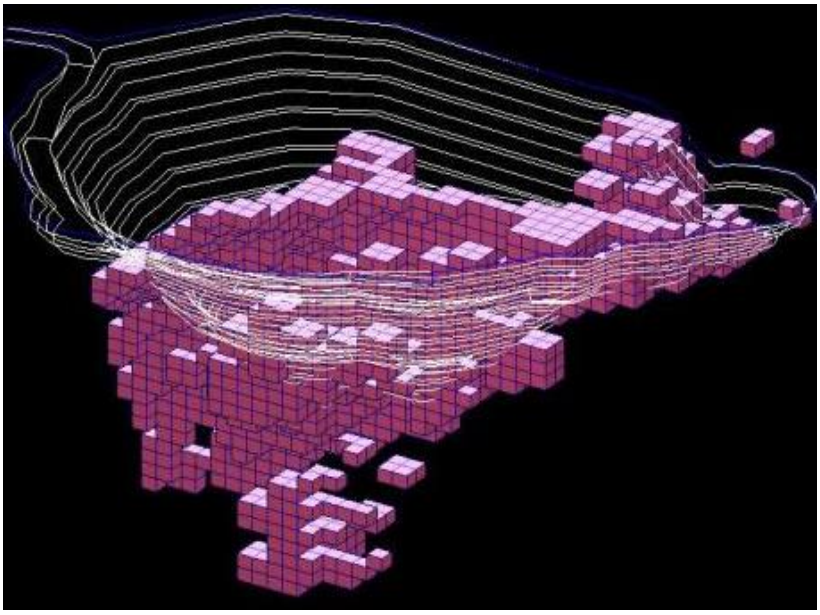

Figure 4.8. Blockmodel section displayed in Surpac software.

4.4. Model validation

A Blockmodel must be performance-tested, validated and revised as necessary, particularly in the early years of mine life, when deductions are made from drillhole data. An important step in a geostatistical evaluation is to validate the model after it has been created and can be undertaken using the following:

- Comparing model values with other estimation techniques
- Basic statistics of model values
- Trend analysis

The graphical validation must make geologic sense [37] and grade distributions within a geological domain should reveal a precise estimate when it shows a normal distribution. If the data distribution is lognormally distributed there should be further data treatments to normalize it as this prevents the squashing of high or low data values (grades).

The best validation tools are comparison of estimated data to production data. High correlation between these sets of data increases the level of confidence in relation to the precision of the resource model.

4.4.1. Kriging efficiency and regression

Block sizes that are to be used should have some relationship with the selective mining unit. Oversmoothing is bound to happen when small block sizes are used for estimation yielding very low precision results and incorrect grade-tonnage curves. The block size should be less than the data spacing and a block size from 1/3 to 1/2 of the drillhole data spacing [12] is proposed as an approximate guideline. Both oversmoothing and undersmoothing result in conditional bias [18, 38]. Conditional bias can therefore be

defined as a condition where there is no good correlation between true grade and estimated grades. The data points do not lie on the line of best fit and are mostly concentrated either above or below the line (Fig. 4.9).

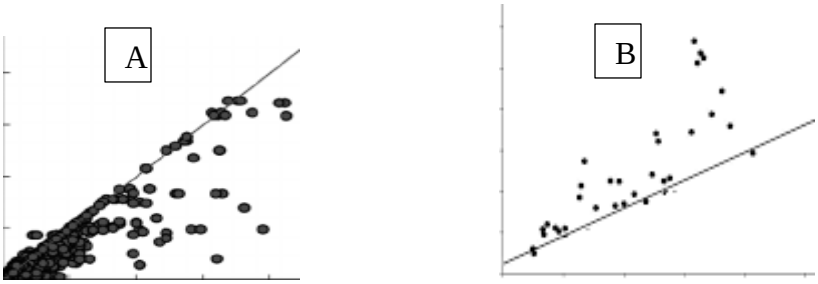

Figure 4.9. Conditional bias (a) Bias for underestimation (b) Bias for overestimation [19]

In oversmoothing, high grade blocks are underestimated and low-grade blocks are overestimated. This affects overall resource estimates and will have a significant effect on economic viability of a mineral project as reconciliation during mining is biased with high variance between actual head grades and block estimates. Undersmoothing on the other hand results in the overestimation of high grade blocks and underestimation of low grade blocks. Both oversmoothing and undersmoothing defines the level of accuracy for the resource estimates as this is shown Fig.4.10.

Figure 4.10. – Regression plots (a) High accuracy (b) low accuracy [19]

CHAPTER 5

SAMPLE DATA ANALYSIS AND DOMAINING

5.1. INTRODUCTION

The drill hole spacing was 25 m x 25 m with a mix of Diamond Drill (DD) and Reverse Circulation Drilling (RC) samples. Mostly, the reverse circulation samples were used for grade control (infill drilling) and diamond drilling was used mainly for exploration.

All the holes were drilled at an angle of 90 degrees downhole to intersect the orebody (A1 tabular reef) at a predetermined spacing of 25 m along strike and dip of the deposit. Ore body models were constrained into the Blockmodel and kriging neighborhood analysis was performed to select the optimal blocks for resource estimation. The kriged results were cross validated and compared to raw data to justify the confidence of the estimates. Fig. 5.1 shows the stepwise approach used for this study.

5.2. Data acquisition and processing

The geological data sampled was within the following geographical limits:

Eastings 7650 mE – 8150 mE

Northings 9750 mN – 10050 mN

Elevation 35 m – 175 m

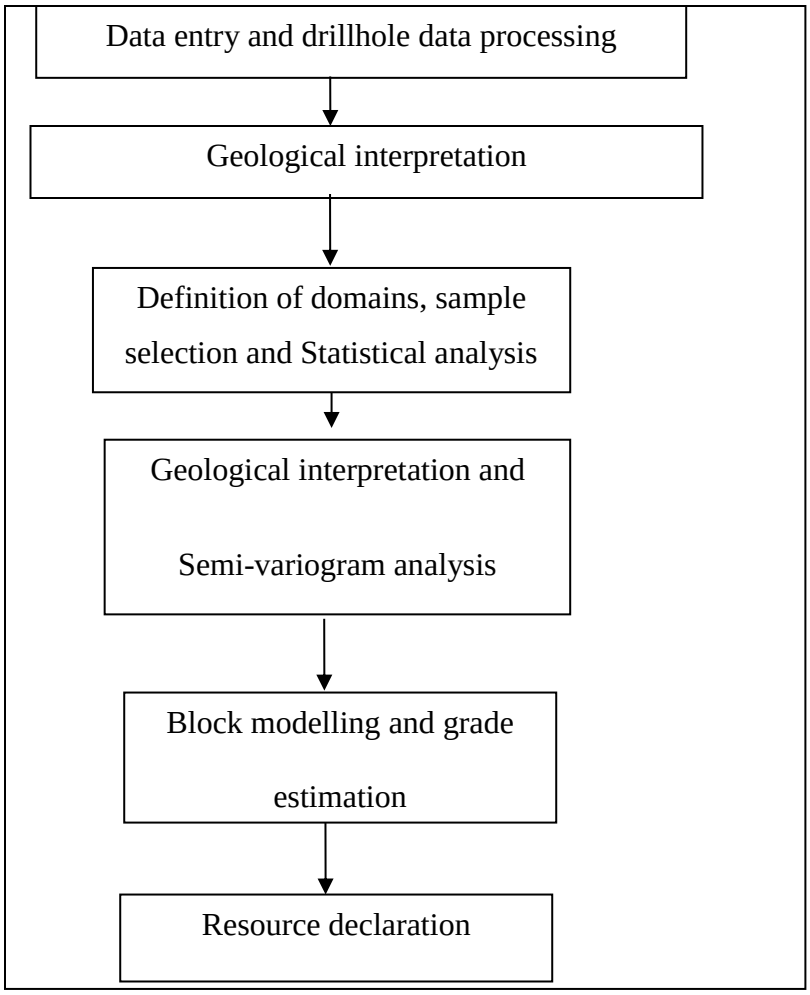

Figure 5.1. Phases in mineral resource Estimation

The total number of DD and RC holes were 15 and 230 holes respectively covering a strike length of 500m. The RC holes were sampled every 1m whereas the DD holes were sampled on lithological contacts. Fig. 5.2. shows a histogram plot for sample length and thickness of the A1 Reef.

Drilling was carried out using LTK46 coring equipment for RC holes and BQ coring equipment for DD holes. The drill cores were extracted using a triple tube wire line system. The raw length descriptive statistics of the geological data is shown in Table 5.1. Assaying was done by using the fire assay standard technique. This technique separates metal concentrates from impurities with the aid of heat and dry agents. [39, 40, 41].

Table 5.1. Raw sample length statistics of A1 Reef

A1 Reef	
Number of samples	914
Total	855.90
Minimum(m)	0.09
Maximum (m)	1.76
Mean(m)	0.94
Standard deviation	0.191
Variance	0.036

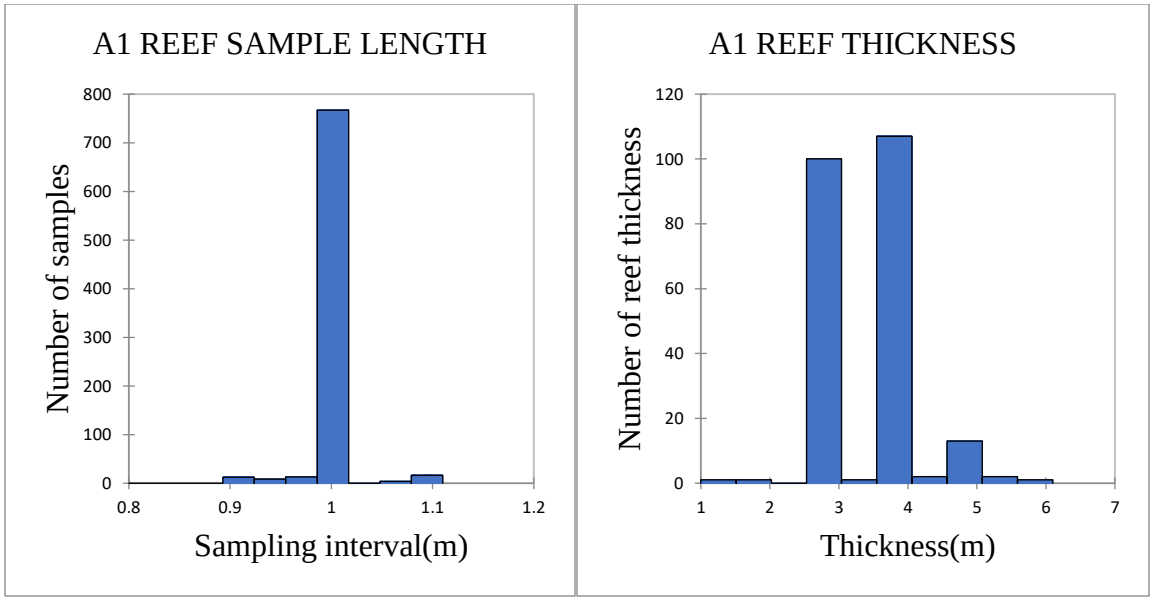

(a) (b)

Figure 5.2. Histogram plots (a) Histogram plot of A1 Reef sample length (b) Analysis of A1 Reef thickness

5.2.1. Database validation

Geological data was uploaded to Surpac database module. Surpac modelling software provides two mandatory tables and other optional tables. In total, five tables were deemed important to capture all relevant information for subsequent orebody modelling and estimation as shown in Table 5.2. Mapped data in the form of text or excel files were converted to ASCII files and filled with different attributes for each table. The mandatory tables for the Tarkwa geological database are collar and survey data. The optional tables consist of geology, assay and zone data.

Many data validation checks were observed and analyzed to present a robust database devoid of data redundancy and errors. These include:

- Missing collar coordinates.
- Missing survey, assay or lithological data.
- Duplicate lithological codes
- Interval errors (missing intervals, overlaps etc.).
- Zero or missing grades.
- Incorrect collar or downhole survey readings.
- Renaming attribute codes in lower or upper case

Table 5.2. Tables used in Surpac to create a drillhole database in Goldfields Ltd.

COLLAR TABLE				
hole_id	hole_type	max_depth (m)	x	Y
AS0855	RC	66	8124.999	9775
AS0933	RC	61	8149.992	9800
GDA18	DD	104	7951.85	10004.9
GDA20	DD	85.5	7999.94	9801.25
SURVEY TABLE				
hole_id	Depth (m)	Azimuth (degrees)	Dip (degrees)	Down
AS0855	0	0	-90	-90
GDA18	0	0	-90	-90
GDA20	0	0	-90	-90
GEOLOGY TABLE				
hole_id	depth_from (m)	depth_to (m)	lith	gr_size
AS0855	0	1	GAP	
AS0855	1	2	GAP	
GDA18	0	0.87	OVB	
ASSAY TABLE				
hole_id	depth_from (m)	depth_to (m)	samp_id	Au(g/t)
AS0855	0	1	AS0855/1	-1
AS0933	0	1	AS0933/1	0.5
GDA18	0	0.87	6090	0.67
ZONE TABLE				
hole_id	depth_from (m)	depth_to (m)	zone	ass_zone
AS0855	0	1	F	-1
AS0933	0	1	OVB	0.5

5.3. Geological modelling and definition of domains

The five tables created were imported into the Surpac database, mapped and displayed. A 2D grid was superimposed to show the extents of the geological data (Fig. 5.3).

The drillhole data was sectioned along the eastings every 25 meters. In total, 20 sections were created, and the lithology coding and grade values were used to interpret the extent of the mineralization.

Geological modelling was basically done within the framework of detailed structural and lithological mapping. The 3D explicit wireframe models of the A1 Reef were created by digitizing sectional interpretations (polylines) of lithology in cross-section across the project area.

A master block was modelled followed by a Digital Terrain Model (DTM) of the investigated fault orientation (Fig. 5.4a). The DTM fault planes were further used to divide the master blocks to help in geological interpretation.

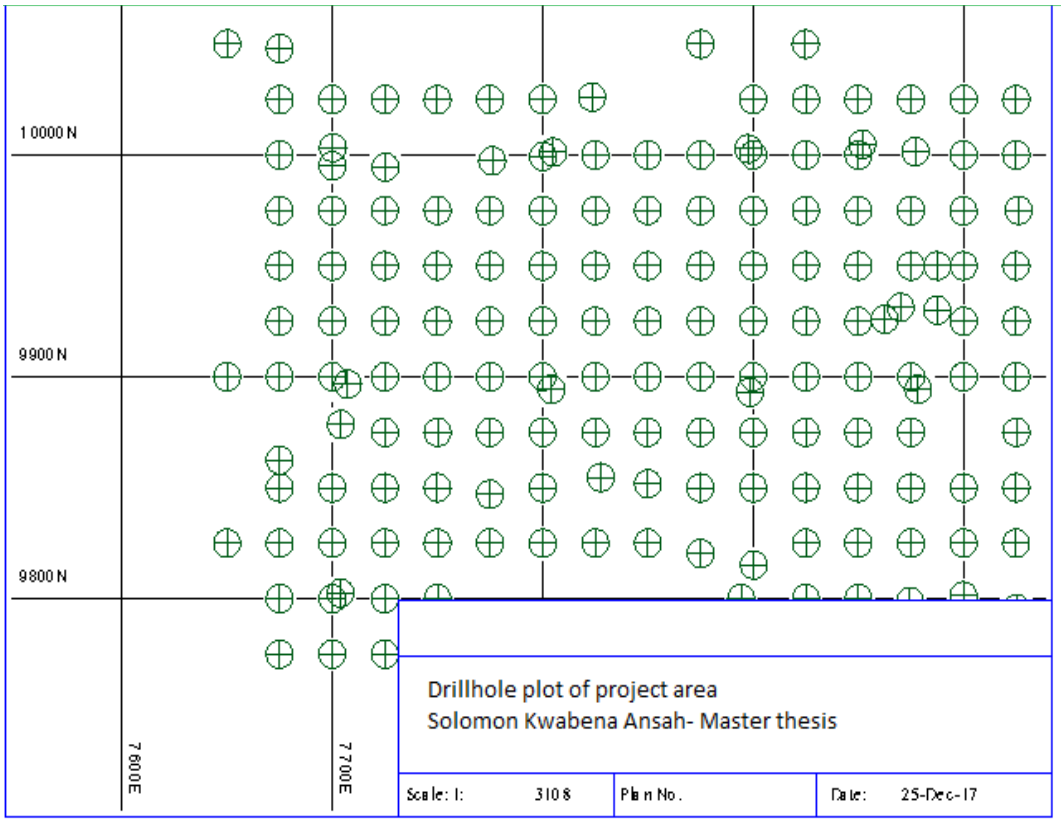

Figure 5.3. Drillhole pattern of the project area

Geological continuity of the reefs was considered good, except where they were disrupted by faults. The A1 Reef is truncated by the fault structure and extra work was done to generate a wireframe model (Fig. 5.4b) to represent its geometry and to confirm the extents, throw and orientation as shown in Fig. 5.6. The waste material, devoid of mineralization which was modelled, divided the reef in three separate domains as shown in Fig. 5.5.

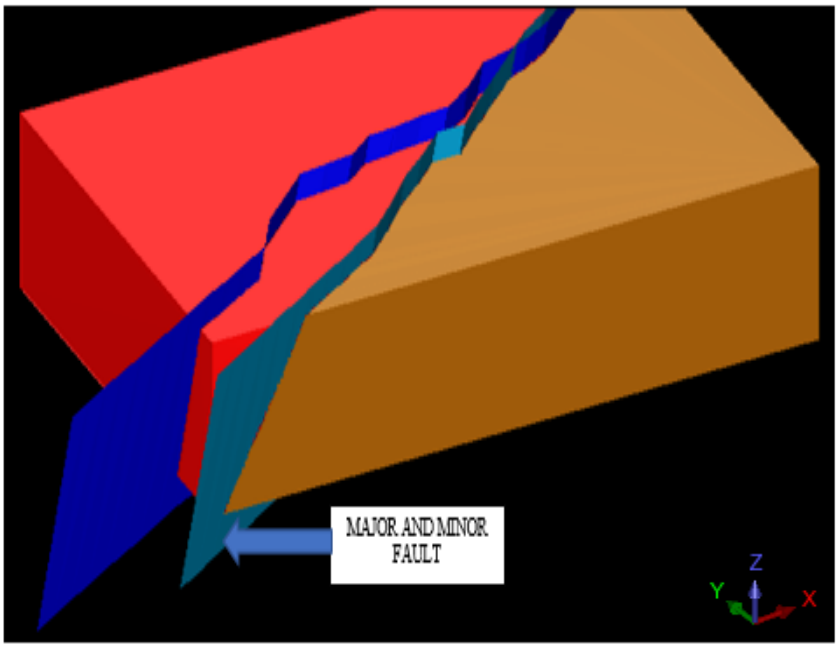

(a)

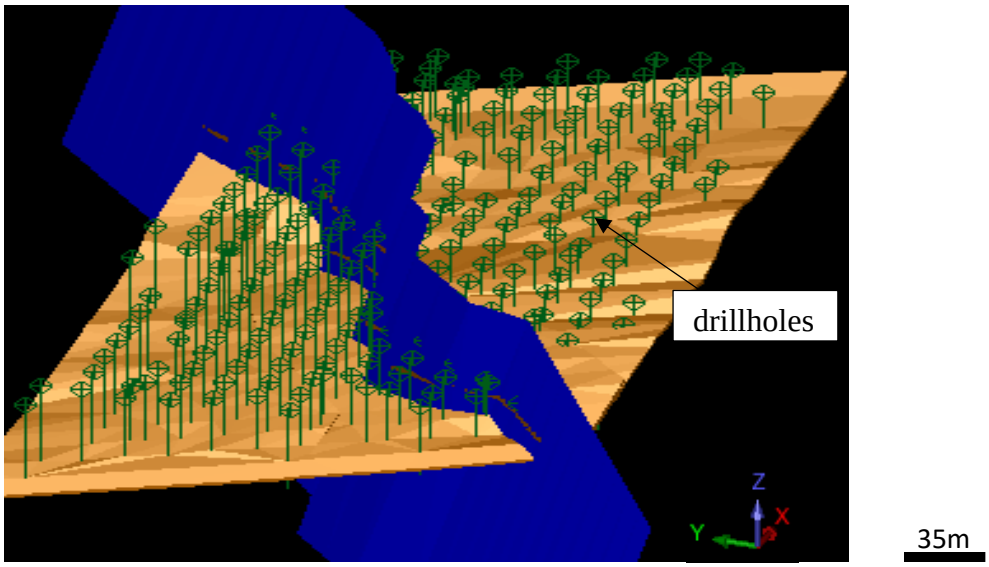

(b)

Figure 5.4. Explicit orebody modelling and interpretation (a) Modelled master block with major fault planes (b) A 3D wireframe generated from polylines with an overlap fault displacing the reef.

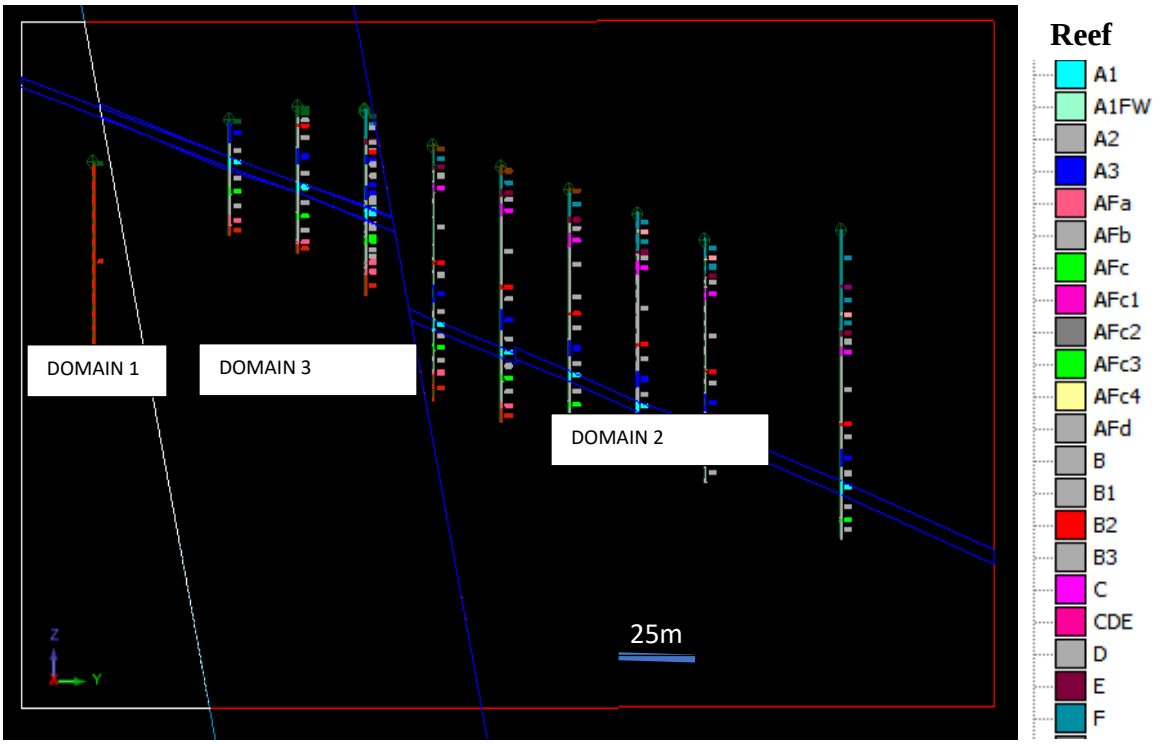

Figure 5.5. Digitization of mineralized zones within fault blocks (stationary domains)

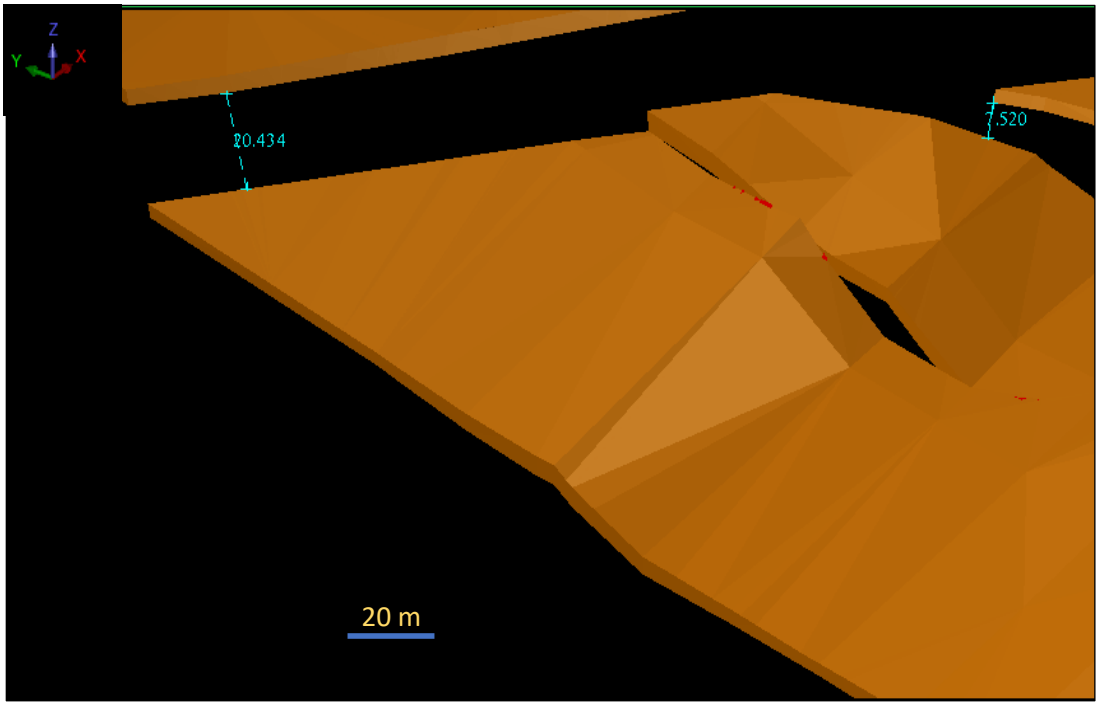

Figure 5.6. Surpac clearance analysis showing some areas of A1 Reef displacement

5.4. Sample selection and statistical analysis

The drillhole data in excel format (.xls) was converted to string files (.str) and data values which were used for further statistical analysis. To ensure that the samples for estimation represent equal volume (support), zonal-downhole compositing was done to ensure that each sample represents the same length at every 1m. It is evident that more than 90% of the samples were taken every 1m in length (Fig. 5.2a). The summary statistics for the composite data used for estimation are tabulated below (Table 5.3).

Table 5.3. Composite data descriptive statistics

A1 Reef	
Total	821
Minimum	0.29
Maximum	1.00
Mean	0.99
Standard deviation	0.057
Variance	0.03

Alternatively, further investigation was done to observe if thickness and accumulation will be good variables for domain definition. It was later abandoned since it is evident that the project area had hard boundaries and this further analysis was beyond the scope of this project. The assay values were exported to Minitab and Excel for data analysis.

5.4.1. Mixing RC and DD samples

A test was carried out to justify the mixing of RC and DD samples for estimation based on the grade and sampling method. because of the tendency of bias resulting from volume variance effect and existence of outliers. It was established that irrespective of the type of sampling method used, the mean does not change. The two populations belong to similar statistical distributions because there are no significant differences between sample mean (Fig. 5.7). A hypothesized value of 0.5 was set in Minitab to be the maximum or threshold mean difference between the sample populations at a significance level of 5%. The RC and DD population recorded means of 1.3426g/t and 1.2570g/t respectively. The observed mean difference was 0.0756, which is far less than 0.5. The two populations were combined for statistical analysis.

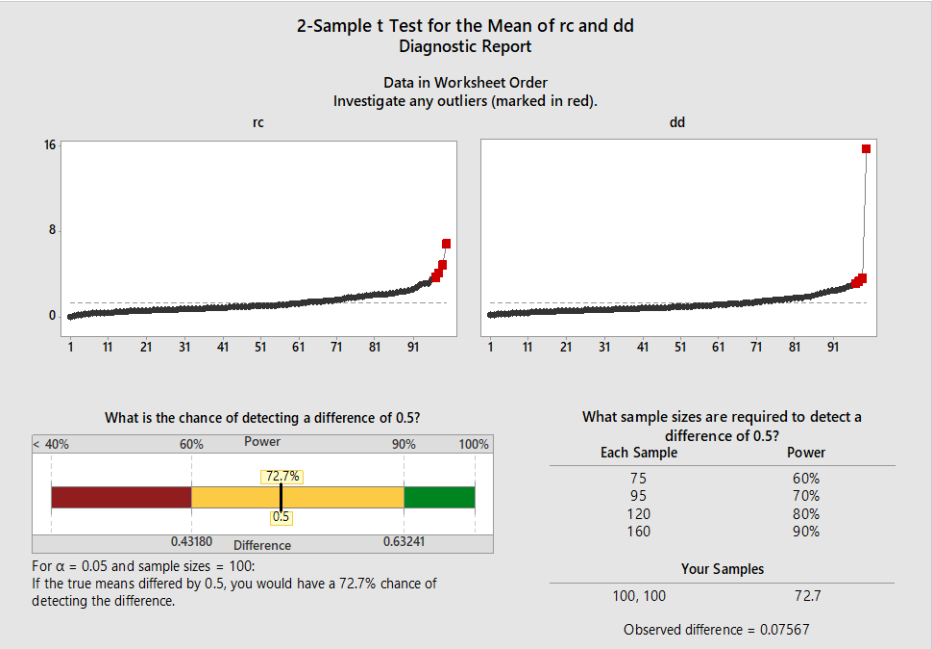

Figure 5.7. Results of T-test analysis in Minitab showing outliers and the probability of detecting the difference between sample mean.

5.4.2. Data distribution analysis

A normality test was run by plotting a histogram and a probability plot to know the kind of distribution the data follows and the spread of data values. A total of 821 composite samples were used and the distribution was positively skewed. It was therefore necessary to separate the data into homogenous domains. The probability plot testing for normality showed that it did not come from a distribution of the same type because the points departed substantially from the line pattern. A P-value of <0.005 recorded shows that it did not follow a normal distribution. The histogram plot of the whole population is shown in Fig. 5.8a.

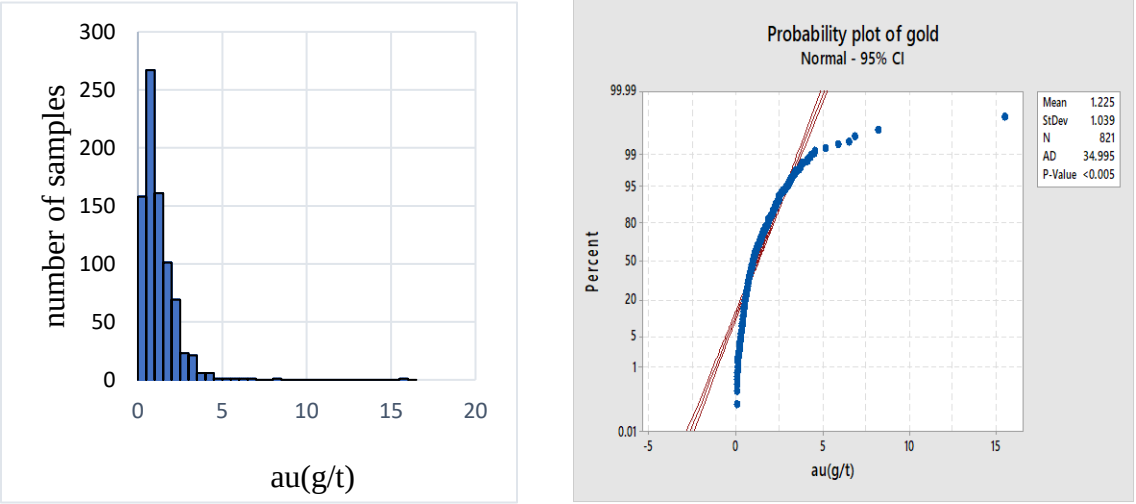

(a) (b)

Figure 5.8. Data distribution analysis (a) Histogram plot of sample data (b) Cumulative probability plot showing a skewed distribution with data points deviating from line of best fit.

In Fig. 5.8b above, it shows that the population must be separated into homogenous domains to establish the correct type of statistical distribution. Boundary analysis was used to help correct this error of mixed populations.

5.5. Boundary analysis

The partitioned reefs formed three different domains as this is evident in Fig.5.9. The domains are classified as Domain1 (D1), Domain 2 (D2) and Domain 3 (D3). The samples within the ore zone were classified separately from an area with no gold concentration, these samples are considered as waste.

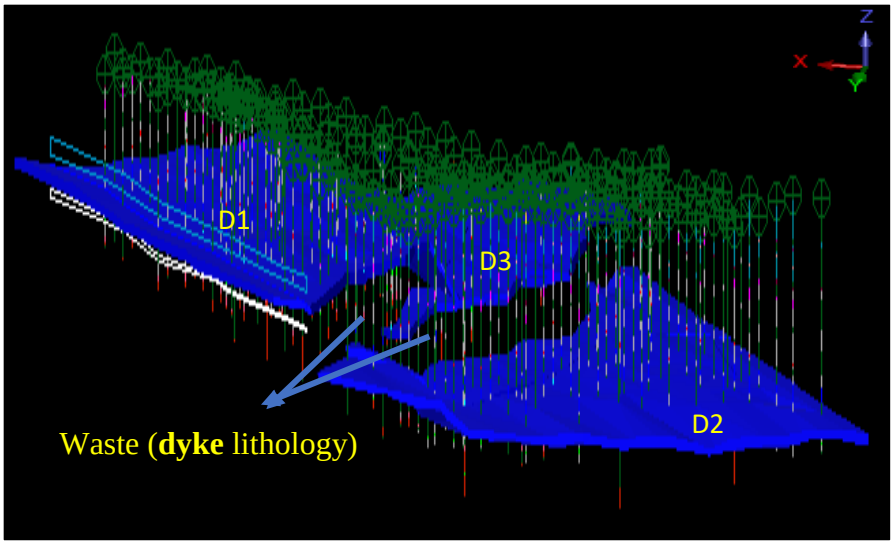

Figure 5.9. A1 Reef partitioned into three domains (D1,D2,D3) due to fault is shown.

The grade variations across boundaries were investigated to justify the existence of hard boundaries as shown in Fig. 5.10 and Fig.5.11. The lag distances at the left hand side of the boundary is displayed in negative values and the lag distances at the right hand side of the boundary are displayed as positive values.

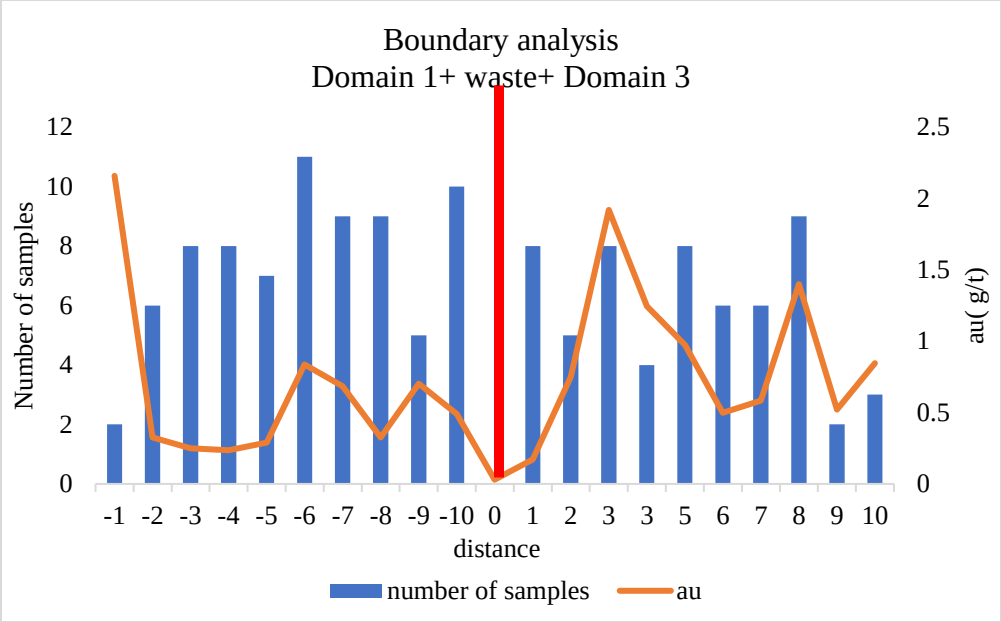

Figure 5.10. Boundary analysis showing an abrupt variation in grade values between Domain 1 and Domain 3 (Domain 1+waste+Domain 3)

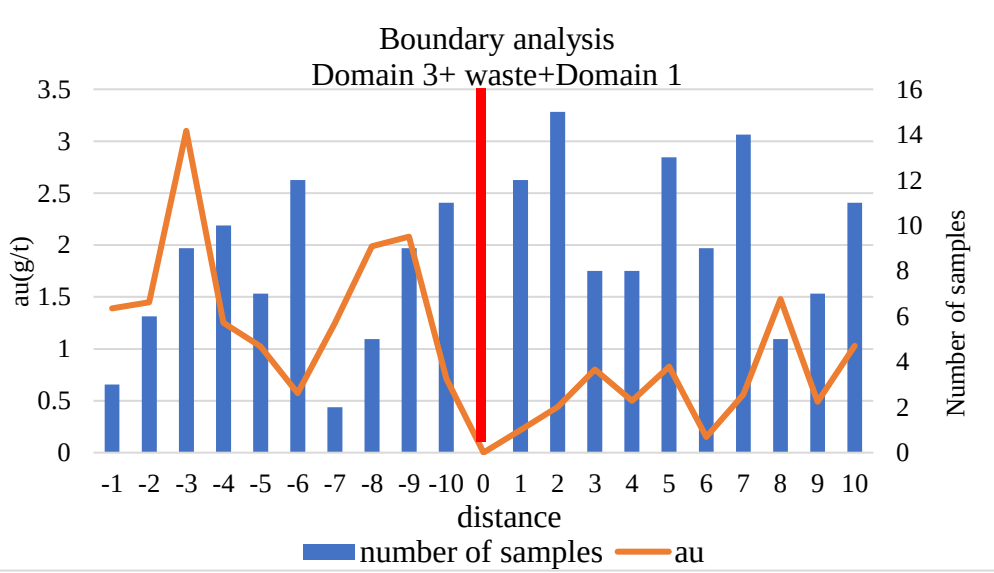

Figure 5.11. Boundary analysis showing an abrupt variation in grade values between Domain 1 and Domain 3 (Domain 1+waste+Domain 3)

5.6. Domain distribution analysis

The domain distribution of the gold mineralization plotted was characterized by positively skewed distribution as is expected for gold [42]. This implies that the sample population contains many low values and relatively very few high values. The positive skewness is confirmed by the histogram of gold grades for the various ore zones. Histogram of gold grades and probability plots are shown in Fig. 5.12. for Domain 1. Appendix B.1 shows the sample plot for Domains 2 and 3. Probability plots showed a p- value less than 0.005.

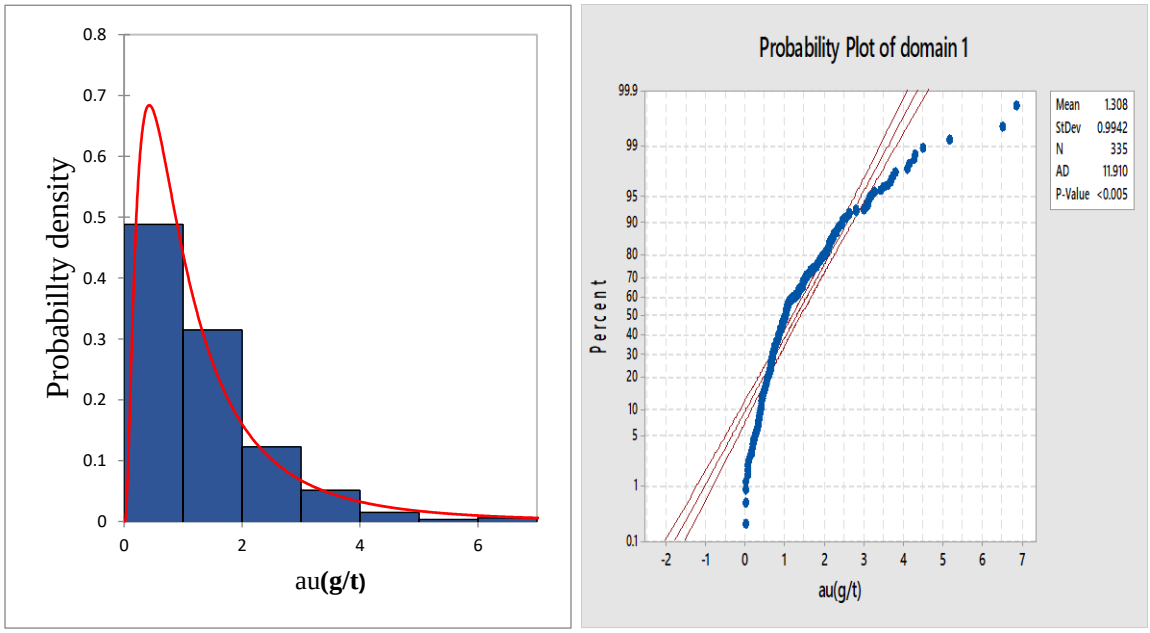

(a) (b)

Figure 5.12. Domain 1 distribution analysis (a) A histogram showing positively skewed distribution for Domain 1 (b) A Probability plot of Domain 1 showing some few outliers.

5.6.1. Data transformation

Many problems arise when dealing with skewed distributions and a more preferred distribution is the normal or the Gaussian distribution. This is because there are many values at the opposite side of the tail for a skewed distribution. This discrepancy causes an imbalance in the frequency of sample values thereby rendering the estimation biased.

Thus, the assay values for gold followed a lognormal distribution and the original data values from the respective domains were transformed by finding a logarithm of the gold value (au).

This is expressed mathematically as [42]:

$au_{normalise} = \ln (au)$

where (5.1)

In is natural logarithm

Au value of gold in grams per tonne (g/t)

To illustrate the use of the transformations for the variables, another graph showing the logarithm of the gold grade of Domain 1(Fig. 5.13a) was plotted. A similar plot was generated for Domains 2 and 3 (see Appendix B.2).

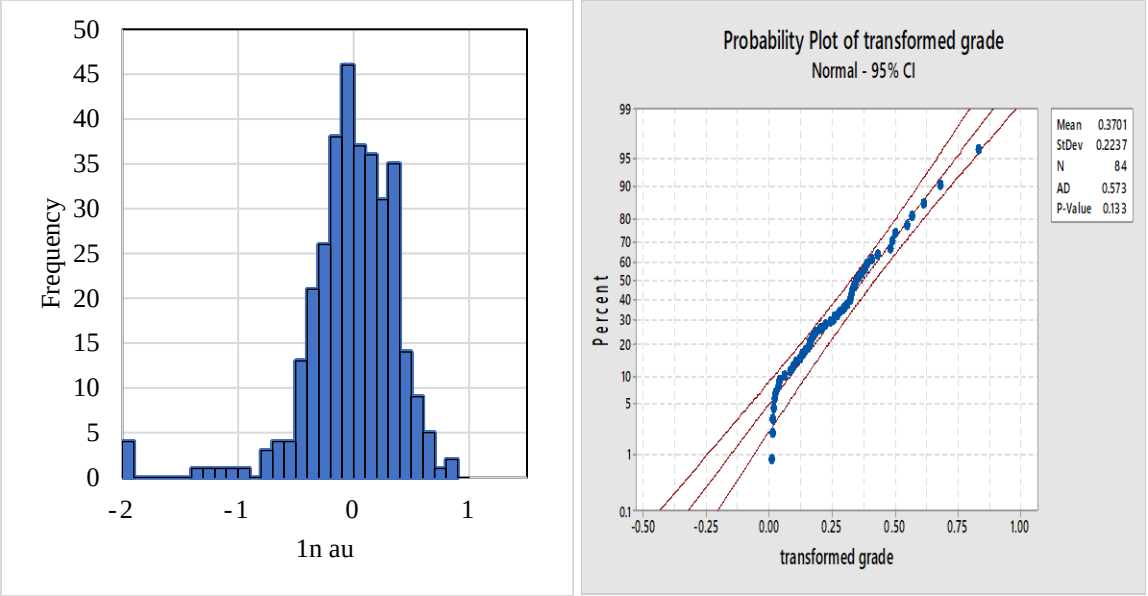

(a) (b)

Figure 5.13. Log distribution analysis (a) Log transformed histogram plot of Domain 1 (b) Log transformed probability plot of Domain 1

In all domains, the level of confidence increased when the probability plots (Fig. 5.13b) tested positive to normality. A P-value greater than 0.005 was recorded and 90% of data points rested near the trend line with few outliers.

5.6.2. Removal of outliers

Data values that were somewhat distant were removed in the domains to produce a robust variogram for geostatistical analysis [22, 42]. There are many methods (histogram plots , confidence interval and percentile) that can be used to determine a top cut value, but in this project Minitab Outlier test tool (Grubb test), histogram plot and geological information of the gold deposit were used to identify outlier values. The variance of all the three domains were low and grade capping was not considered necessary. However, based on geological

information from previous mine grade control estimates and sedimentological logging, a value of 5 g/t was chosen. Surpac tool was also used to remove extreme values by generating codes to cut and cap them to 5g/t as shown graphically in Fig. 5.14. A similar analysis was performed for Domain 2 and 3 (see Appendix B.3).

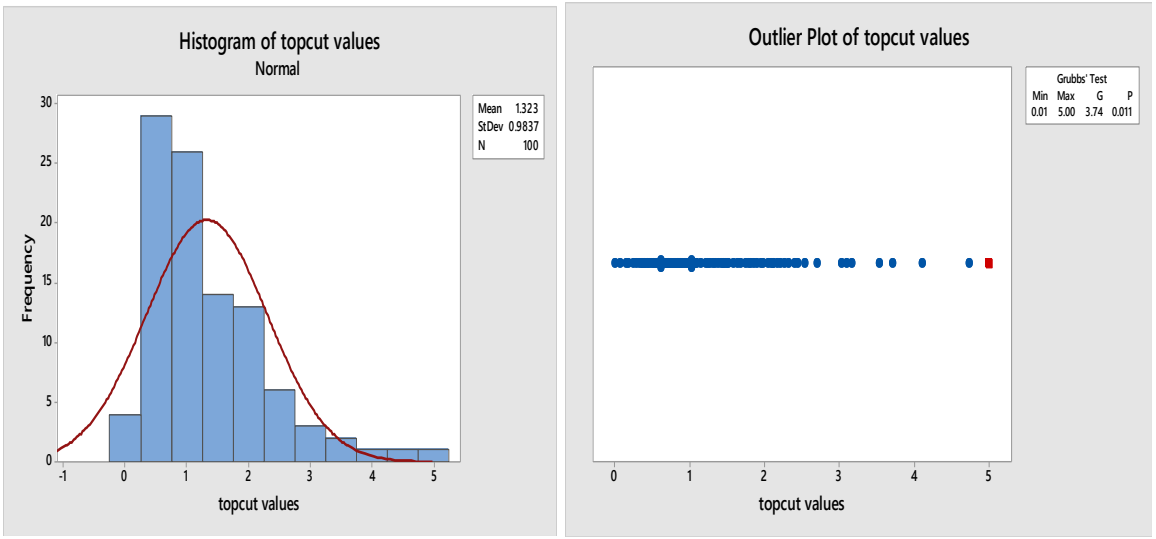

(a) (b)

Figure 5.14. Removal of outlier analysis (a) Histogram of capped gold grades (b) Plot of outlier test results (domain1)

5.7. Variogram analysis

The semi-variogram was used to measure the spatial trends in the data. The composited geological data was imported into Surpac for geostatistical analysis. Grades were not estimated for the waste domain and therefore no variograms were computed for it.

Downhole semi-variograms for downhole samples were also generated with a nugget of 0.26 g/t in the vertical direction (90^{o}) as shown in Fig. 5.15. Semi-variograms were

generated for all three (3) domains and lag sizes were generally kept close to the drill spacing of 25 m to capture sample variance. The resulting semi-variogram is usually erratic if lag distances are not close to sample spacing. Three semi variograms were produced to correspond to the three principal directions being downhole (minor), along dip (semi-major) and strike (major).

Domain 3 variograms obtained for Reef A1 was not robust due to the lack of data pairs in the domain. Conversely, Domains 1 and 2 had a very strong semi-variogram which was considered to a good representation of the global semi-variogram structure.

The orientation used for the variogram computation is specified together with a summary of the data values masked for variogram calculation. The longest direction of continuity was generally along the eastings(X) (rotated to match the strike of mineralization) with the intermediate direction of continuity along the Y axis (rotated to match the down dip direction of mineralization). The sill value representing the population variance of the ore grade data recorded a maximum value of 1. The Nugget effect for the reef variograms were generally 27% (Co =0.27) of the sill (Co+C) as shown in Table 5.4 and Table 5.5. Ranges along strike (direction of maximum continuity) were shorter because of the continuity of the ore body and the less variability between grade values. It mostly varied from 28 m to 100 m and 90 m to 160 m for structure 1 and 2 (nested) respectively along strike. The range for the shortest direction of continuity (were perpendicular to the reefs), was between 2 m and 3.5 m. In all three (3) domains, it exhibited geometric anisotropy with a sill value of 1 and different ranges along various directions. This is expected to be the case and thus justifies the validity of the semi-variogram models.

The combined experimental and modeled downhole variograms (90 degrees) in all three directions for each domain are presented graphically below (Fig. 5.15). The major and semi-major anisotropic ratios describe the relationship between the principal directions. The two variogram maps were extracted along the minor axis to generate the anisotropic ratio and the kriging parameters for the estimation process. The individual variograms, showing more detail and the experimental data from which, the models were generated, is presented in Fig. 5.16. See Appendix D for other 2-D and other directional variograms.

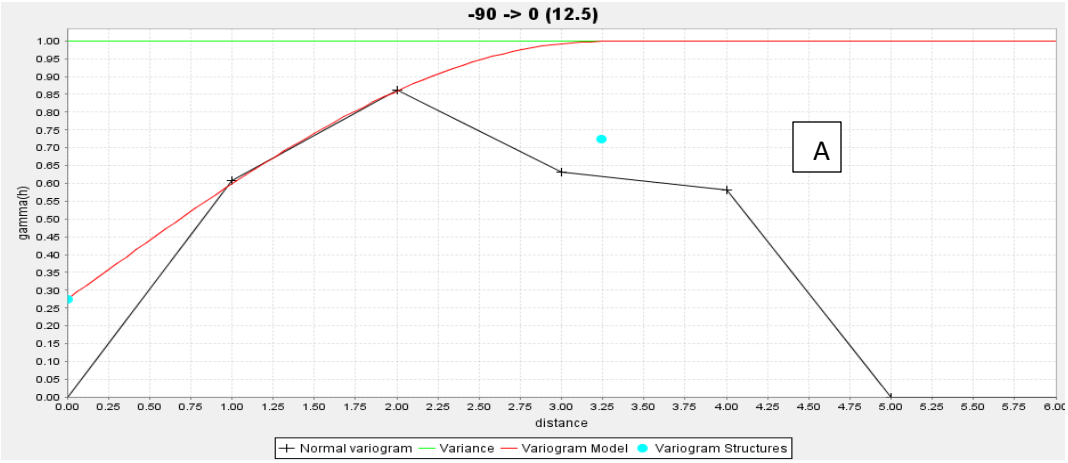

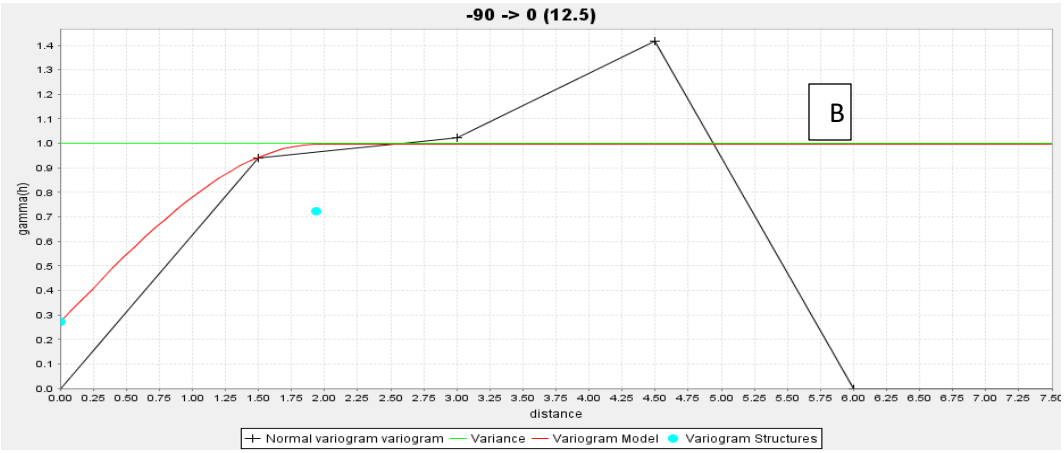

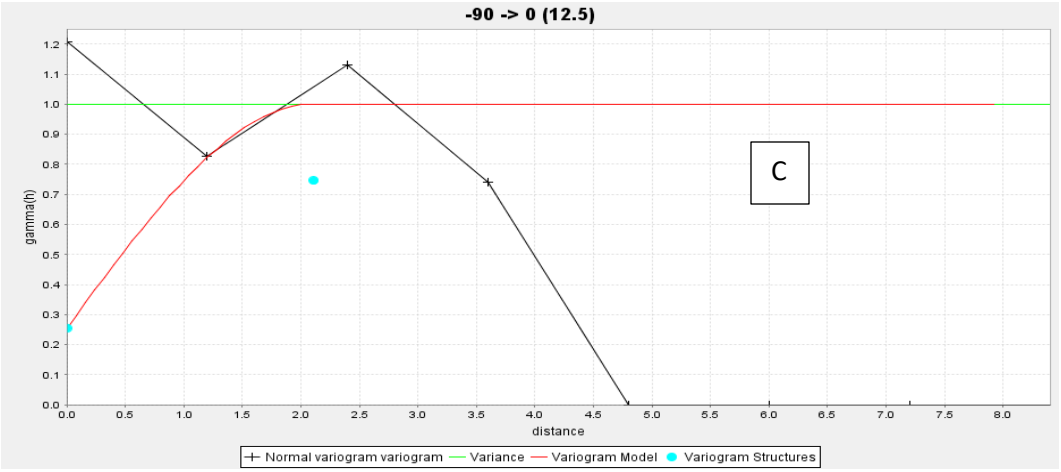

(c)

Figure 5.15. Downhole variograms for 90^0 direction (a) Downhole variogram of Domain 1 (b) Downhole variogram of Domain 2 (c) Downhole variogram of Domain 3

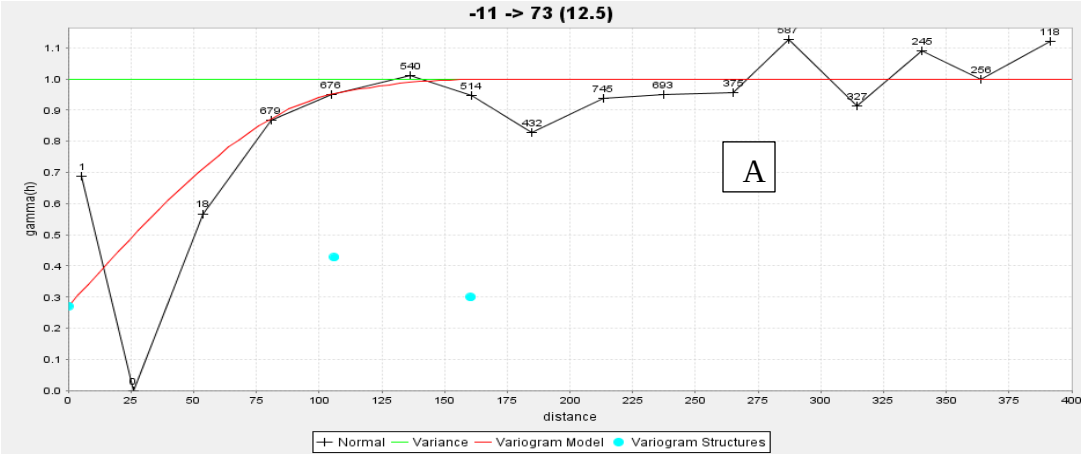

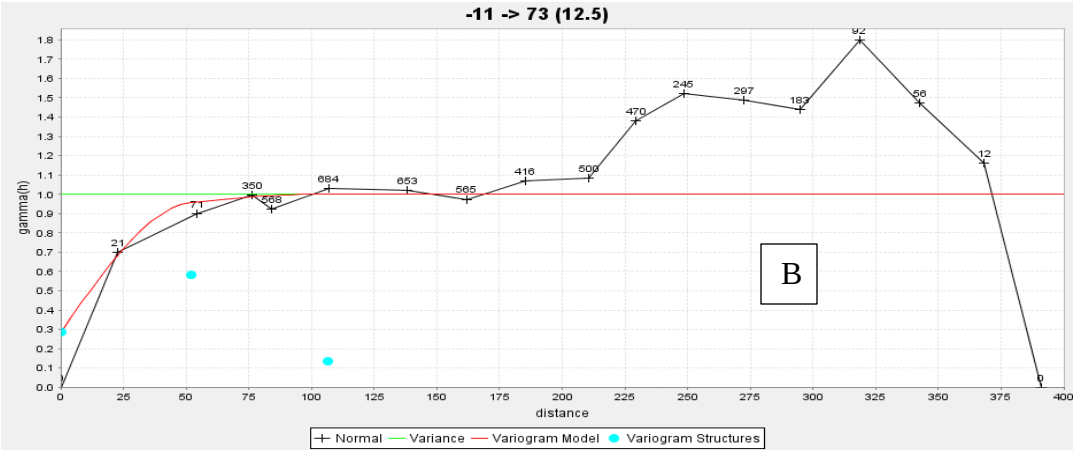

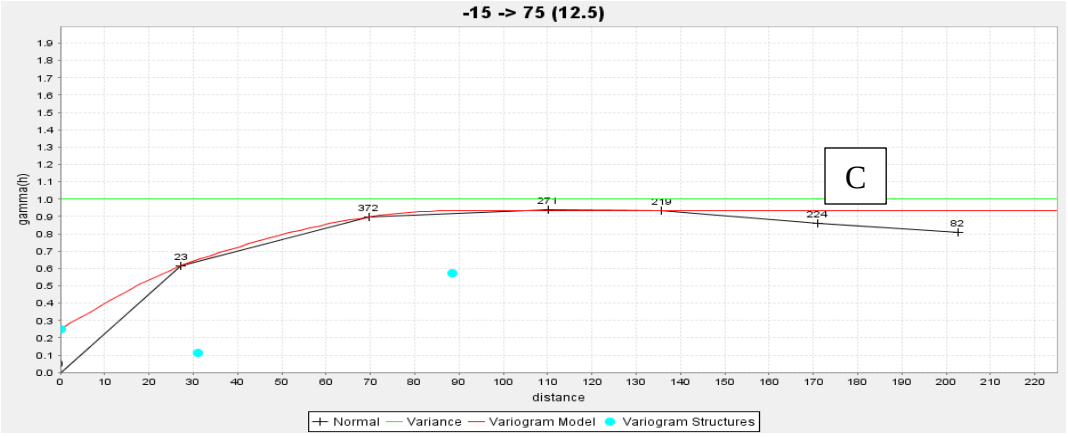

Figure 5.16. Semi-variograms (a) A1 Reef semi-variogram of Domain 1 along 71º (b) A1 Reef semi-variogram of Domain 2 along 73º (c) A1 Reef semi-variogram of Domain 3 along 80º

Table 5.4. A1 Reef semi-variogram parameters for all domains (minor)

Domain	Azimuth	Dip	Spread	Spread Limit	Nugget(C_o)	C	Range
1	0	-90	12.5	25	0.27	0.72	3.25
2	0	-90	12.5	25	0.27	0.72	1.9
3	0	-90	12.5	25	0.25	0.75	2.109

Table 5.5. A1 Reef semi-variogram parameters for all domains (major)

Domain	Summary	Azimuth	Nugget(C_O)	C_1	C_2	r_1	r_2
1	Major	71	0.27	0.43	0.29	106.1	160.409
2	Major	73	0.27	0.58	0.13	52	107
3	Major	75	0.25	0.11	0.62	28	91

5.7.1. Alternative case

To evaluate the importance of dividing the data into domains, semi-variograms for the A1 Reef without the definition of domains was modelled (with inclusion of waste material), cross validated and the results compared to the separated geological data. The semi-variogram model for A1 Reef with all three domains combined is shown in Fig. 5.17 with its corresponding parameters in Table 5.6.

Table 5.6. A1 Reef semi-variogram parameters for reef - no domains

Domain	Summary	Azimuth	Nugget (C_O)	C_1	C_2	r_1	r_2
No domaining	Major	81	0.69	0.10	0.22	64.5	169

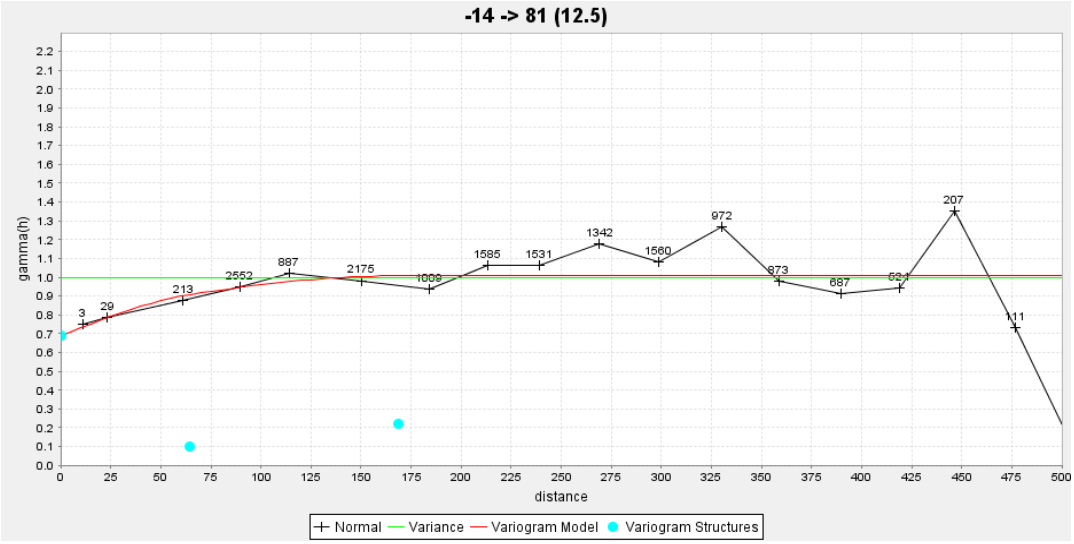

Figure 5.17. A1 Reef semi-variogram of A1 Reef along 81^{o} with 3 Domains combined

The nugget for the alternative case increased more than 40 % (0.69) as compared to the domained reefs. Prior to variogram validation, this observation is an indicator of less robust estimates for A1 Reef when all three geological domains are combined. Thus, the randomness introduced makes prediction of unsampled locations more difficult and biased.

5.8. Cross validation

The estimation of unsampled locations depends heavily on the semi-variogram model as the representation of the true spatial structure for that measurement in that area. The kriged estimates were cross validated to justify the precision of the semi variogram model. The estimated block grades were compared to the true grades in this process. The true grades (actual sample measurements) in this case were analogous to the composite grades because grade compositing was done every 1 m to reduce spatial variability. In this process, a sample from the data set was removed and re-estimated using the remaining samples [43].

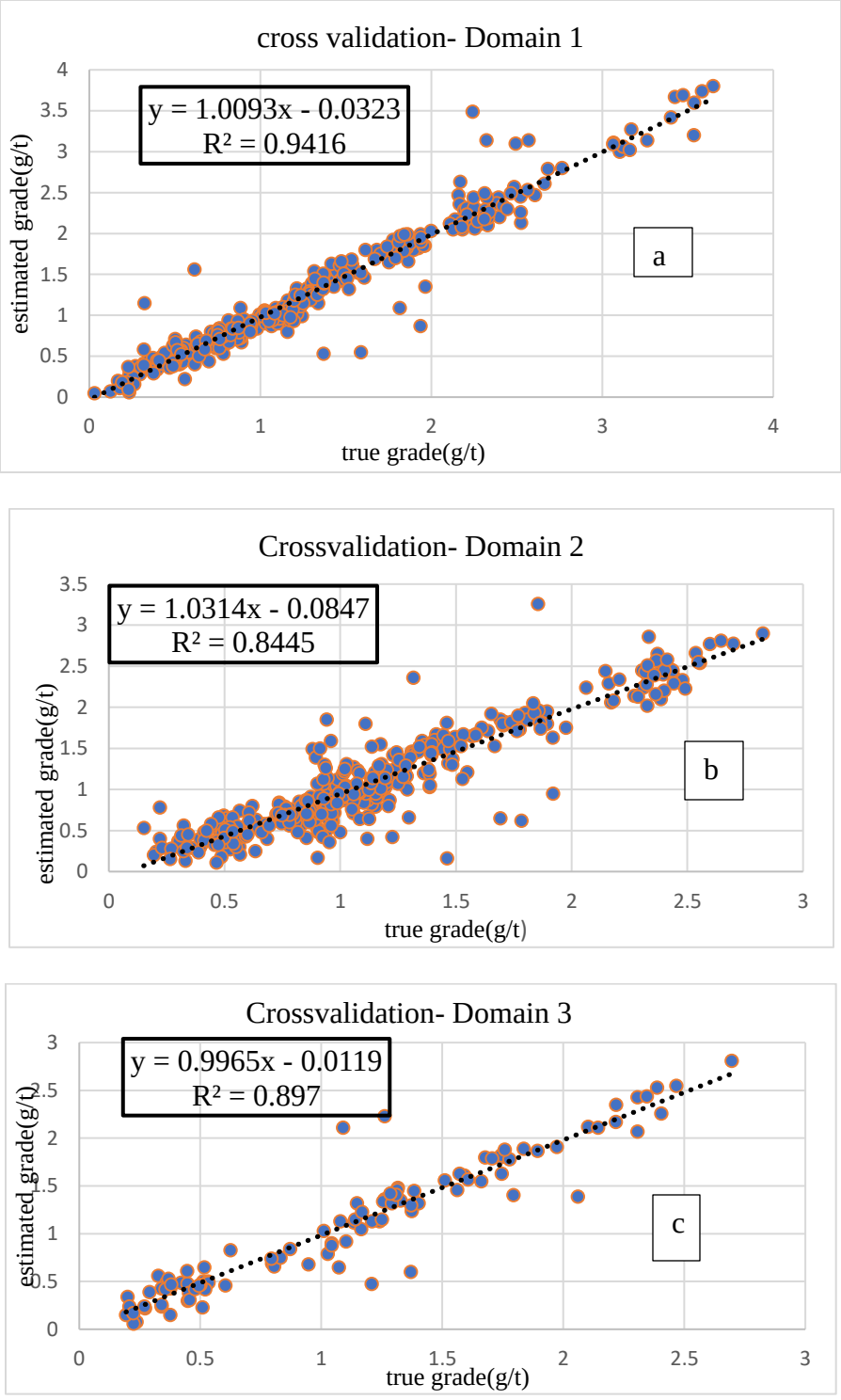

Figure 5.18. Cross validation plots (a) Scatter plots of Domain 1 (b) Scatter plots Domain 2 (c) Scatter plots of Domain 3

The model showed a robust coefficient of determination greater than 0.84, signifying limited over smoothing during the estimation process as shown in Fig. 5.18.

For the alternative case, the coefficient of determination dropped to 0.39 (Fig.5.19) with results largely impacted by high nugget effect of 0.7.

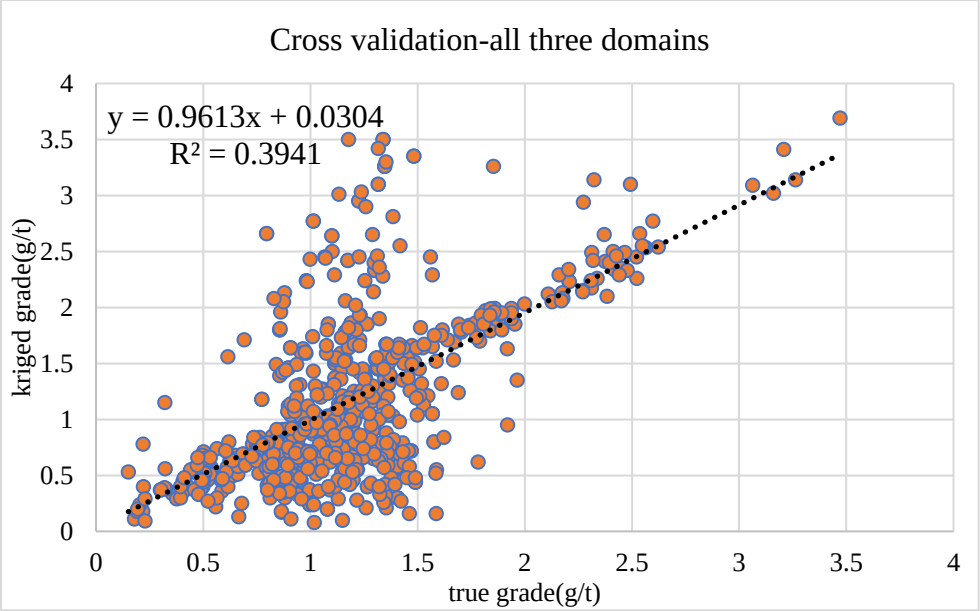

Figure 5.19. Scatter plots of true grades on estimated grades (three combined domains)

CHAPTER 6

BLOCK MODELLING AND RESOURCE ESTIMATION

6.1. Block modelling

A sub-celled Blockmodel was generated for the updated portion of the model with the parent block size equal to the optimal block size of 10 m by 10 m by 3 m. The number of discretization points was set to 3 for x, y and z. This means that 27 sub-blocks were created and the mean grades for the sub-blocks were assigned to the block. The limits of the data guided the choice of the Blockmodel extents and later filled with attributes (Table 6.1.). Fig. 6.1 shows a constrained A1 Reef estimated model colored by grade range.

Table 6.1. Blockmodel summary

BLOCKMODEL EXTENTS			
	x	y	z
Minimum	7650	9750	35
Maximum	8150	10050	175
User block size	10	10	3
Minimum block size	10	10	3
ATTRIBUTES	DESCRIPTION		
au_ok	OK		
Sg	specific gravity		
Reef	Mineralized ore zone		

6.2. Grade interpolation

A specific gravity of 2.65 was used for tonnage calculation. This may deviate a little from the actual value but was still maintained for tonnage calculation.

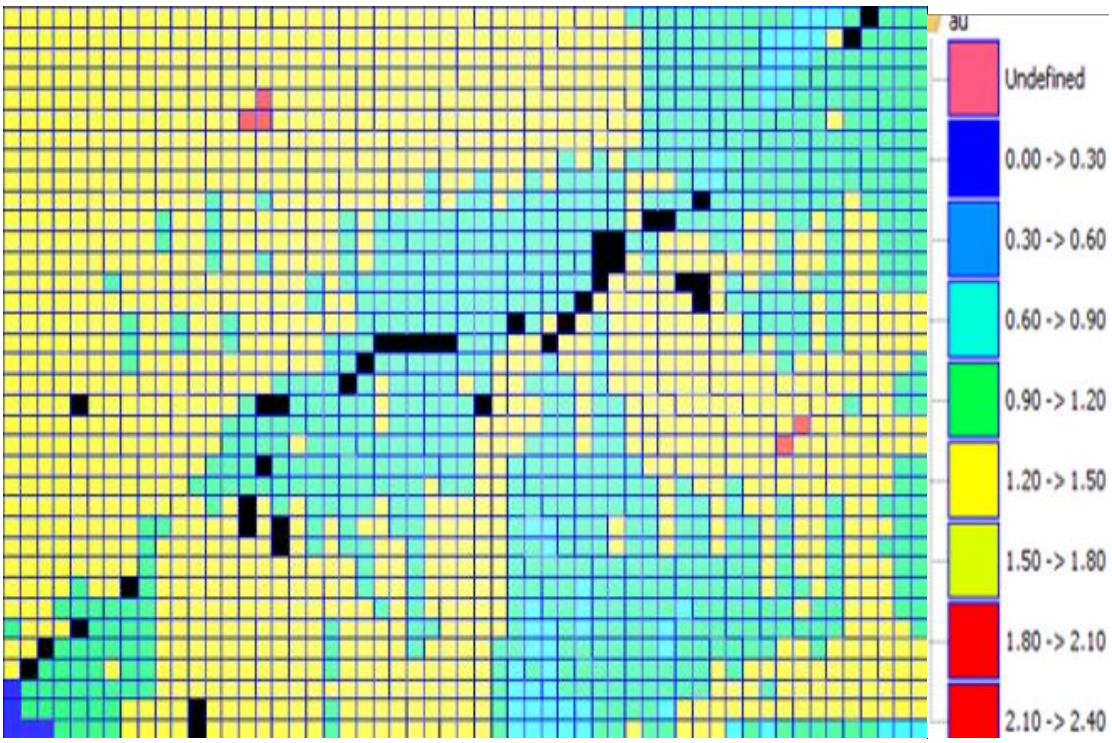

Figure 6.1. Blockmodel of the project area colored by grade range (Black dots show the graphic workspace).

Table 6.2. OK estimates of A1 Reef

Domain	Volume(m^3)	Sg	Tonnes	Grade(g/t)
1	270600	2.65	717090	1.383
2	343200	2.65	909480	1.206
3	99300	2.65	263145	1.148
Total	**713100**	**2.65**	**1889715**	**1.262**

6.3. Blockmodel validation

The Blockmodel was validated to assess the confidence of the mineral estimates. The validation methods used include:

i. Comparing model values to alternative technique

The 3 domains were combined omitting the waste material and used for further analysis. Blockmodel estimates using IDW were interpolated into the Blockmodel and compared to the OK estimates since it has been established as a way of validating OK estimates [11]. IDW is more biased as compared to OK but its serves as an alternative estimation technique in Goldfields Ghana Limited for resource estimation and OK validation. Fig. 6.2 shows the regression plot with a coefficient of determination of 90%. This indicates that underestimation of high grade blocks has been controlled and the confidence of the estimates is very high.

In addition, the estimated grades for both methods were compared to each other on every 3m bench elevation (Fig. 6.3) which recorded a mean grade of 1.25g/t and 1.23g/t for OK and IDW respectively.

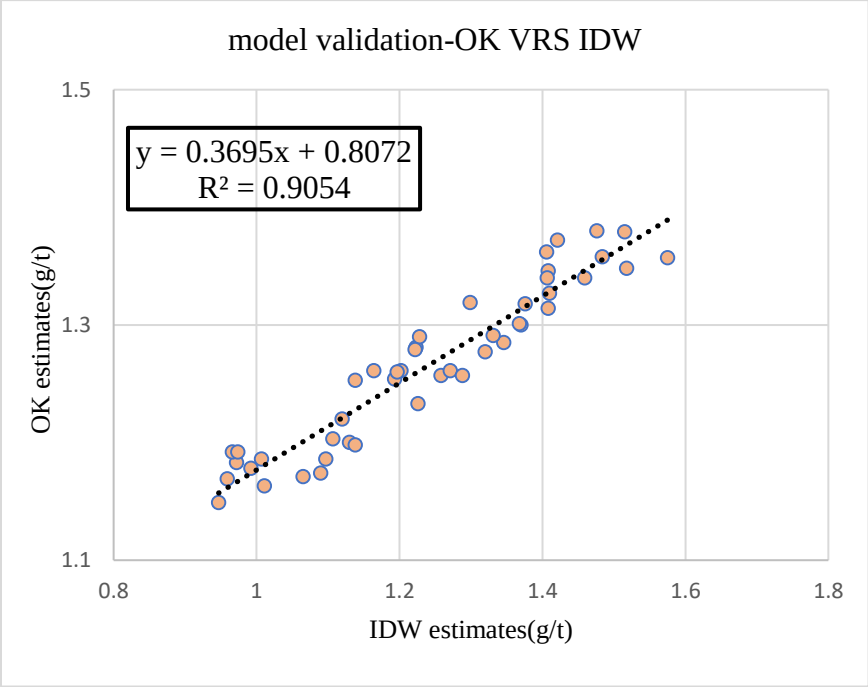

Figure 6.2. Scatter plots of OK estimates vs. IDW estimates (positive correlation)

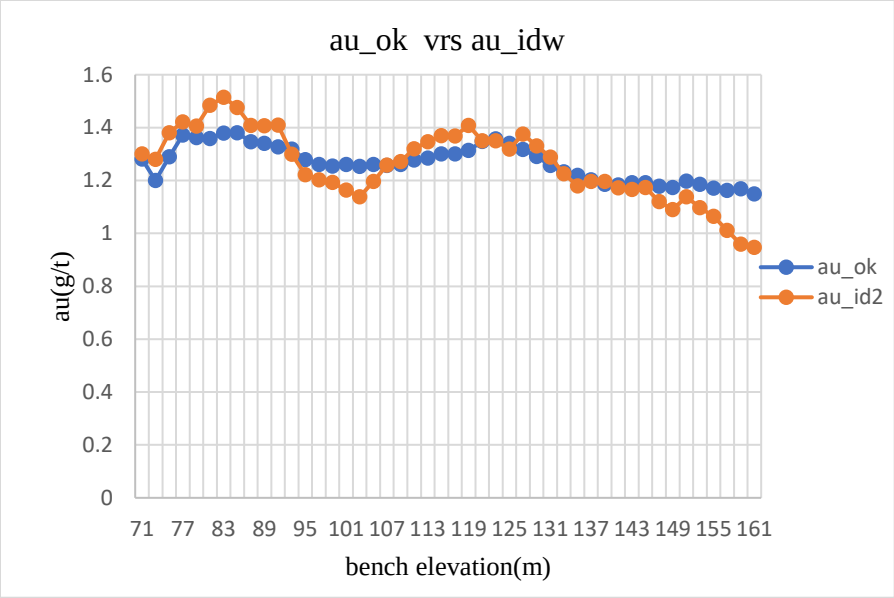

Figure 6.3. Comparison of grades (au_OK vs. IDW) on different elevation

ii. Basic statistics of model values

The grade distribution of the block estimate (Fig. 6.4) showed a normal distribution with a mean grade of 1.262g/t. The normal grade distribution proved that there is no clustering of data values that could result in overestimation or underestimation. The table below summarizes the Blockmodel descriptive statistics.

Table 6.3. Blockmodel estimates statistics

number of samples	Minimum(g/t)	Maximum(g/t)	mean(g/t)	std. deviation
2396	0.001	1.969	1.262	0.203

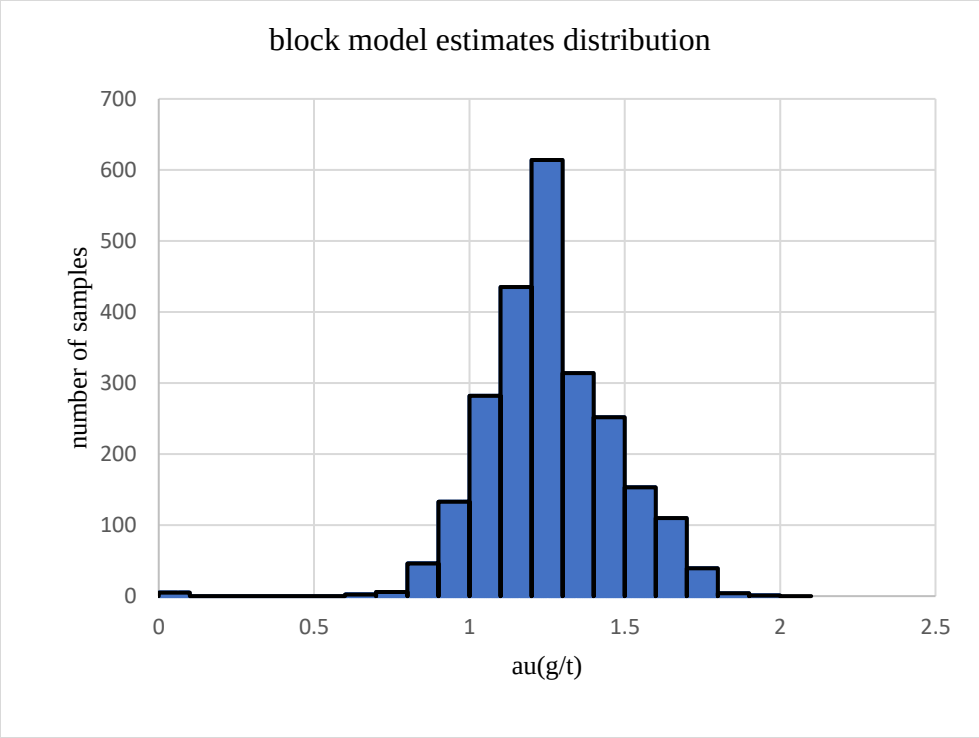

Figure 6.4. Histogram of Blockmodel estimates (normal)

iii. Trend analysis

A comparison of the estimated block values with the composite data (true values) was analyzed. The essence of this was to identify areas where the composite data compared well with model values and vice versa.

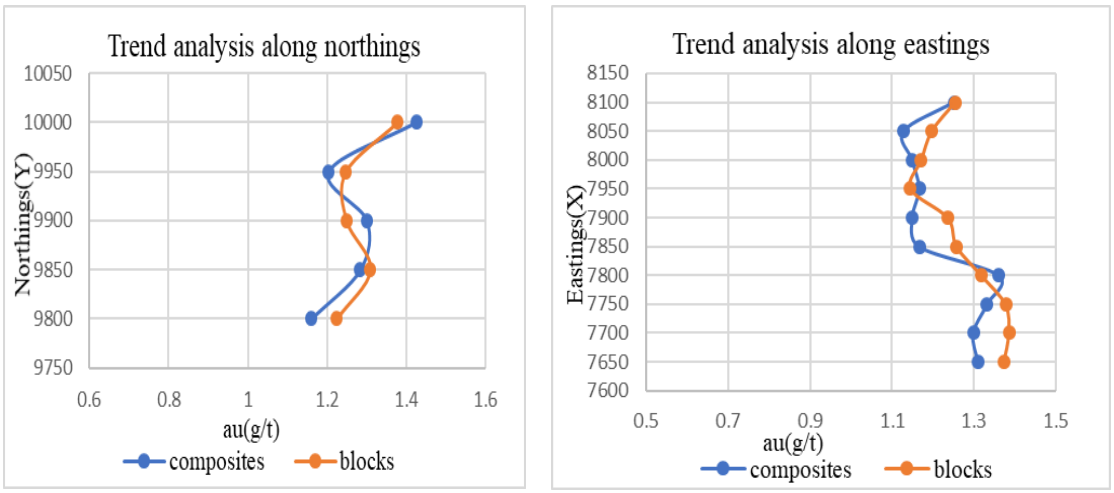

Figure 6.5. Trend analysis (a) Comparison of composite data to Blockmodel values along northing direction (b) Comparison of composite data to Blockmodel values along easting direction

The comparison was made along two principal directions i.e. eastings and northings as shown in Fig. 6.5. The linear relationship between true values (composites) and Blockmodel values, along eastings and northings were determined using a scatterplot with a Coefficient of determination 0.93. This showed a strong relationship between the two variables and expressed below in Fig. 6.6.

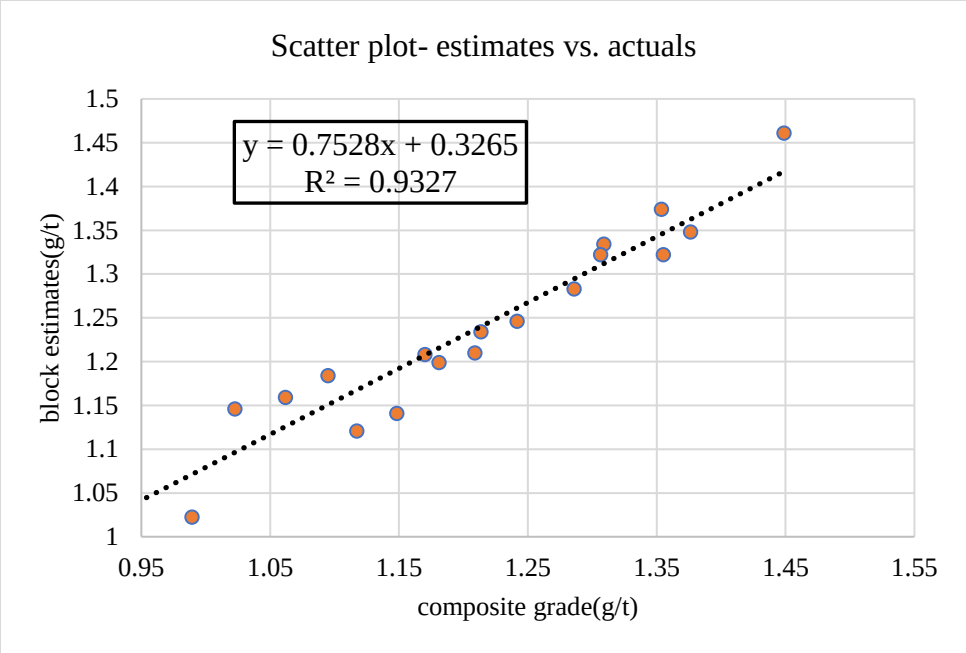

Figure 6.6. Scatter plot of block estimates on composites along eastings (7650E-8150E)

6.4. Risk Assessment

Table 6.4 outlines the evaluation of the risk associated with the various processes and steps involved in generating the geostatistical resource estimate for A1 Reef as a representative example for all the structural domains. This is in accordance with the current JORC Code published in 2012 [44].

Table 6.4. Risk assessment

Item	Comments
Database integrity	The drillhole database was provided by Goldfields Ghana Ltd. for this project was audited and passed all database validation checks. **Low risk**
Quality of assay data	The laboratory accuracy is acceptable with no significant sample contamination. Quality assurance quality control checks were put in place to ensure the reliability and credibility of reported grades from assay. All checks were done by Goldfields mineral resource team and a separate report (confidential) capturing all the standards used in assay showed that there was no significant sample contamination. **Low to moderate risk**
Bulk density	A fixed bulk density value of 2.70 t/m^3 was used for tonnage calculation. This might deviate a little as mostly the bulk density values range from 2.50 to 2.70 t/m^3. This may affect tonnage results by 10% to 20%. **Moderate risk**
Geological Interpretation	Geological continuity is good except areas disrupted by faults. An overall exploration (from mapping and literature) to grade control showed similar models and this helped significantly in the definition of geological domains prior to geostatistical estimation. **Low risk to moderate risk**
Estimation and modelling techniques	Semi-variograms were modeled for each domain for A1 Reef. Optimal estimation parameters were determined and used in building a robust strong model. OK was used for estimation as the number of assay data available was sufficient to generate a reliable estimate using OK. The Blockmodel estimates were validated using IDW Other validation tools were done by comparing block values to

	composite values, basic statistics and semi-variogram cross validation. **Low risk**

CHAPTER 7

CONCLUSION AND RECOMMENDATION

7.1. Conclusions

The major findings of this research, conclusions and recommendations are as follows**:**

- It can be concluded that the original data sample values followed a lognormal distribution with high concentration of low grade values.
- Geological interpretation of the orebody helped in the definition of geological domains. A normal fault partitioned the main reef into different domains with an abrupt variation of grades along the contact when boundary analysis was carried out.
- Domaining and statistical analyses are very important in mineral resource estimation and a good data analysis will result in an unbiased estimated and a smoothed grade interpolation. Detailed statistical investigation will reveal the data properties and statistical trends within a domain.
- Information gained from the nature of grade distribution will assist in choosing an appropriate estimation model.
- An alternative case was also analyzed on A1 Reef without geological domains. Correlation between true and kriged grades was low. This is due to the intrusion of waste (thrust fault) and high nugget as manifested in the semi-variogram model.

- The total Blockmodel estimates were validated with composite data, IDW estimates with a perfect normalized distribution. The correlation coefficient in all domains was greater than 82%.
- The total tonnes for the A1 Reef was 1889715 tonnes with an average grade of 1.262 g/t as estimated using OK.

7.2. Overall recommendations

- The hard boundaries defined in this research should be used as a standard model to partition drillhole data in the Akontasi central pit to form homogenous domains.
- Mineral resource estimation should always be performed within these homogenous domain boundaries to improve estimates and if possible used further to validate other grade control estimates.
- The methodology adopted in this research project should be extended as a standard operating procedure for other portions of the deposit during geostatistical analysis.

7.3. Recommendations for future work

- A follow up analysis is recommended to investigate the existence of soft boundary for the same type of deposit and how geological variables like grade, thickness and accumulation will help in the definition of domains.
- Since the best validation tool is the comparison of estimated data to raw data, mineral resource estimates can be compared to mine production data for reconciliation purposes and to quantify the level of conditional bias.

- Another analysis should be made on block size optimisation. This will help to select the optimal block size for mineral resource estimation. Alternatively, other estimation techniques like Simple Kriging and Indicator Kriging can be used to test the level of confidence of block estimates [12].

REFERENCES

[1] David, M., "Geostatistical Ore Reserve Estimation", pp. 364, 1977.

[2] Karpeta, W. P., "A Review of the Geology, Mining and Exploration of the Tarkwa Mine Area", Ghana Goldfields Ghana Ltd., Ghana, pp. 225, 2000.

[3] Hirst, T., "The Geology of the Tarkwa Goldfields and adjacent country", Gold Coast Geological Survey, Bulletin No.10, 1938.

[4] Griffis, R.J., and Agezo, F.L, "Gold deposits of Ghana", Mineral Occurences and Exploration potential of Northern Ghana., Ghana Minerals Commission Report, Accra, pp. 132, 2002.

[5] Davis, D.W., Hirdes,W., Schaltegger, U., and Nunoo, E.A, "U-Pb age constraints on deposition and provenance of Birimian and gold-bearing Tarkwaian sediments in Ghana", West Africa, Ghana Accra, Precambrian Res 67, pp. 89–107, 1994.

[6] Junner, N. R., Hirst, T., and Service, H., "The Tarkwa Gold, Gold Coast Geological Survey Memoir", Vol. 3, No. 6, Accra, pp.75, 1942.

[7] Sestini, G., "Sedimentology of a paleoplacer: the gold-bearing Tarkwaian of Ghana", in: Amstutz GC, Bernard AJ (eds) Ores in sediments. Springer, Berlin Heidelberg New York, pp.275–305, 1973.

[8] Strogen, P., "The sedimentology, stratigraphy and structure ofthe Tarkwaian, Western Region, and its relevance to gold exploration and development", In: Proc Int Conf. Geology of Ghana with Special Emphasis on Gold, Accra, 1988, pp. R/1–R/39, 1988.

[9] Hirdes W. and Nunoo, B., "The Proterozoic paleoplacers at Tarkwa Gold Mine, SW Ghana: sedimentology, mineralogy, and precise age dating of the Main Reef and West Reef

and bearing on the investigations on the source area aspects". In: Oberthu¨r T (ed) Metallogenesis of selected gold deposits in Africa. Geol Jahrb pp. 247–311, 1994.

[10] Kesse, G. O., "The Rock and Mineral Resources of Ghana", Ballkema Publishers, Rotterdam, Netherlands, pp. 610, 1985.

[11] Lonrho Ltd., "Tarkwa and Abosso Mines, feasibility study". Ministry of Lands and Mineral Resources, Accra, 1974.

[12] Journel, A.G. and Huijgregts, C.J., "Mining Geostatistics", Academic Press, London, pp. 600, 1978.

[13] Isaaks, E.H. and Srivastava, R.M., "An introduction to applied geostatistics", Oxford University Press, New York, pp. 561, 1989.

[14] Goovaerts, P., "Geostatistics for natural resources evaluation", Oxford University Press, New York, pp. 483, 1997.

[15] Royle, A.G., "How to use geostatistics for ore reserve classification", World Mining, Vol. 30, pp. 52–56, 1992.

[16] Matheron, G., "Principles of Geostatistics", Economic Geology, pp.1246-1266, 1982.

[17] Dominy, S.C., Annels, A.E., and Noppe, M., "estimates", In Proceedings of the 8th AusIMM Underground Operators' Conference, 8th AusIMM Underground Operators' Conference, Townsville, QLD, Australia, Vol. 11, pp.77-98, 2002.

[18] Clark, I., "The art of cross-validation in geostatistical applications", APCOM, 19th Proceedings, pp. 211–220, 1986.

[19] Krige, D.G., "A practical analysis of effects of spatial structure and data available and used, on conditional biases on Ordinary Kriging", 5th International Geostatistics Congress, Wollongong, Australia, 1996.

[20] Al-Hassan, S., "Statistical Models", University of Mines and Technology, Unpublished MSc Lecture Notes, Tarkwa, pp. 127, 2011.

[21] Royle, A.G., "How to use geostatistics for ore reserve classification", World Mining, Vol. 30, pp. 52–56, 1992.

[22] Rossi, M.E. and Deutsch, C.V., "Mineral Resource Estimation", Springer Science Business Media, Dordrecht, pp. 332, 2014.

[23] Emery, X., and Ortiz, J. M., "Estimation of mineral resources using grade domains: critical analysis and a suggested methodology", Journal of the South African Institute of Mining and Metallurgy (ISI), 105(4), pp. 247-255, 2005.

[24] Ortiz, J. M. and Emery, X., "Geostatistical estimation of mineral resources with soft boundaries: a comparative study", Journal of the South African Institute of Mining and Metallurgy (ISI), 106(8): pp. 577-584, 2006.

[25] Owusu, S., "Comparison of kriging and Inverse Distance Weighting", University of Mines and Technology, unpublished MSc thesis report, Ghana, Tarkwa, pp. 130, 2011.

[26] Snowden, D.V., "Practical interpretation of mineral resource and ore reserve classification guidelines, Mineral Resource and Ore Reserve Estimation", The AUSIMM Guide to Good Practice, Monograph 23, pp.643-652, 2001.

[27] Matheron, G., "Traité de Géostatistique Appliqué", Vols 1 and 2, 1962.

[28] Deutsch, C.V., “Power point presentation on Boundaries”, University of Alberta, Centre for Computational Gesostatistics, CCG, Canada, Alberta, March 2011. Unpublished document.

[29] Larrondo, P. and Deutsch C.V., “Accounting for geological boundaries in geostatistical modelling of multiple rock types”, In: Leuangthong O, Deutsch CV (eds) Geostatistics Banff, 2004, Vol 1, Springer, November, pp. 3–12, 2005.

[30] Elliot, S.M. and Bywater A., “Reconciliation of the Mckinnons Gold Deposit”, Cobar, New South Wales. Mineral Resource and Ore Reserve Estimation—The AUSIMM Guide to Good Practice. Edwards, A.C. (Ed.). Melbourne, The Australasian Institute of Mining and Metallurgy, pp. 257–268, 1997.

[31] Larrondo, P. F. “Accounting for Geological Boundaries in Geostatistical Modelling Of Multiple Rock Types”. M. Sc. Thesis, University of Alberta, Edmonton, Alberta, 2004.

[32] Marsal, D., “Statistics for Geoscientists”, University of Stuttgart, Stuttgart, 1987.

[33] Dowd, P. A., “Geostatistical Ore Reserve Estimation - A case study on a Disseminated Nickel Deposit. Case Histories in Mineral Deposits Evaluation”, Geological Society Special Publication, London, (Annels, A. E. ed.), pp. 243-256, 1992.

[34] Sinclair, A.J. and Blackwell G.H., “Applied mineral inventory estimation”, Cambridge University Press, New York, pp. 381, 2002.

[35] Krige, D.G., “On the departure of ore value distributions from the log-normal model in South African gold mines”, J.S.A.I.M., South Africa, November 1960, January and August 1961.

[36] Dominy S.C., Annels, A.E, “Geology in the Resource and Reserve Estimation of Narrow Vein Deposits”, Exploration and Mining Geology, Mining Technology IMM Transactions section A,Vol. 6, No. 4, pp. 317-333, 1997.

[37] Glacken, I. M., and Snowden, D.V., “Mineral Resource Estimation, in Mineral Resource and Ore Reserve Estimation-The AUSIMM Guide to Good Practice, pp 189-198, The Australasian Institute of Mining and Metallurgy, Melbourne, 2001.

[38] Elliott, S.M., Snowden, D.V., Bywater, A., Standing, C.A., and Ryba, A, “Reconciliation of the McKinnons Gold Deposit”, Cobar, New South Wales, in Proceedings Third International Mining Geology Conference, Melbourne ,pp 113-122,1997.

[39] Fulton C.H., “Manual of Fire Assaying”; McGraw-Hill Book Company Inc., New York, pp. 54-66, 1929.

[40] Shepard, O. C. and Dietrich, F. W., “Fire Assaying”; McGraw-Hill Book Company Inc., New York, 1940.

[41] Bugbee, E. E. A., “Textbook of Fire Assaying”, 3rd ed.; Wiley, New York, 1948.

[42] Davis, J. C., “Statistics and data analysis in geology”, John Wiley and Sons, New York. pp. 1986.

[43] Journel, A. G. and Rossi M.E., “When do we need a trend model”, Math Geol 22(8), pp.715–738, 1989.

[44] JORC, The Joint Ore Reserves Committee, “Australasian Code for Reporting of Identified Mineral Resources and Ore Reserves (The JORC Code)”, The Australasian Institute of Mining and Metallurgy, Australia Institute of Geoscientists, and Minerals Councils of Australia, pp. 1-43, 20

APPENDIX A

A.1. Drillhole data for geostatistical analysis

Northings	Eastings	Elevation	grade(au)	Hole Id	grade cut
9774.999	8124.999	143.805	0.91	AS0855	0.91
9774.999	8124.999	142.805	0.72	AS0855	0.72
9774.999	8124.999	141.805	0.3	AS0855	0.3
9799.999	8149.992	135.2	0.36	AS0933	0.36
9799.999	8149.992	134.2	1.55	AS0933	1.55
9799.999	8149.992	133.2	1.01	AS0933	1.01
9799.999	8149.992	132.2	1.2	AS0933	1.2
9825.001	8149.993	126.923	0.71	AS0935	0.71
9825.001	8149.993	125.923	1.82	AS0935	1.82
9825.001	8149.993	124.923	3.41	AS0935	3.41
9875.001	8149.996	111.068	0.52	AS0939	0.52
9875.001	8149.996	110.068	2.94	AS0939	2.94
9875.001	8149.996	109.068	1.65	AS0939	1.65
9875.001	8149.996	108.068	2.54	AS0939	2.54
9800	8125.008	137.675	0.85	AS0949	0.85
9800	8125.008	136.675	0.37	AS0949	0.37
9800	8125.008	135.675	1.59	AS0949	1.59
9800	8125.008	134.675	1.63	AS0949	1.63
9825.001	8124.993	130.203	0.88	AS0951	0.88
9825.001	8124.993	129.203	0.79	AS0951	0.79
9825.001	8124.993	128.203	0.87	AS0951	0.87
9825.001	8124.993	127.203	0.1	AS0951	0.1
9850.866	8125.018	120.892	0.68	AS0953	0.68
9850.866	8125.018	119.892	0.82	AS0953	0.82
9850.866	8125.018	118.892	1.59	AS0953	1.59
9850.866	8125.018	117.892	2.29	AS0953	2.29
9875.003	8125.024	114.708	1.05	AS0955	1.05
9875.003	8125.024	113.708	1.64	AS0955	1.64
9875.003	8125.024	112.708	3.35	AS0955	3.35
9875.003	8125.024	111.708	2.33	AS0955	2.33
9949.99	8149.98	92.15	0.99	AS1037	0.99
9949.99	8149.98	91.15	1.64	AS1037	1.64
9949.99	8149.98	90.15	0.82	AS1037	0.82
9949.99	8149.98	89.15	1.14	AS1037	1.14

9975.981	8149.974	84.397	0.94	AS1039	0.94
9975.981	8149.974	83.397	0.78	AS1039	0.78
9975.981	8149.974	82.397	1.26	AS1039	1.26
9975.981	8149.974	81.397	0.4	AS1039	0.4
9900.522	8125.682	109.563	0.3	AS1049	0.3
9900.522	8125.682	108.563	3.1	AS1049	3.1
9900.522	8125.682	107.563	0.73	AS1049	0.73
9900.522	8125.682	106.563	0.72	AS1049	0.72
9924.999	8124.995	102.618	0.46	AS1051	0.46
9924.999	8124.995	101.618	1.19	AS1051	1.19
9924.999	8124.995	100.618	1.67	AS1051	1.67
9924.999	8124.995	99.618	1.04	AS1051	1.04
9950.034	8137.495	93.899	1.07	AS1053A	1.07
9950.034	8137.495	92.899	0.65	AS1053A	0.65
9950.034	8137.495	91.899	0.87	AS1053A	0.87
9950.034	8137.495	90.899	1	AS1053A	1
9975.68	8125.746	88.981	0.53	AS1055	0.53
9975.68	8125.746	87.981	0.24	AS1055	0.24
9975.015	8137.519	87.884	0.94	AS1055A	0.94
9975.015	8137.519	86.884	0.98	AS1055A	0.98
9975.015	8137.519	85.884	0.37	AS1055A	0.37
9975.015	8137.519	84.884	2.64	AS1055A	2.64
10049.985	8149.958	65.284	0.65	AS1137	0.65
10049.985	8149.958	64.284	1.21	AS1137	1.21
10049.985	8149.958	63.284	1.86	AS1137	1.86
10025.001	8124.989	73.803	1.5	AS1151	1.5
10025.001	8124.989	72.803	1.78	AS1151	1.78
10025.001	8124.989	71.803	1.73	AS1151	1.73
10025.001	8124.989	70.803	2.77	AS1151	2.77
10025.001	8124.989	69.803	0.79	AS1151	0.79
9750.04	8099.962	152.468	0.5	AT0805	0.5
9750.04	8099.962	151.468	0.74	AT0805	0.74
9750.04	8099.962	150.468	1.46	AT0805	1.46
9750.04	8099.962	149.468	0.85	AT0805	0.85
9774.996	8099.998	146.305	0.57	AT0807	0.57
9774.996	8099.998	145.305	0.37	AT0807	0.37
9774.996	8099.998	144.305	1.8	AT0807	1.8
9775.004	8074.996	149.717	0.51	AT0823	0.51
9775.004	8074.996	148.717	0.63	AT0823	0.63

9775.004	8074.996	147.717	0.87	AT0823	0.87
9774.997	8050.005	153.067	1	AT0839	1
9774.997	8050.005	152.067	2.66	AT0839	2.66
9774.997	8050.005	151.067	0.91	AT0839	0.91
9774.997	8050.005	150.067	0.46	AT0839	0.46
9775.001	8024.999	156.421	0.2	AT0855	0.2
9775.001	8024.999	155.421	0.71	AT0855	0.71
9775.001	8024.999	154.421	1.18	AT0855	1.18
9775.001	8024.999	153.421	0.79	AT0855	0.79
9825.003	8099.992	132.213	0.84	AT0903	0.84
9825.003	8099.992	131.213	0.87	AT0903	0.87
9825.003	8099.992	130.213	1.16	AT0903	1.16
9850.865	8100.003	123.165	0.53	AT0905	0.53
9850.865	8100.003	122.165	0.44	AT0905	0.44
9850.865	8100.003	121.165	2.95	AT0905	2.95
9850.865	8100.003	120.165	1.03	AT0905	1.03
9875	8099.995	116.166	0.8	AT0907	0.8
9875	8099.995	115.166	3.26	AT0907	3.26
9875	8099.995	114.166	15.5	AT0907	3.5
9875	8099.995	113.166	1.93	AT0907	1.93
9802.364	8074.866	141.591	0.5	AT0917	0.5
9802.364	8074.866	140.591	1.64	AT0917	1.64
9802.364	8074.866	139.591	1.6	AT0917	1.6
9824.998	8074.983	135.105	0.64	AT0919	0.64
9824.998	8074.983	134.105	2.42	AT0919	2.42
9824.998	8074.983	133.105	1.85	AT0919	1.85
9850.868	8075.008	125.492	0.58	AT0921	0.58
9850.868	8075.008	124.492	0.51	AT0921	0.51
9850.868	8075.008	123.492	0.69	AT0921	0.69
9850.868	8075.008	122.492	1.46	AT0921	1.46
9875.001	8075.004	117.719	0.61	AT0923	0.61
9875.001	8075.004	116.719	1.71	AT0923	1.71
9875.001	8075.004	115.719	2.14	AT0923	2.14
9875.001	8075.004	114.719	0.63	AT0923	0.63
9793.361	8050.047	150.044	0.91	AT0933	0.91
9793.361	8050.047	149.044	0.47	AT0933	0.47
9793.361	8050.047	148.044	0.72	AT0933	0.72
9793.361	8050.047	147.044	0.9	AT0933	0.9
9793.361	8050.047	146.044	1.04	AT0933	1.04

9824.99	8049.98	137.772	0.67	AT0935	0.67
9824.99	8049.98	136.772	0.91	AT0935	0.91
9824.99	8049.98	135.772	1.27	AT0935	1.27
9850	8049.98	130.16	0.74	AT0937	0.74
9850	8049.98	129.16	0.29	AT0937	0.29
9850	8049.98	128.16	2.5	AT0937	2.5
9850	8049.98	127.16	1.02	AT0937	1.02
9874.999	8049.98	119.811	0.66	AT0939	0.66
9874.999	8049.98	118.811	1.37	AT0939	1.37
9874.999	8049.98	117.811	2.06	AT0939	2.06
9874.999	8049.98	116.811	0.56	AT0939	0.56
9795.487	8025.092	150.556	0.59	AT0949	0.59
9795.487	8025.092	149.556	0.33	AT0949	0.33
9795.487	8025.092	148.556	1.96	AT0949	1.96
9824.931	8024.932	140.362	0.99	AT0951	0.99
9824.931	8024.932	139.362	1.49	AT0951	1.49
9824.931	8024.932	138.362	1.12	AT0951	1.12
9849.999	8025.016	131.845	0.4	AT0953	0.4
9849.999	8025.016	130.845	1.3	AT0953	1.3
9849.999	8025.016	129.845	1.02	AT0953	1.02
9874.985	8025.032	121.267	0.78	AT0955	0.78
9874.985	8025.032	120.267	1.85	AT0955	1.85
9874.985	8025.032	119.267	0.95	AT0955	0.95
9898.341	8103.323	111.685	1.8	AT1001	1.8
9898.341	8103.323	110.685	2.4	AT1001	2.4
9898.341	8103.323	109.685	1.12	AT1001	1.12
9925	8099.998	101.333	1.67	AT1003	1.67
9925.025	8112.529	102.575	0.52	AT1003A	0.52
9925.025	8112.529	101.575	0.84	AT1003A	0.84
9925.025	8112.529	100.575	3.03	AT1003A	3.03
9950	8099.978	97.183	0.9	AT1005	0.9
9950	8099.978	96.183	1.93	AT1005	1.93
9950	8099.978	95.183	2.55	AT1005	2.55
9950	8099.978	94.183	1.21	AT1005	1.21
9975.01	8112.471	89.399	0.76	AT1007A	0.76
9975.01	8112.471	88.399	0.95	AT1007A	0.95
9975.01	8112.471	87.399	0.55	AT1007A	0.55
9975.01	8112.471	86.399	1.45	AT1007A	1.45
9898.138	8078.566	113.742	0.7	AT1017	0.7

9898.138	8078.566	112.742	2.24	AT1017	2.24
9898.138	8078.566	111.742	1.13	AT1017	1.13
9898.138	8078.566	110.742	0.27	AT1017	0.27
9925.001	8075	108.444	1.04	AT1019	1.04
9925.001	8075	107.444	0.16	AT1019	0.16
9925.001	8075	106.444	0.59	AT1019	0.59
9925.001	8075	105.444	1.04	AT1019	1.04
9925.001	8075	104.444	0.65	AT1019	0.65
9950.027	8087.477	98.543	0.72	AT1021A	0.72
9950.027	8087.477	97.543	1.75	AT1021A	1.75
9950.027	8087.477	96.543	2.65	AT1021A	2.65
9950.027	8087.477	95.543	1	AT1021A	1
9976.04	8075.053	90.625	4.07	AT1023	3.5
9976.04	8075.053	89.625	1.36	AT1023	1.36
9896.747	8053.467	116.657	0.66	AT1033	0.66
9896.747	8053.467	115.657	1.53	AT1033	1.53
9896.747	8053.467	114.657	2.46	AT1033	2.46
9925	8050.005	108.096	0.32	AT1035	0.32
9925	8050.005	107.096	0.79	AT1035	0.79
9925	8050.005	106.096	1.2	AT1035	1.2
9925	8050.005	105.096	1.82	AT1035	1.82
9950	8050	100.93	0.48	AT1037	0.48
9950	8050	99.93	3.42	AT1037	3.42
9950	8050	98.93	2.29	AT1037	2.29
9950	8050	97.93	0.98	AT1037	0.98
9975.035	8050.842	94.476	0.63	AT1039	0.63
9975.035	8050.842	93.476	0.69	AT1039	0.69
9975.035	8050.842	92.476	1.66	AT1039	1.66
9975.035	8050.842	91.476	0.82	AT1039	0.82
9899.999	8025.007	116.342	1.07	AT1049	1.07
9899.999	8025.007	115.342	1.19	AT1049	1.19
9899.999	8025.007	114.342	2.02	AT1049	2.02
9925.001	8025.007	110.512	0.21	AT1051	0.21
9925.001	8025.007	109.512	0.21	AT1051	0.21
9930.014	8037.523	108.061	0.58	AT1051A	0.58
9930.014	8037.523	107.061	1.54	AT1051A	1.54
9930.014	8037.523	106.061	1.53	AT1051A	1.53
9930.014	8037.523	105.061	0.63	AT1051A	0.63
9949.022	8037.473	102.834	1.32	AT1053A	1.32

9949.022	8037.473	101.834	2.45	AT1053A	2.45
9949.022	8037.473	100.834	2.28	AT1053A	2.28
9949.022	8037.473	99.834	0.28	AT1053A	0.28
9975.118	8026.092	95.737	0.42	AT1055	0.42
9975.118	8026.092	94.737	0.42	AT1055	0.42
9975.118	8026.092	93.737	0.26	AT1055	0.26
9975.118	8026.092	92.737	0.57	AT1055	0.57
9975.118	8026.092	91.737	2.36	AT1055	2.36
9999.998	8100.009	83.089	1.55	AT1101	1.55
9999.998	8100.009	82.089	1.52	AT1101	1.52
9999.998	8100.009	81.089	0.42	AT1101	0.42
9999.998	8100.009	80.089	1.67	AT1101	1.67
10025.001	8099.992	76.318	0.95	AT1103	0.95
10025.001	8099.992	75.318	0.48	AT1103	0.48
10025.001	8099.992	74.318	1.8	AT1103	1.8
10025.001	8099.992	73.318	0.56	AT1103	0.56
9999.997	8075.007	85.478	0.8	AT1117	0.8
9999.997	8075.007	84.478	1.9	AT1117	1.9
9999.997	8075.007	83.478	0.79	AT1117	0.79
9999.997	8075.007	82.478	0.33	AT1117	0.33
9750.002	8000.016	165.921	0.6	AU0805	0.6
9750.002	8000.016	164.921	0.41	AU0805	0.41
9750.002	8000.016	163.921	1.49	AU0805	1.49
9750.002	8000.016	162.921	0.64	AU0805	0.64
9775.003	7999.98	158.21	0.79	AU0807	0.79
9775.003	7999.98	157.21	0.53	AU0807	0.53
9775.003	7999.98	156.21	2.13	AU0807	2.13
9750.001	7974.995	169.184	0.48	AU0821	0.48
9750.001	7974.995	168.184	0.61	AU0821	0.61
9750.001	7974.995	167.184	1.39	AU0821	1.39
9775.026	7974.827	162.808	0.35	AU0823	0.35
9775.026	7974.827	161.808	0.49	AU0823	0.49
9775.026	7974.827	160.808	0.94	AU0823	0.94
9775.026	7974.827	159.808	1.07	AU0823	1.07
9774.987	7949.967	168.861	0.77	AU0839	0.77
9774.987	7949.967	167.861	0.17	AU0839	0.17
9774.987	7949.967	166.861	0.42	AU0839	0.42
9774.987	7949.967	165.861	1.81	AU0839	1.81
9774.987	7949.967	164.861	0.92	AU0839	0.92

9775.015	7924.98	167.524	0.63	AU0855	0.63
9775.015	7924.98	166.524	0.67	AU0855	0.67
9775.015	7924.98	165.524	0.48	AU0855	0.48
9775.015	7924.98	164.524	0.08	AU0855	0.08
9825.004	7999.982	143.597	0.24	AU0903	0.24
9825.004	7999.982	142.597	0.48	AU0903	0.48
9825.004	7999.982	141.597	1.43	AU0903	1.43
9825.004	7999.982	140.597	1.31	AU0903	1.31
9850.001	8000.004	136.272	0.96	AU0905	0.96
9850.001	8000.004	135.272	0.46	AU0905	0.46
9850.001	8000.004	134.272	0.37	AU0905	0.37
9850.001	8000.004	133.272	2.24	AU0905	2.24
9850.001	8000.004	132.272	1.59	AU0905	1.59
9798.751	7974.554	156.001	0.58	AU0917	0.58
9798.751	7974.554	155.001	0.43	AU0917	0.43
9798.751	7974.554	154.001	1.3	AU0917	1.3
9798.751	7974.554	153.001	0.59	AU0917	0.59
9825.001	7974.998	145.448	0.36	AU0919	0.36
9825.001	7974.998	144.448	0.9	AU0919	0.9
9825.001	7974.998	143.448	1.14	AU0919	1.14
9850.001	7974.994	138.06	0.62	AU0921	0.62
9850.001	7974.994	137.06	0.7	AU0921	0.7
9850.001	7974.994	136.06	2.45	AU0921	2.45
9850.001	7974.994	135.06	0.71	AU0921	0.71
9875.001	7974.997	131.107	1.31	AU0923	1.31
9875.001	7974.997	130.107	0.65	AU0923	0.65
9875.001	7974.997	129.107	2.43	AU0923	2.43
9875.001	7974.997	128.107	1.09	AU0923	1.09
9875.001	7974.997	127.107	1.23	AU0923	1.23
9799.997	7950.007	156.847	0.43	AU0933	0.43
9799.997	7950.007	155.847	0.71	AU0933	0.71
9799.997	7950.007	154.847	2.05	AU0933	2.05
9825.126	7949.82	151.409	0.6	AU0935	0.6
9825.126	7949.82	150.409	0.63	AU0935	0.63
9825.126	7949.82	149.409	0.86	AU0935	0.86
9825.126	7949.82	148.409	1.07	AU0935	1.07
9850.001	7949.993	141.576	0.4	AU0937	0.4
9850.001	7949.993	140.576	1.2	AU0937	1.2
9850.001	7949.993	139.576	0.66	AU0937	0.66

9875	7950.006	133.894	0.4	AU0939	0.4
9875	7950.006	132.894	0.55	AU0939	0.55
9875	7950.006	131.894	1.66	AU0939	1.66
9875	7950.006	130.894	0.91	AU0939	0.91
9800.006	7924.97	160.854	0.3	AU0949	0.3
9800.006	7924.97	159.854	2.08	AU0949	2.08
9800.006	7924.97	158.854	0.75	AU0949	0.75
9824.969	7925.014	151.543	0.46	AU0951	0.46
9824.969	7925.014	150.543	2.23	AU0951	2.23
9824.969	7925.014	149.543	0.96	AU0951	0.96
9850.002	7924.996	143.801	0.36	AU0953	0.36
9850.002	7924.996	142.801	0.56	AU0953	0.56
9850.002	7924.996	141.801	1.19	AU0953	1.19
9850.002	7924.996	140.801	0.86	AU0953	0.86
9875.014	7925.009	135.353	0.54	AU0955	0.54
9875.014	7925.009	134.353	1.12	AU0955	1.12
9875.014	7925.009	133.353	0.73	AU0955	0.73
9900.013	8000	121.26	0.8	AU1001A	0.8
9900.013	8000	120.26	2.9	AU1001A	2.9
9900.013	8000	119.26	1.55	AU1001A	1.55
9900.013	8000	118.26	0.44	AU1001A	0.44
9925.001	7999.995	113.984	0.7	AU1003	0.7
9925.001	7999.995	112.984	0.87	AU1003	0.87
9925.001	7999.995	111.984	2.81	AU1003	2.81
9925.001	7999.995	110.984	1.37	AU1003	1.37
9950	7999.997	106.028	0.53	AU1005	0.53
9950	7999.997	105.028	1.45	AU1005	1.45
9950	7999.997	104.028	3.3	AU1005	3.3
9950	7999.997	103.028	0.48	AU1005	0.48
9900	7975	123.012	0.66	AU1017	0.66
9900	7975	122.012	3.01	AU1017	3.01
9900	7975	121.012	1.25	AU1017	1.25
9930.006	7987.494	113.655	0.74	AU1019A	0.74
9930.006	7987.494	112.655	1.24	AU1019A	1.24
9930.006	7987.494	111.655	2.45	AU1019A	2.45
9930.006	7987.494	110.655	1.05	AU1019A	1.05
9900	7950.007	126.584	0.71	AU1033	0.71
9900	7950.007	125.584	0.86	AU1033	0.86
9900	7950.007	124.584	2.44	AU1033	2.44

9900	7950.007	123.584	1.15	AU1033	1.15
9775.002	7899.989	172.643	0.7	AV0807	0.7
9775.002	7899.989	171.643	0.18	AV0807	0.18
9775.002	7899.989	170.643	0.25	AV0807	0.25
9775.002	7899.989	169.643	1.71	AV0807	1.71
9775.002	7899.989	168.643	1.42	AV0807	1.42
9774.999	7875.011	175.342	0.13	AV0823	0.13
9774.999	7875.011	174.342	0.11	AV0823	0.11
9774.999	7875.011	173.342	0.71	AV0823	0.71
9774.999	7875.011	172.342	1.22	AV0823	1.22
9774.999	7875.011	171.342	0.97	AV0823	0.97
9775.001	7850.014	175.596	1.07	AV0839	1.07
9815.214	7900.288	160.316	0.34	AV0903	0.34
9815.214	7900.288	159.316	0.37	AV0903	0.37
9815.214	7900.288	158.316	1.74	AV0903	1.74
9815.214	7900.288	157.316	0.69	AV0903	0.69
9850	7899.992	146.724	0.29	AV0905	0.29
9850	7899.992	145.724	0.24	AV0905	0.24
9850	7899.992	144.724	1.44	AV0905	1.44
9850	7899.992	143.724	0.6	AV0905	0.6
9874.996	7900.002	138.626	0.45	AV0907	0.45
9874.996	7900.002	137.626	0.82	AV0907	0.82
9874.996	7900.002	136.626	1.03	AV0907	1.03
9799.998	7875.011	167.516	0.7	AV0917	0.7
9799.998	7875.011	166.516	0.89	AV0917	0.89
9799.998	7875.011	165.516	1.26	AV0917	1.26
9799.998	7875.011	164.516	1.85	AV0917	1.85
9820.4	7875.05	160.528	1.5	AV0919	1.5
9820.4	7875.05	159.528	2.97	AV0919	2.97
9820.4	7875.05	158.528	0.38	AV0919	0.38
9849.999	7875.007	149.031	0.51	AV0921	0.51
9849.999	7875.007	148.031	1.25	AV0921	1.25
9849.999	7875.007	147.031	0.92	AV0921	0.92
9800.003	7850.001	169.326	0.76	AV0933	0.76
9800.003	7850.001	168.326	0.64	AV0933	0.64
9800.003	7850.001	167.326	1.29	AV0933	1.29
9800.003	7850.001	166.326	1.39	AV0933	1.39
9824.998	7849.998	160.781	0.41	AV0935	0.41
9824.998	7849.998	159.781	1.75	AV0935	1.75

9824.998	7849.998	158.781	0.94	AV0935	0.94
9800.003	7824.993	169.766	0.64	AV0949	0.64
9800.003	7824.993	168.766	0.45	AV0949	0.45
9800.003	7824.993	167.766	4.51	AV0949	3.5
9800.003	7824.993	166.766	2.86	AV0949	2.86
9800.003	7824.993	165.766	1.81	AV0949	1.81
9775.001	7800.004	167.176	2.58	AW0807	2.58
9775.001	7800.004	166.176	1.14	AW0807	1.14
9775.001	7800.004	165.176	1.29	AW0807	1.29
9801.25	7999.94	150.767	0.5596	GDA20	0.5596
9801.25	7999.94	149.66	3.7748	GDA20	3.5
9801.25	7999.94	148.553	0.95	GDA20	0.95
9930.99	8116.28	100.959	0.9973	GDA58	0.9973
9930.99	8116.28	99.876	2.3891	GDA58	2.3891
9930.99	8116.28	98.794	3.2011	GDA58	3.2011
9930.99	8116.28	97.711	1.0773	GDA58	1.0773
9894.39	7978.45	123.906	0.6943	GDA59	0.6943
9894.39	7978.45	122.959	1.9214	GDA59	1.9214
9894.39	7978.45	122.011	1.5207	GDA59	1.5207
9894.39	7978.45	121.064	1.1587	GDA59	1.1587
9995.49	8096.91	85.738	0.154	GDA60	0.154
9995.49	8096.91	84.654	0.499	GDA60	0.499
9995.49	8096.91	83.57	1.1409	GDA60	1.1409
9995.49	8096.91	82.486	1.1525	GDA60	1.1525
9995.49	8096.91	81.402	2.1582	GDA60	2.1582
9800.08	7894.24	165.84	0.3265	GDA61	0.3265
9800.08	7894.24	164.76	0.25	GDA61	0.25
9800.08	7894.24	163.68	0.2354	GDA61	0.2354
9800.08	7894.24	162.6	0.2907	GDA61	0.2907
9800.08	7894.24	161.52	0.8373	GDA61	0.8373
9801.81	8101.59	138.644	0.684	GDA62	0.684
9801.81	8101.59	137.711	0.3254	GDA62	0.3254
9801.81	8101.59	136.779	0.7026	GDA62	0.7026
9801.81	8101.59	135.846	0.4892	GDA62	0.4892
Northings	**Eastings**	**Elevation**	**grade(au)**	**Hole Id**	**grade cut**
10025.001	8074.981	50.985	0.75	AT1119	0.75
10025.001	8074.981	49.985	1.92	AT1119	1.92
9999.997	8050.008	63.335	0.01	AT1133	0.01
9999.997	8050.008	62.335	0.01	AT1133	0.01

9999.997	8050.008	61.335	0.01	AT1133	0.01
9999.997	8050.008	60.335	0.01	AT1133	0.01
10025	8050.004	50.957	0.4	AT1135	0.4
10025	8050.004	49.957	0.54	AT1135	0.54
10025	8050.004	48.957	1.06	AT1135	1.06
10025	8050.004	47.957	0.64	AT1135	0.64
10000.003	8025.011	59.768	1.01	AT1149	1.01
10000.003	8025.011	58.768	1.32	AT1149	1.32
10000.003	8025.011	57.768	4.09	AT1149	3.5
10000.003	8025.011	56.768	0.25	AT1149	0.25
10025	8025.011	53.72	0.41	AT1151	0.41
10025	8025.011	52.72	0.85	AT1151	0.85
10025	8025.011	51.72	0.88	AT1151	0.88
10025	8025.011	50.72	1.55	AT1151	1.55
9974.776	7999.93	77.803	0.83	AU1007	0.83
9974.776	7999.93	76.803	1.85	AU1007	1.85
9974.776	7999.93	75.803	0.65	AU1007	0.65
9975.001	7974.995	57.88	0.99	AU1023	0.99
9975.001	7974.995	56.88	3.27	AU1023	3.27
9975.001	7974.995	55.88	1.49	AU1023	1.49
9975.001	7974.995	54.88	0.31	AU1023	0.31
9975.001	7974.995	53.88	0.85	AU1023	0.85
9950	7950	66.55	1.13	AU1037	1.13
9950	7950	65.55	2.47	AU1037	2.47
9950	7950	64.55	0.84	AU1037	0.84
9975.001	7949.976	59.031	0.5	AU1039	0.5
9975.001	7949.976	58.031	1.33	AU1039	1.33
9975.001	7949.976	57.031	0.99	AU1039	0.99
9975.001	7949.976	56.031	0.34	AU1039	0.34
9949.997	7924.997	70.611	0.51	AU1053	0.51
9949.997	7924.997	69.611	1.02	AU1053	1.02
9949.997	7924.997	68.611	0.38	AU1053	0.38
9949.997	7924.997	67.611	0.99	AU1053	0.99
9975.001	7925.001	62.094	0.34	AU1055	0.34
9975.001	7925.001	61.094	1.11	AU1055	1.11
9975.001	7925.001	60.094	2.12	AU1055	2.12
9975.001	7925.001	59.094	0.44	AU1055	0.44
9999.996	8000.013	58.373	0.72	AU1101	0.72
9999.996	8000.013	57.373	2.79	AU1101	2.79

9999.996	8000.013	56.373	1.82	AU1101	1.82
10025	8000.004	41.436	0.62	AU1103	0.62
10025	8000.004	40.436	0.9	AU1103	0.9
10025	8000.004	39.436	1.46	AU1103	1.46
10025	8000.004	38.436	1.77	AU1103	1.77
10001.515	7977.15	47.904	0.8	AU1117	0.8
10001.515	7977.15	46.904	0.9	AU1117	0.9
10001.515	7977.15	45.904	1.45	AU1117	1.45
10001.515	7977.15	44.904	0.97	AU1117	0.97
10025.003	7974.986	42.621	0.87	AU1119	0.87
10025.003	7974.986	41.621	2.44	AU1119	2.44
10025.003	7974.986	40.621	0.8	AU1119	0.8
10000.001	7949.979	50.431	0.76	AU1133	0.76
10000.001	7949.979	49.431	1.8	AU1133	1.8
10000.001	7949.979	48.431	1.48	AU1133	1.48
10000.001	7949.979	47.431	0.8	AU1133	0.8
10025.006	7949.985	44.021	0.67	AU1135	0.67
10025.006	7949.985	43.021	2.2	AU1135	2.2
10025.006	7949.985	42.021	0.73	AU1135	0.73
10000.004	7925	53.836	0.41	AU1149	0.41
10000.004	7925	52.836	0.72	AU1149	0.72
10000.004	7925	51.836	1.43	AU1149	1.43
10024.983	7925.011	47.621	1.15	AU1151	1.15
10024.983	7925.011	46.621	3.8	AU1151	3.5
10024.983	7925.011	45.621	2.8	AU1151	2.8
10024.983	7925.011	44.621	0.71	AU1151	0.71
10049.947	7924.915	38.906	0.87	AU1153	0.87
10049.947	7924.915	37.906	3.74	AU1153	3.5
10049.947	7924.915	36.906	2.63	AU1153	2.63
10049.947	7924.915	35.906	0.53	AU1153	0.53
9924.999	7899.971	84.623	1.06	AV1003	1.06
9924.999	7899.971	83.623	3	AV1003	3
9924.999	7899.971	82.623	0.06	AV1003	0.06
9924.999	7899.971	81.623	0.05	AV1003	0.05
9950.001	7899.978	73.415	0.79	AV1005	0.79
9950.001	7899.978	72.415	0.87	AV1005	0.87
9950.001	7899.978	71.415	0.84	AV1005	0.84
9950.001	7899.978	70.415	0.87	AV1005	0.87
9975.004	7900.022	65.85	0.66	AV1007	0.66

9975.004	7900.022	64.85	0.65	AV1007	0.65
9975.004	7900.022	63.85	2.36	AV1007	2.36
9975.004	7900.022	62.85	0.48	AV1007	0.48
9925.001	7875.014	84.255	0.65	AV1019	0.65
9925.001	7875.014	83.255	1.18	AV1019	1.18
9925.001	7875.014	82.255	1.52	AV1019	1.52
9925.001	7875.014	81.255	1.09	AV1019	1.09
9949.998	7875.019	76.861	0.2	AV1021	0.2
9949.998	7875.019	75.861	0.44	AV1021	0.44
9949.998	7875.019	74.861	1.03	AV1021	1.03
9949.998	7875.019	73.861	0.88	AV1021	0.88
9974.999	7875.013	68.157	0.55	AV1023	0.55
9974.999	7875.013	67.157	1.08	AV1023	1.08
9974.999	7875.013	66.157	3.06	AV1023	3.06
9974.999	7875.013	65.157	1.43	AV1023	1.43
9925	7850.007	86.837	0.63	AV1035	0.63
9925	7850.007	85.837	2.37	AV1035	2.37
9925	7850.007	84.837	0.85	AV1035	0.85
9950.002	7849.987	78.302	0.28	AV1037	0.28
9950.002	7849.987	77.302	2.29	AV1037	2.29
9950.002	7849.987	76.302	2.05	AV1037	2.05
9950.002	7849.987	75.302	0.37	AV1037	0.37
9975.002	7850.005	72.56	0.9	AV1039	0.9
9975.002	7850.005	71.56	0.26	AV1039	0.26
9975.002	7850.005	70.56	0.41	AV1039	0.41
9975.002	7850.005	69.56	0.67	AV1039	0.67
9975.002	7850.005	68.56	1.03	AV1039	1.03
9899.999	7824.987	96.414	1.26	AV1049	1.26
9899.999	7824.987	95.414	1.33	AV1049	1.33
9899.999	7824.987	94.414	2.17	AV1049	2.17
9924.999	7824.97	89.348	2.12	AV1051	2.12
9924.999	7824.97	88.348	3.49	AV1051	3.49
9924.999	7824.97	87.348	0.47	AV1051	0.47
9950.002	7824.982	80.802	0.63	AV1053	0.63
9950.002	7824.982	79.802	2.11	AV1053	2.11
9950.002	7824.982	78.802	0.78	AV1053	0.78
9974.999	7825.021	73.127	0.66	AV1055	0.66
9974.999	7825.021	72.127	0.96	AV1055	0.96
9974.999	7825.021	71.127	0.72	AV1055	0.72

9974.999	7825.021	70.127	0.49	AV1055	0.49
10000	7899.992	56.887	0.43	AV1101	0.43
10000	7899.992	55.887	0.89	AV1101	0.89
10000	7899.992	54.887	1.65	AV1101	1.65
10000	7899.992	53.887	0.7	AV1101	0.7
10025.01	7900.011	50.27	1.04	AV1103	1.04
10025.01	7900.011	49.27	1.96	AV1103	1.96
10025.01	7900.011	48.27	1.46	AV1103	1.46
10025.01	7900.011	47.27	2.1	AV1103	2.1
9999.999	7874.973	60.501	0.33	AV1117	0.33
9999.999	7874.973	59.501	0.55	AV1117	0.55
9999.999	7874.973	58.501	0.36	AV1117	0.36
9999.999	7874.973	57.501	1.51	AV1117	1.51
10049.974	7875.002	44.281	0.44	AV1121	0.44
10049.974	7875.002	43.281	1.82	AV1121	1.82
10049.974	7875.002	42.281	0.95	AV1121	0.95
10000	7849.986	62.221	1.39	AV1133	1.39
10000	7849.986	61.221	0.62	AV1133	0.62
10000	7849.986	60.221	2.44	AV1133	2.44
10000	7849.986	59.221	0.74	AV1133	0.74
10000	7824.981	65.121	0.07	AV1149	0.07
10000	7824.981	64.121	1.45	AV1149	1.45
10000	7824.981	63.121	1.94	AV1149	1.94
10026.1	7823.399	58.915	2.31	AV1151	2.31
10026.1	7823.399	57.915	1.66	AV1151	1.66
10026.1	7823.399	56.915	3.2	AV1151	3.2
10026.1	7823.399	55.915	1.09	AV1151	1.09
9874.985	7750.022	112.665	1.06	AW0939	1.06
9874.985	7750.022	111.665	2.06	AW0939	2.06
9874.985	7750.022	110.665	1.62	AW0939	1.62
9849.998	7725.022	124.624	0.24	AW0953	0.24
9849.998	7725.022	123.624	3.11	AW0953	3.11
9849.998	7725.022	122.624	2.32	AW0953	2.32
9875.003	7724.984	114.637	0.48	AW0955	0.48
9875.003	7724.984	113.637	2.57	AW0955	2.57
9875.003	7724.984	112.637	1.02	AW0955	1.02
9900	7799.97	100.066	0.88	AW1001	0.88
9900	7799.97	99.066	1.54	AW1001	1.54
9900	7799.97	98.066	0.53	AW1001	0.53

9925.001	7799.982	92.806	0.94	AW1003	0.94
9925.001	7799.982	91.806	2.29	AW1003	2.29
9925.001	7799.982	90.806	1.42	AW1003	1.42
9950.002	7799.96	84.284	0.37	AW1005	0.37
9950.002	7799.96	83.284	1.01	AW1005	1.01
9950.002	7799.96	82.284	0.94	AW1005	0.94
9950.002	7799.96	81.284	0.53	AW1005	0.53
9974.998	7800.013	76.907	0.64	AW1007	0.64
9974.998	7800.013	75.907	1.75	AW1007	1.75
9974.998	7800.013	74.907	1.54	AW1007	1.54
9974.998	7800.013	73.907	0.58	AW1007	0.58
9900	7775.015	102.299	2.44	AW1017	2.44
9900	7775.015	101.299	1.63	AW1017	1.63
9900	7775.015	100.299	0.45	AW1017	0.45
9924.995	7775.025	95.519	0.6	AW1019	0.6
9924.995	7775.025	94.519	3.6	AW1019	3.5
9924.995	7775.025	93.519	2.13	AW1019	2.13
9950.004	7775.013	86.795	0.66	AW1021	0.66
9950.004	7775.013	85.795	3.42	AW1021	3.42
9950.004	7775.013	84.795	0.98	AW1021	0.98
9974.998	7775.032	78.654	0.74	AW1023	0.74
9974.998	7775.032	77.654	3.67	AW1023	3.5
9974.998	7775.032	76.654	1.8	AW1023	1.8
9899.995	7750.001	104.571	1.09	AW1033	1.09
9899.995	7750.001	103.571	0.6	AW1033	0.6
9899.995	7750.001	102.571	0.16	AW1033	0.16
9924.991	7749.994	97.776	1.04	AW1035	1.04
9924.991	7749.994	96.776	2.19	AW1035	2.19
9924.991	7749.994	95.776	3.14	AW1035	3.14
9949.999	7749.995	88.758	0.99	AW1037	0.99
9949.999	7749.995	87.758	1.68	AW1037	1.68
9949.999	7749.995	86.758	1.29	AW1037	1.29
9975	7750.012	81.975	0.45	AW1039	0.45
9975	7750.012	80.975	1.27	AW1039	1.27
9975	7750.012	79.975	1.44	AW1039	1.44
9899.986	7725.015	107.739	0.84	AW1049	0.84
9899.986	7725.015	106.739	0.93	AW1049	0.93
9899.986	7725.015	105.739	2.47	AW1049	2.47
9899.986	7725.015	104.739	2.61	AW1049	2.61

9925.003	7725.021	100.004	0.63	AW1051	0.63
9925.003	7725.021	99.004	1.1	AW1051	1.1
9925.003	7725.021	98.004	2.22	AW1051	2.22
9925.003	7725.021	97.004	0.68	AW1051	0.68
9950.002	7724.991	91.483	0.6	AW1053	0.6
9950.002	7724.991	90.483	2.09	AW1053	2.09
9950.002	7724.991	89.483	0.6	AW1053	0.6
9975	7724.991	84.491	0.67	AW1055	0.67
9975	7724.991	83.491	1.82	AW1055	1.82
9975	7724.991	82.491	1.35	AW1055	1.35
9975	7724.991	81.491	0.34	AW1055	0.34
9999.341	7800.221	68.724	0.72	AW1101	0.72
9999.341	7800.221	67.724	1.69	AW1101	1.69
9999.341	7800.221	66.724	2.26	AW1101	2.26
9999.341	7800.221	65.724	0.84	AW1101	0.84
10025.046	7799.929	59.059	1.05	AW1103	1.05
10025.046	7799.929	58.059	4.14	AW1103	3.5
10025.046	7799.929	57.059	2.45	AW1103	2.45
9997.34	7776.04	72.014	0.57	AW1117	0.57
9997.34	7776.04	71.014	1.99	AW1117	1.99
9997.34	7776.04	70.014	1.88	AW1117	1.88
9997.34	7776.04	69.014	0.74	AW1117	0.74
10025.007	7774.962	62.657	1.04	AW1119	1.04
10025.007	7774.962	61.657	1.79	AW1119	1.79
10025.007	7774.962	60.657	6.84	AW1119	3.5
10025.007	7774.962	59.657	0.67	AW1119	0.67
10024.985	7750.003	65.626	1.1	AW1135	1.1
10024.985	7750.003	64.626	1.7	AW1135	1.7
10024.985	7750.003	63.626	3.09	AW1135	3.09
10024.985	7750.003	62.626	0.78	AW1135	0.78
9994.508	7725.254	77.796	0.68	AW1149	0.68
9994.508	7725.254	76.796	2.23	AW1149	2.23
9994.508	7725.254	75.796	0.69	AW1149	0.69
10025.068	7725.075	68.623	0.34	AW1151	0.34
10025.068	7725.075	67.623	1.03	AW1151	1.03
10025.068	7725.075	66.623	4.26	AW1151	3.5
10025.068	7725.075	65.623	0.4	AW1151	0.4
9800	7700.002	145.494	0.63	AX0901	0.63
9800	7700.002	144.494	0.94	AX0901	0.94

9800	7700.002	143.494	0.54	AX0901	0.54
9825	7700.005	134.203	0.99	AX0903	0.99
9825	7700.005	133.203	1.05	AX0903	1.05
9825	7700.005	132.203	0.79	AX0903	0.79
9850.002	7699.984	125.406	0.38	AX0905	0.38
9850.002	7699.984	124.406	2.34	AX0905	2.34
9850.002	7699.984	123.406	1.8	AX0905	1.8
9878.488	7704.091	115.478	0.55	AX0907	0.55
9878.488	7704.091	114.478	1.07	AX0907	1.07
9878.488	7704.091	113.478	0.22	AX0907	0.22
9800	7675.002	140.901	0.29	AX0917	0.29
9800	7675.002	139.901	0.93	AX0917	0.93
9800	7675.002	138.901	0.18	AX0917	0.18
9824.999	7674.998	134.631	1.99	AX0919	1.99
9824.999	7674.998	133.631	1.61	AX0919	1.61
9824.999	7674.998	132.631	0.55	AX0919	0.55
9824.999	7674.998	131.631	0.11	AX0919	0.11
9849.998	7675.02	127.572	0.65	AX0921	0.65
9849.998	7675.02	126.572	1.89	AX0921	1.89
9849.998	7675.02	125.572	6.49	AX0921	3.5
9862.502	7675.008	123.253	1.45	AX0923	1.45
9862.502	7675.008	122.253	1.52	AX0923	1.52
9862.502	7675.008	121.253	1.25	AX0923	1.25
9825	7650.009	138.072	0.84	AX0935	0.84
9825	7650.009	137.072	1.85	AX0935	1.85
9825	7650.009	136.072	1.97	AX0935	1.97
9900	7700.005	110.488	0.4	AX1001	0.4
9900	7700.005	109.488	0.93	AX1001	0.93
9900	7700.005	108.488	2.15	AX1001	2.15
9900	7700.005	107.488	2.12	AX1001	2.12
9925	7699.996	102.683	0.43	AX1003	0.43
9925	7699.996	101.683	1.19	AX1003	1.19
9925	7699.996	100.683	4.49	AX1003	3.5
9925	7699.996	99.683	2.03	AX1003	2.03
9949.986	7700.001	94.444	0.69	AX1005	0.69
9949.986	7700.001	93.444	0.76	AX1005	0.76
9949.986	7700.001	92.444	1.66	AX1005	1.66
9949.986	7700.001	91.444	2.23	AX1005	2.23
9975	7699.999	85.576	0.41	AX1007	0.41

9975	7699.999	84.576	0.9	AX1007	0.9
9975	7699.999	83.576	1.37	AX1007	1.37
9975	7699.999	82.576	1.05	AX1007	1.05
9900.001	7674.993	111.232	1.35	AX1017	1.35
9900.001	7674.993	110.232	5.15	AX1017	3.5
9900.001	7674.993	109.232	1.25	AX1017	1.25
9925	7675.004	103.922	0.81	AX1019	0.81
9925	7675.004	102.922	1.9	AX1019	1.9
9925	7675.004	101.922	1.18	AX1019	1.18
9925	7675.004	100.922	0.36	AX1019	0.36
9950.001	7675.014	97.619	0.38	AX1021	0.38
9950.001	7675.014	96.619	0.93	AX1021	0.93
9950.001	7675.014	95.619	1.51	AX1021	1.51
9950.001	7675.014	94.619	1.51	AX1021	1.51
9975.004	7674.984	87.444	1.32	AX1023	1.32
9975.004	7674.984	86.444	1.15	AX1023	1.15
9975.004	7674.984	85.444	0.18	AX1023	0.18
9899.999	7650.021	113.804	0.71	AX1033	0.71
9899.999	7650.021	112.804	1	AX1033	1
9899.999	7650.021	111.804	0.8	AX1033	0.8
10024.956	7699.991	70.777	1.03	AX1103	1.03
10024.956	7699.991	69.777	1.45	AX1103	1.45
10024.956	7699.991	68.777	4.3	AX1103	3.5
10000.003	7675.042	81.593	1.03	AX1117	1.03
10000.003	7675.042	80.593	3.02	AX1117	3.02
10000.003	7675.042	79.593	2.05	AX1117	2.05
10024.933	7675.074	71.866	0.76	AX1119	0.76
10024.933	7675.074	70.866	1.56	AX1119	1.56
10024.933	7675.074	69.866	1.95	AX1119	1.95
10024.933	7675.074	68.866	0.45	AX1119	0.45
10047.999	7675.005	66.919	0.84	AX1121	0.84
10047.999	7675.005	65.919	3.14	AX1121	3.14
10047.999	7675.005	64.919	3.69	AX1121	3.5
10049.999	7650.009	67.927	0.63	AX1137	0.63
10049.999	7650.009	66.927	1.32	AX1137	1.32
10049.999	7650.009	65.927	0.67	AX1137	0.67
10004.86	7951.85	51.344	2.13	GDA18	2.13
10004.86	7951.85	50.371	2.5326	GDA18	2.5326
10004.86	7951.85	49.399	2.1738	GDA18	2.1738

10004.86	7951.85	48.426	0.39	GDA18	0.39
10001.22	7805.02	68.113	1.39	GDA46	1.39
10001.22	7805.02	67.218	1.4473	GDA46	1.4473
10001.22	7805.02	66.323	3.1	GDA46	3.1
10001.22	7805.02	65.427	1.2506	GDA46	1.2506
10002.75	7897.69	56.706	1.0235	GDA85	1.0235
10002.75	7897.69	55.799	0.5739	GDA85	0.5739
10002.75	7897.69	54.891	1.2443	GDA85	1.2443
10002.75	7897.69	53.984	0.9742	GDA85	0.9742
9896.7	7707.41	108.774	0.4989	GDA91	0.4989
9896.7	7707.41	107.802	0.5838	GDA91	0.5838
9896.7	7707.41	106.83	1.399	GDA91	1.399
9896.7	7707.41	105.858	0.5212	GDA91	0.5212
9896.7	7707.41	104.886	0.0921	GDA91	0.0921
10003.27	7700.34	78.151	0.8461	GDA92	0.8461
10003.27	7700.34	77.174	1.988	GDA92	1.988
10003.27	7700.34	76.196	2.0799	GDA92	2.0799
10003.27	7700.34	75.219	0.7106	GDA92	0.7106
Northings	**Eastings**	**Elevation**	**grade(au)**	**Hole Id**	**grade cut**
9950	7974.998	81.563	0.44	AU1021	0.44
9950	7974.998	80.563	0.08	AU1021	0.08
9926.003	7962.504	114.052	0.5	AU1035A	0.5
9926.003	7962.504	113.052	0.83	AU1035A	0.83
9926.003	7962.504	112.052	0.15	AU1035A	0.15
9899.991	7925.007	109.526	0.56	AU1049	0.56
9899.991	7925.007	108.526	1.48	AU1049	1.48
9899.991	7925.007	107.526	0.49	AU1049	0.49
9875	7874.971	120.011	1.03	AV0923	1.03
9875	7874.971	119.011	0.43	AV0923	0.43
9875	7874.971	118.011	1.42	AV0923	1.42
9851.795	7849.981	130.063	0.9	AV0937	0.9
9851.795	7849.981	129.063	1.13	AV0937	1.13
9851.795	7849.981	128.063	1.12	AV0937	1.12
9874.999	7849.963	123.114	0.49	AV0939	0.49
9874.999	7849.963	122.114	1.32	AV0939	1.32
9874.999	7849.963	121.114	2.35	AV0939	2.35
9825	7825.004	141.988	0.23	AV0951	0.23
9825	7825.004	140.988	1.8	AV0951	1.8
9825	7825.004	139.988	2.43	AV0951	2.43

9825	7825.004	138.988	0.24	AV0951	0.24
9854.739	7827.606	132.911	0.5	AV0953	0.5
9854.739	7827.606	131.911	1.63	AV0953	1.63
9854.739	7827.606	130.911	1.35	AV0953	1.35
9875.005	7825.046	127.29	0.68	AV0955	0.68
9875.005	7825.046	126.29	0.79	AV0955	0.79
9875.005	7825.046	125.29	2.44	AV0955	2.44
9900.001	7900.016	111.549	0.88	AV1001	0.88
9900.001	7900.016	110.549	0.48	AV1001	0.48
9900.001	7900.016	109.549	1.36	AV1001	1.36
9900.001	7900.016	108.549	2.11	AV1001	2.11
9900	7874.999	112.675	1.39	AV1017	1.39
9900	7874.999	111.675	0.92	AV1017	0.92
9900	7874.999	110.675	0.69	AV1017	0.69
9900.002	7849.99	114.804	0.66	AV1033	0.66
9900.002	7849.99	113.804	2.53	AV1033	2.53
9900.002	7849.99	112.804	1.46	AV1033	1.46
9775.006	7775.002	164.946	1.56	AW0823	1.56
9775.006	7775.002	163.946	0.06	AW0823	0.06
9775.006	7775.002	162.946	0.26	AW0823	0.26
9774.997	7725	168.757	2.12	AW0855	2.12
9774.997	7725	167.757	1.91	AW0855	1.91
9774.997	7725	166.757	1.05	AW0855	1.05
9800	7800.02	154.118	0.45	AW0901	0.45
9800	7800.02	153.118	5.89	AW0901	3.5
9800	7800.02	152.118	1.15	AW0901	1.15
9824.998	7799.996	146.081	0.38	AW0903	0.38
9824.998	7799.996	145.081	1.24	AW0903	1.24
9824.998	7799.996	144.081	0.53	AW0903	0.53
9850	7799.984	135.859	0.43	AW0905	0.43
9850	7799.984	134.859	1.34	AW0905	1.34
9850	7799.984	133.859	1.61	AW0905	1.61
9874.998	7799.968	131.432	0.65	AW0907	0.65
9874.998	7799.968	130.432	1.32	AW0907	1.32
9874.998	7799.968	129.432	1.55	AW0907	1.55
9800.001	7775.003	156.494	1.13	AW0917	1.13
9800.001	7775.003	155.494	1.63	AW0917	1.63
9800.001	7775.003	154.494	0.84	AW0917	0.84
9825.001	7775.016	149.015	1.8	AW0919	1.8

9825.001	7775.016	148.015	1.45	AW0919	1.45
9847.001	7774.997	143.422	2.07	AW0921	2.07
9847.001	7774.997	142.422	0.65	AW0921	0.65
9847.001	7774.997	141.422	0.15	AW0921	0.15
9875.005	7775.014	132.494	0.75	AW0923	0.75
9875.005	7775.014	131.494	0.74	AW0923	0.74
9875.005	7775.014	130.494	0.39	AW0923	0.39
9800	7750.011	160.094	1.57	AW0933	1.57
9800	7750.011	159.094	1.82	AW0933	1.82
9800	7750.011	158.094	1.32	AW0933	1.32
9824.999	7750.01	152.841	2.26	AW0935	2.26
9824.999	7750.01	151.841	2.11	AW0935	2.11
9824.999	7750.01	150.841	0.42	AW0935	0.42
9850	7749.99	145.66	0.3	AW0937	0.3
9850	7749.99	144.66	1.13	AW0937	1.13
9850	7749.99	143.66	1.78	AW0937	1.78
9850	7749.99	142.66	0.49	AW0937	0.49
9850	7749.983	146.981	0.47	AW0937A	0.47
9850	7749.983	145.981	1.41	AW0937A	1.41
9850	7749.983	144.981	1.79	AW0937A	1.79
9850	7749.983	143.981	0.34	AW0937A	0.34
9800	7725.002	162.474	2.81	AW0949	2.81
9800	7725.002	161.474	1.87	AW0949	1.87
9800	7725.002	160.474	1.42	AW0949	1.42
9825	7724.997	155.44	2.55	AW0951	2.55
9825	7724.997	154.44	1.88	AW0951	1.88
9825	7724.997	153.44	2.17	AW0951	2.17
9825	7724.997	152.44	1.46	AW0951	1.46
9774.993	7699.999	171.446	0.46	AX0807	0.46
9774.993	7699.999	170.446	1.3	AX0807	1.3
9774.993	7699.999	169.446	0.24	AX0807	0.24
9775.003	7675	173.289	0.24	AX0823	0.24
9775.003	7675	172.289	1.23	AX0823	1.23
9775.003	7675	171.289	0.31	AX0823	0.31
9796.87	7802.22	159.994	0.17	GDA47	0.17
9796.87	7802.22	158.921	0.4227	GDA47	0.4227
9796.87	7802.22	157.849	8.1487	GDA47	3.5
9796.87	7802.22	156.776	1.4053	GDA47	1.4053
9893.16	7898.44	111.105	0.4758	GDA84	0.4758

9893.16	7898.44	110.095	0.6032	GDA84	0.6032
9893.16	7898.44	109.085	2.2317	GDA84	2.2317
9894.28	7804.13	100.34	0.4178	GDA88	0.4178
9894.28	7804.13	99.44	0.6133	GDA88	0.6133
9894.28	7804.13	98.54	0.4667	GDA88	0.4667
9894.28	7804.13	97.64	0.4567	GDA88	0.4567

A.2. Data for boundary analysis

DOMAIN 1 + WASTE+ DOMAIN 3				
eastings	**elevation**	**domain code**	**au**	**number of samples**
8096.91	81.402	-1	2.1582	2
7894.24	165.84	-2	0.3265	6
7894.24	164.76	-3	0.25	8
7894.24	163.68	-4	0.2354	8
7894.24	162.6	-5	0.2907	7
7894.24	161.52	-6	0.8373	11
8101.59	138.644	-7	0.684	9
8101.59	137.711	-8	0.3254	9
8101.59	136.779	-9	0.7026	5
8101.59	135.846	-10	0.4892	10
8136.43	131.05	0	0.03	0
8074.981	51.985	1	0.17	8
8074.981	50.985	2	0.75	5
8074.981	49.985	3	1.92	8
7897.69	54.891	3	1.2443	4
7897.69	53.984	5	0.9742	8
7707.41	108.774	6	0.4989	6
7707.41	107.802	7	0.5838	6
7707.41	106.83	8	1.399	9
7707.41	105.858	9	0.5212	2
7707.41	104.886	10	0.8461	3
DOMAIN 3 + WASTE+ DOMAIN 1				
eastings	**elevation**	**domain code**	**au**	**number of samples**
7805.02	68.113	-1	1.39	3
7805.02	67.218	-2	1.4473	6
7805.02	66.323	-3	3.1	9

7805.02	65.427	-4	1.2506	10
7897.69	56.706	-5	1.0235	7
7897.69	55.799	-6	0.5739	12
7897.69	54.891	-7	1.2443	2
7700.34	77.174	-8	1.988	5
7700.34	76.196	-9	2.0799	9
7700.34	75.219	-10	0.7106	11
7835	78.48	0	0.001	0
7974.998	82.563	1	0.22	12
7974.998	81.563	2	0.44	15
7974.998	80.563	3	0.8	8
7962.504	114.052	4	0.5	8
7962.504	113.052	5	0.83	13
7962.504	112.052	6	0.15	9
7925.007	109.526	7	0.56	14
7925.007	108.526	8	1.48	5
7925.007	107.526	9	0.49	7
7874.971	120.011	10	1.03	11

A.3. OK vs. IDW estimates by elevation

Z	Volume	Tonnes	Au (g/t)	auid2(g/t)
71	14331	37977	1.279	1.222
74	14769	39138	1.261	1.202
77	14485	38385	1.254	1.193
80	15369	40728	1.261	1.164
83	14392	38139	1.253	1.138
86	13423	35571	1.26	1.197
89	13354	35388	1.257	1.258
92	13723	36366	1.261	1.271
95	13808	36591	1.277	1.32
98	15008	39771	1.285	1.346
101	15669	41523	1.3	1.37
104	15308	40566	1.301	1.368
107	15815	41910	1.314	1.408
110	14469	38343	1.348	1.35
113	14647	38815	1.357	1.35

116	16561	43887	1.34	1.319
119	15154	40158	1.318	1.376
122	15446	40932	1.291	1.331
125	15539	41178	1.257	1.288
128	17177	45519	1.233	1.226
131	17862	47334	1.22	1.18
134	18584	49248	1.203	1.197
137	16954	44928	1.186	1.197
140	17015	45090	1.183	1.172
143	15900	42135	1.192	1.166
146	16362	43359	1.192	1.174
149	17931	47517	1.178	1.12
152	17599	46637	1.174	1.09
155	14931	39567	1.198	1.138
158	15138	40116	1.186	1.097
161	13723	36366	1.171 **Variance =0.003** **Mean=1.25**	1.065 **Variance=0.009** **Mean= 1.23**

A.4. Block estimates descriptive statistics

BLOCK ESTIMATES DESCRIPTIVE STATISTICS				
File	**Solo Prjt.mdl**	**Solo Prjt.mdl**	**Solo Prjt.mdl**	**Solo Prjt.mdl**
Variable	au	X	Y	Z
Number of samples	2397	2397	2397	2397
Minimum value	0.001	7630.798	9728.579	26.73
Maximum value	1.968664	8180.798	10078.579	188.73
Mean	1.262423	7916.534337	9903.130523	106.936508
Median	1.250788	7920.798	9908.579	107.73
Geometric Mean	1.231599	7914.903087	9902.577739	97.535411
Variance	0.041238	25797.09027	10946.53437	1726.536829
Standard Deviation	0.203072	160.614726	104.625687	41.551616
Coeffcient of Variation	0.160859	0.020289	0.010565	0.388563
Moment 1 Arithmetic Mean	0.009552	1207374627	214092696.5	5594857.346
Skewness	-0.210372	-0.067637	-0.016311	-0.075506

Kurtosis	5.616667	1.814264	1.786687	1.876884
Natural Log Mean	0.208313	8.976503	9.20055	4.580216
Log Variance	0.129867	0.000412	0.000112	0.206989
10.0 Percentile	1.021579	7690.798	9758.579	47.73
20.0 Percentile	1.101223	7750.798	9788.579	62.73
30.0 Percentile	1.163065	7810.798	9828.579	77.73
40.0 Percentile	1.211324	7870.798	9868.579	95.73
50.0 Percentile (median)	1.250788	7920.798	9908.579	107.73
60.0 Percentile	1.285033	7975.798	9938.579	122.73
70.0 Percentile	1.345908	8030.798	9978.579	134.73
80.0 Percentile	1.427976	8080.798	10008.579	149.73
90.0 Percentile	1.53518	8130.798	10048.579	161.73
95.0 Percentile	1.624277	8160.798	10068.579	170.73
97.5 Percentile	1.677498	8170.798	10078.579	176.73

APPENDIX B

B.1. Domain statistical analysis

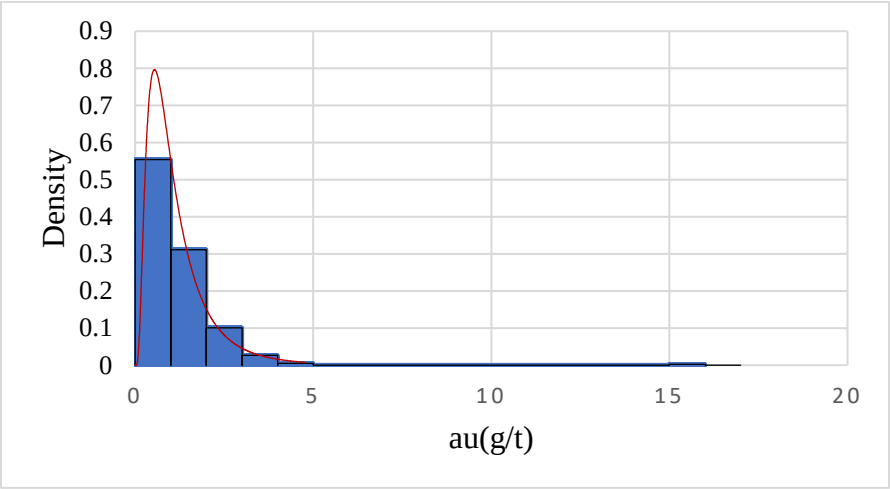

(a)

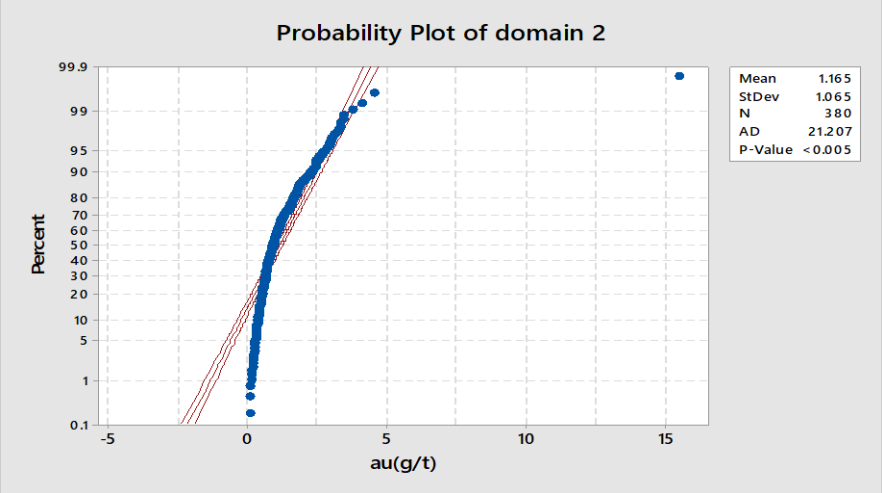

(b)

Figure B.1. Domain 2 data distribution analysis (a) Histogram showing positively skewed distribution (b) Probability plot of skewed distribution

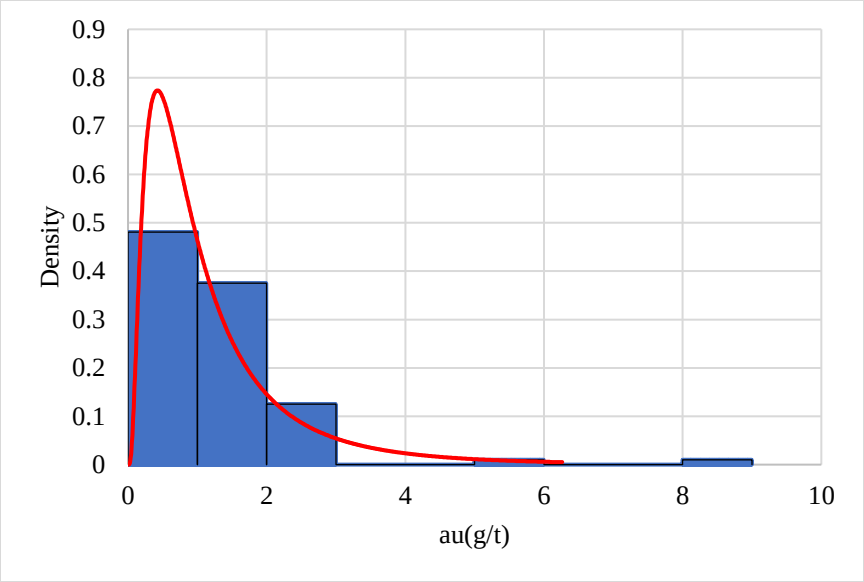

(a)

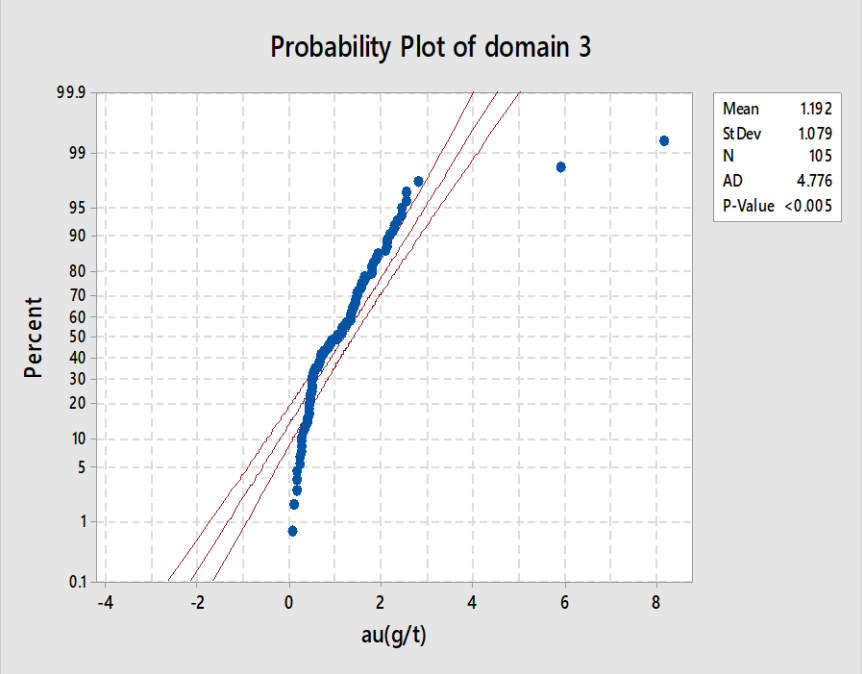

(b)

Figure B.2. Domain 3 distribution analysis (a) Histogram showing positively skewed distribution (b) Probability plot of skewed distributions

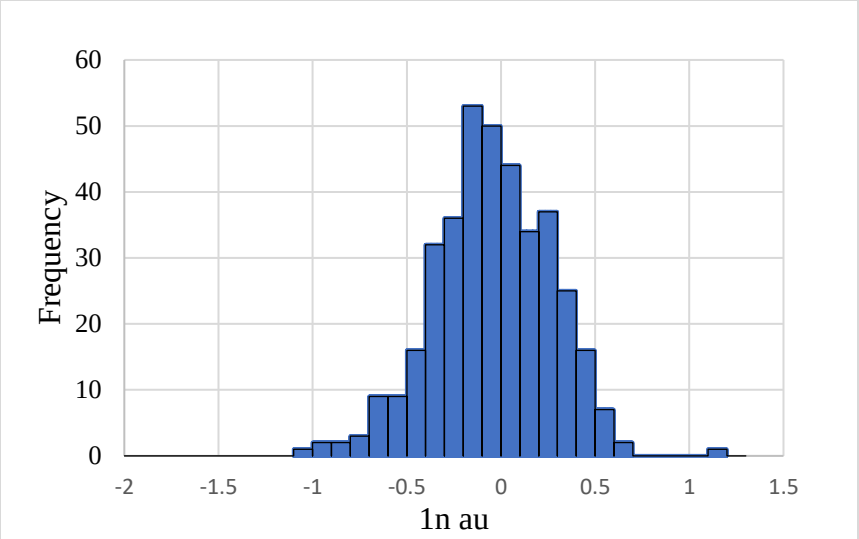

(a)

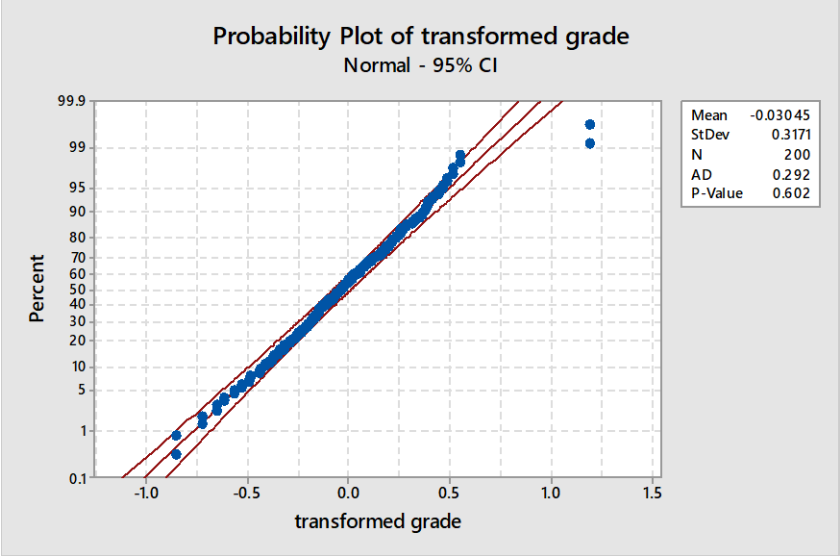

(b)

Figure B.3. Domain 2 log distribution analysis distribution analysis (a) Log transformed histogram plot of Domain 2 (b) Log transformed probability plot of Domain 2

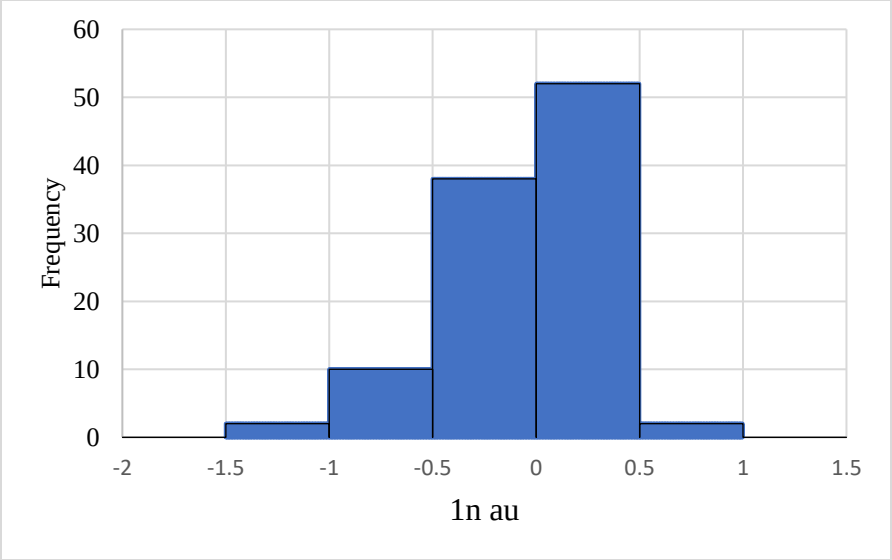

(a)

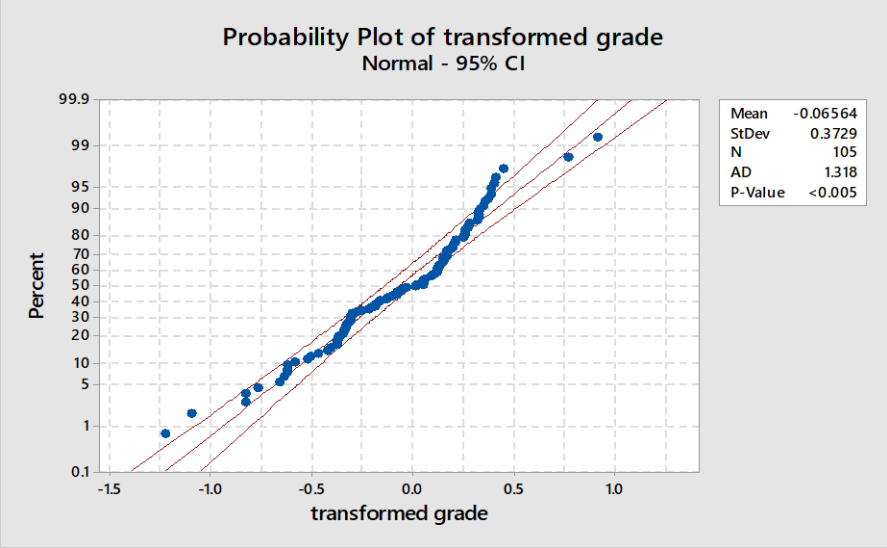

(b)

Figure B.4. Domain 3 log distribution analysis distribution analysis (a) Log transformed histogram plot of Domain 3 (b) Log transformed probability plot of Domain 3

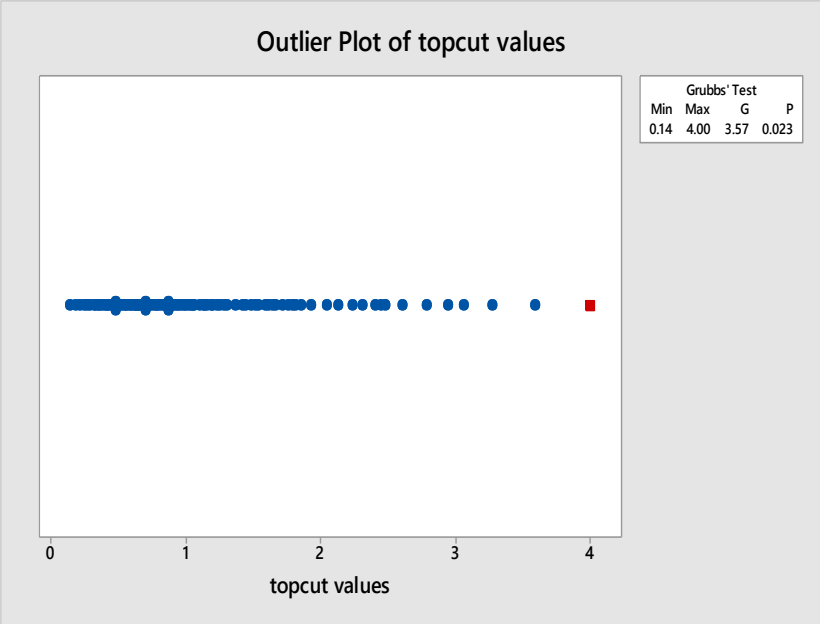

Figure B.5. Plot of outlier test results (Domain 2)

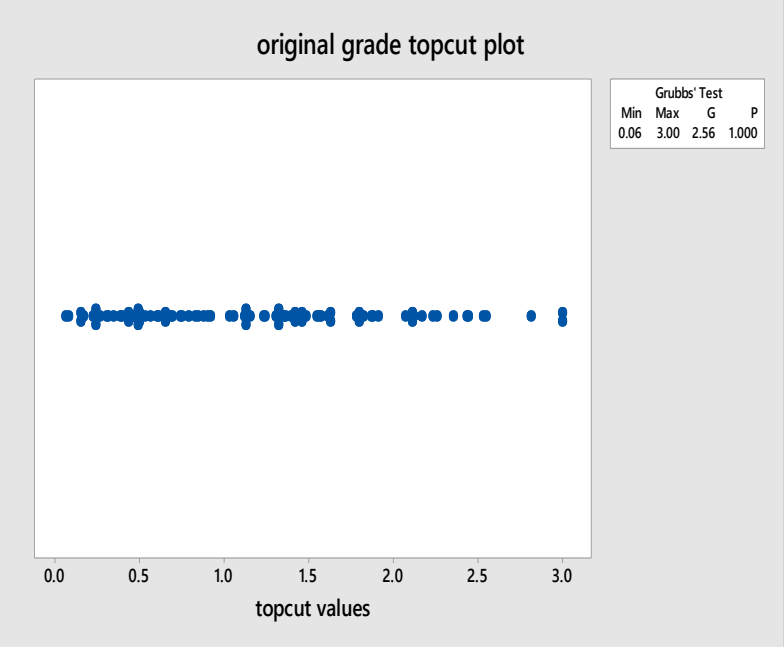

Figure B.6. Plot of outlier test results (Domain 3)

APPENDIX C

C.1. Script for Trend Analysis

```
 ##########################################################################
# Macro Name    : c:/solomon/abugyee fresh/a1 harboundary/basic stats/dom1 bs/trendanalysis.tcl
# Version       : Surpac 6.5.1
# Creation Date: Mon Jan 01 21:25:00 2018
# Description   :
set status [ SclFunction "RECALL ANY FILE" {
 file="solo_prjt.mdl"
 mode="openInNewLayer"
set status [ SclFunction "BM STRING REPORT" {
 frm20190={
    fileType="String"
    type="Centroids"
    location="bm_centroids_A"
    id="11"
    report_attributes="some"
    block_size="N"
    constrain="Y"
    attributes={
       attribute="au"
    class_att=""
    class_range="-999,999"
    cent_type="User block resolution"
    outputIJK="N"
 frm20111={
       constraints=table { not op contype location id rnga rngb lbound ubound ext }
```

```
        { "" "=" "BLOCK" "reef" "A1" "" "" "" "" "" }
      conexp=""
      confile=""
      keep_blocks="N"
set status [ SclFunction "TREND ANALYSIS" {} ]
set status [ SclFunction "RECALL ANY FILE" {
  file="bm_centroids_a11.str"
  mode="openInNewLayer
set status [ SclFunction "DRAW DESC" {
  frm00089={
      range1=""
      range2=""
      range3=""
      ifld_num="d1"
      textalignment="<"
      position="Centroid"
      layer_name="bm_centroids_a11.str"
set status [ SclFunction "node_show_all" {
  action="node_show_all"
  context="graphics"
set status [ SclFunction "ERASE LINES" {
  frm00089={
      range1=""
      range2=""
      range3=""
      textalignment="<"
      layer_name="bm_centroids_a11.str"
set status [ SclFunction "TREND ANALYSIS" {
```

```
frm20414={
      fname="bm_vs_compo_trendana"
   report_format=".csv - Comma Separated (Spreadsheet)"
   dfields=table { location id str dfield label min max } {
    { "testcombi" "" "" "D7" "" "" "" }
    { "testcombi" "" "" "D7" "" "" "" }
    { "testcombi" "" "" "D7" "" "" "" }
    { "testcombi" "" "" "D7" "" "" "" }
    { "testcombi" "" "" "D7" "" "" "" }
    { "testcombi" "" "" "D7" "" "" "" }
    { "bm_centroids_a" "11" "" "D1" "" "" "" }
    { "bm_centroids_a" "11" "" "D1" "" "" "" }
    { "bm_centroids_a" "11" "" "D1" "" "" "" }
    { "bm_centroids_a" "11" "" "D1" "" "" "" }
    { "bm_centroids_a" "11" "" "D1" "" "" "" }
    { "bm_centroids_a" "11" "" "D1" "" "" "" }
   range="10,100,10"
   negative="NEGATIVES"
   dfields_Constraints=table { min0 max0 min1 max1 min2 max2 } {
    { "" "" "9800" "9850" "" "" }
    { "" "" "9850" "9900" "" "" }
    { "" "" "9900" "9950" "" "" }
    { "" "" "9950" "10000" "" "" }
    { "" "" "10000" "10050" "" "" }
    { "" "" "10050" "10100" "" "" }
    { "" "" "9800" "9850" "" "" }
    { "" "" "9850" "9900" "" "" }
    { "" "" "9900" "9950" "" "" }
```

```
        { "" "" "9950" "10000" "" "" }
        { "" "" "10000" "10050" "" "" }
        { "" "" "10050" "10100" "" "" }
set status [ SclFunction "MACRO PLAYBACK" {} ]
```

C.2. Script for block estimates vrs. composites

```
set status [ SclFunction "EXIT GRAPHICS" {
  frm00108={
     exit_mode="E"
set status [ SclFunction "RECALL ANY FILE" {
  file="a1_dom_bs1.str"
  mode="openInNewLayer"
set status [ SclFunction "STRING RENUMBER RANGE" {
  frm00068={
         old_str_range="1,2"
     new_str_range="30003"
set status [ SclFunction "ZOOM OUT" {} ]
set status [ SclFunction "2D GRID" {
  frm00140={
     ygrid_inc="100"
     ylabel_inc="1"
     xgrid_inc="100"
     xlabel_inc="1"
     grid="above"
     maximum="200.00"
     minimum="0"
set status [ SclFunction "RECALL FILE" {
  frm00236={
         location="bm_centroids_a1.str"
```

```
      rid="1"
      string_rng=""
      ftype="S"
      swa_desc="Y"
      append="R"
      styles_file=""
      rescale="N"
      swa_name="bm_centroids_a1.str"
set status [ SclFunction "ERASE STRINGS" {
  frm00089={
      range1=""
      range2=""
      range3=""
      ifld_num="d1"
      textalignment="<"
      legend_location="no legend"
      layer_name="bm_centroids_a1.str"
set status [ SclFunction "DRAW MARKERS" {
  frm00089={
         range1=""
      range2=""
      range3=""
      ifld_num="d1"
      textalignment="<"
      position="All points"
      legend_location="no legend"
      layer_name="bm_centroids_a1.str"
set status [ SclFunction "TREND ANALYSIS" {
```

```
 frm20414={
    _action=display
    fname="bm_vs_composites"
    report_format=".csv - Comma Separated (Spreadsheet)"
    dfields=table { location id str dfield label min max } {
     { "a1_dom_bs1" "1" "" "D1" "" "" "" }
        { "a1_dom_bs1" "1" "" "D1" "" "" "" }
     { "a1_dom_bs1" "1" "" "D1" "" "" "" }
        { "a1_dom_bs1" "1" "" "D1" "" "" "" }
     { "bm_centroids" "1" "" "D1" "" "" "" }
     { "bm_centroids" "1" "" "D1" "" "" "" }
     { "bm_centroids" "1" "" "D1" "" "" "" }
     { "bm_centroids" "1" "" "D1" "" "" "" }
    range="0,100,25"
    negative="NEGATIVES"
    dfields_Constraints=table { min0 max0 min1 max1 min2 max2 } {
     { "" "" "9800" "9825" "" "" }
     { "" "" "9825" "9850" "" "" }
     { "" "" "9850" "9875" "" "" }
     { "" "" "9875" "9900" "" "" }
     { "" "" "9800" "9825" "" "" }
     { "" "" "9825" "9850" "" "" }
     { "" "" "9850" "9875" "" "" }
     { "" "" "9875" "9900" "" "" }
set status [ SclFunction "RECALL ANY FILE" {
 file="bm_vs_composites.xls"
 mode="none"
```

APPENDIX D

D.1. Global directional semi-variogram structures

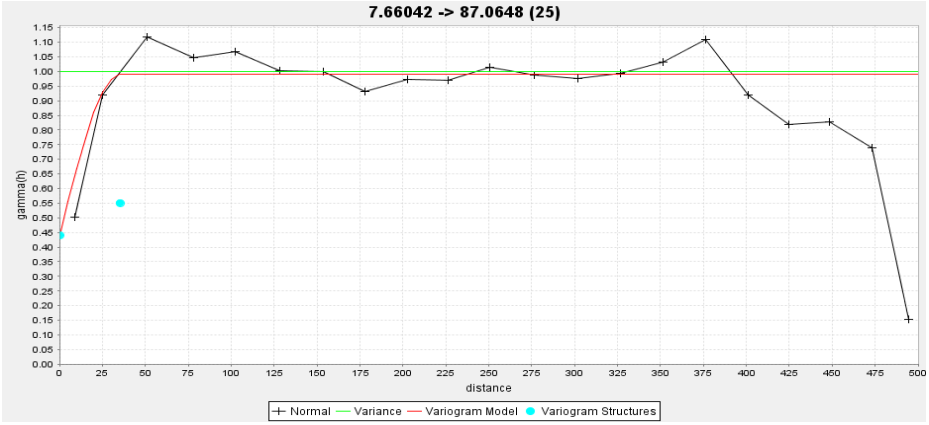

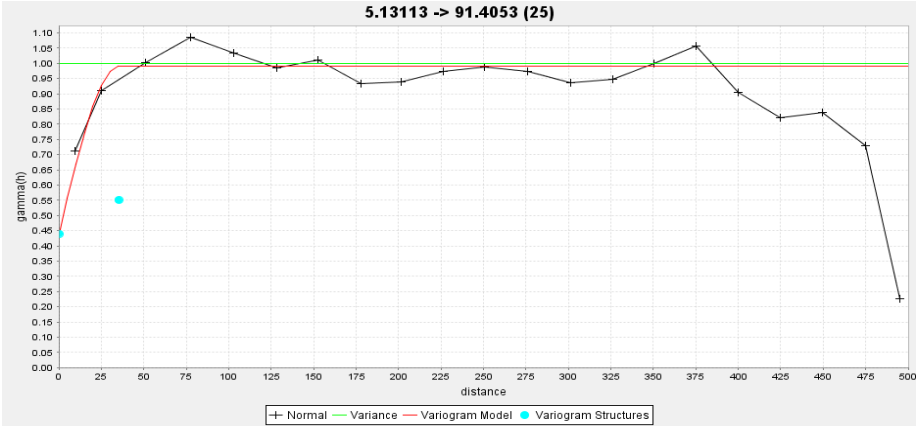

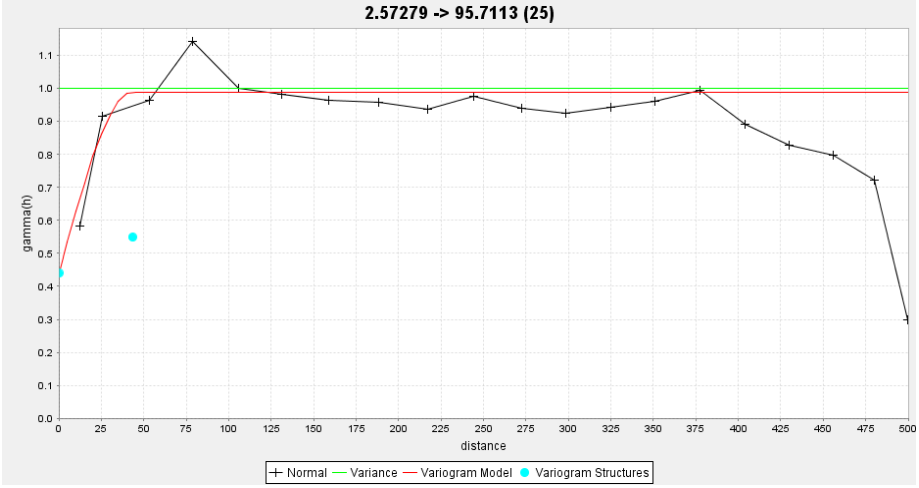

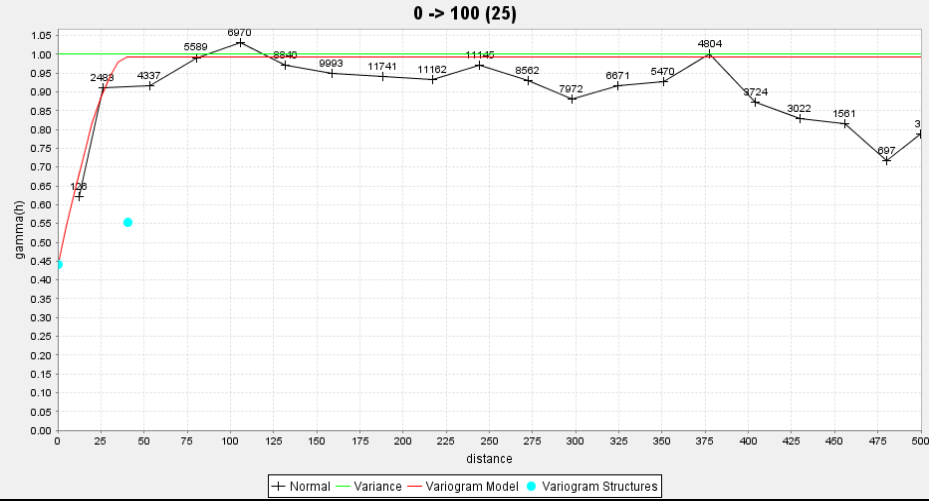
0 -> 100 (25)
gamma(h)
distance
Normal
Variance
Variogram Model
Variogram Structures

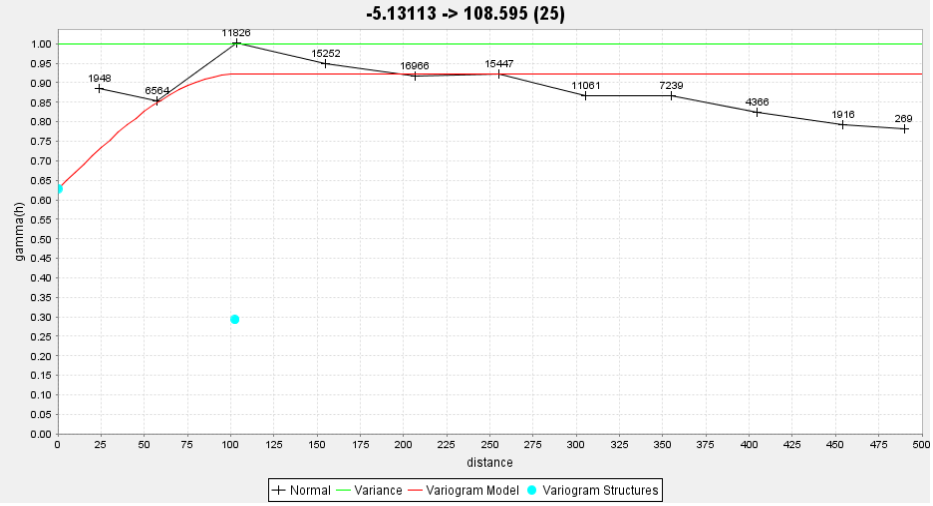
-5.13113 -> 108.595 (25)
gamma(h)
distance
Normal
Variance
Variogram Model
Variogram Structures

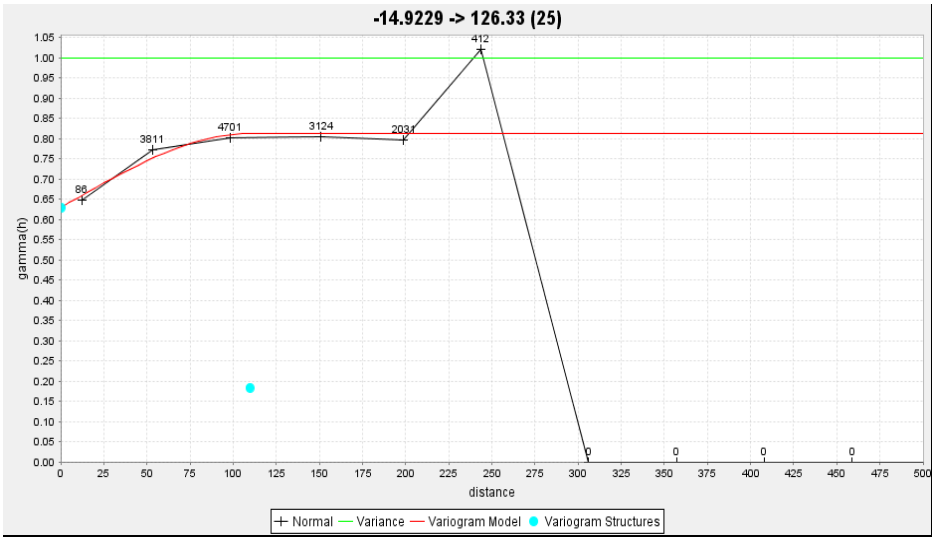
-14.9229 -> 126.33 (25)
gamma(h)
distance
Normal
Variance
Variogram Model
Variogram Structures

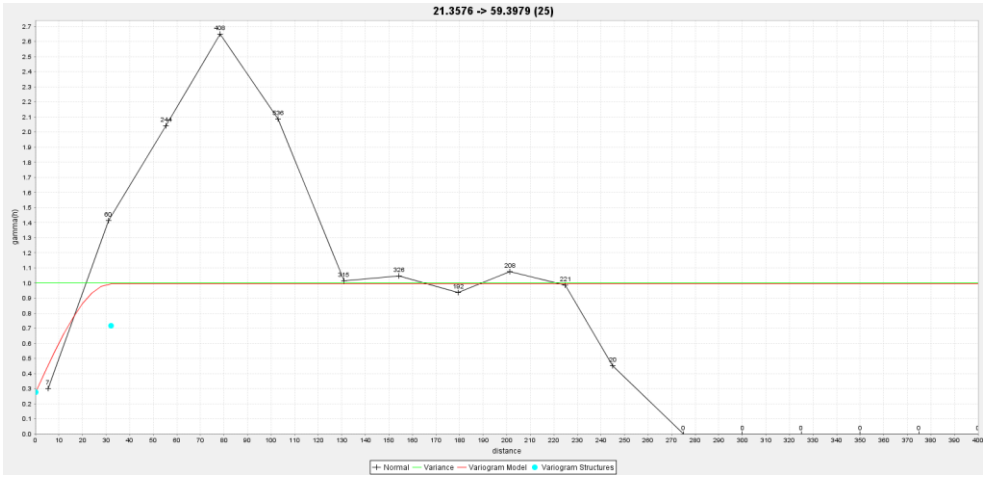
21.3576 -> 59.3979 (25)
gamma(h)
distance
Normal
Variance
Variogram Model
Variogram Structures


23.2374 -> 54.3897 (25)
gamma(h)
distance
Normal
Variance
Variogram Model
Variogram Structures

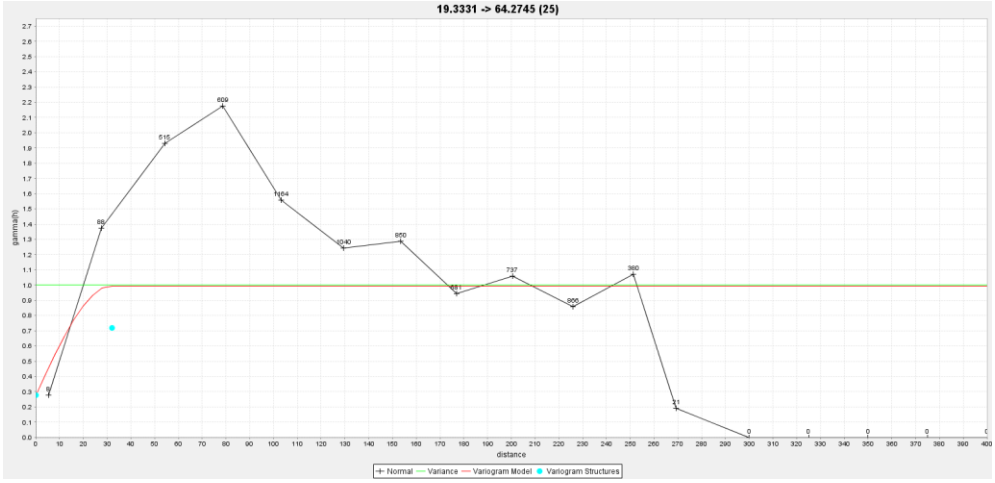
19.3331 -> 64.2745 (25)
gamma(h)
distance
Normal
Variance
Variogram Model
Variogram Structures

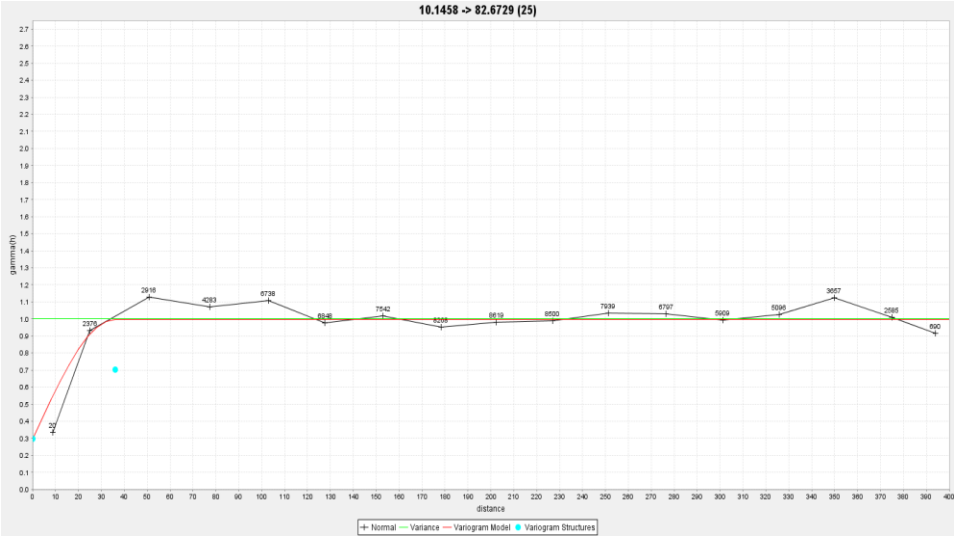
10.1458 -> 82.6729 (25)
gamma(h)
distance
Normal
Variance
Variogram Model
Variogram Structures

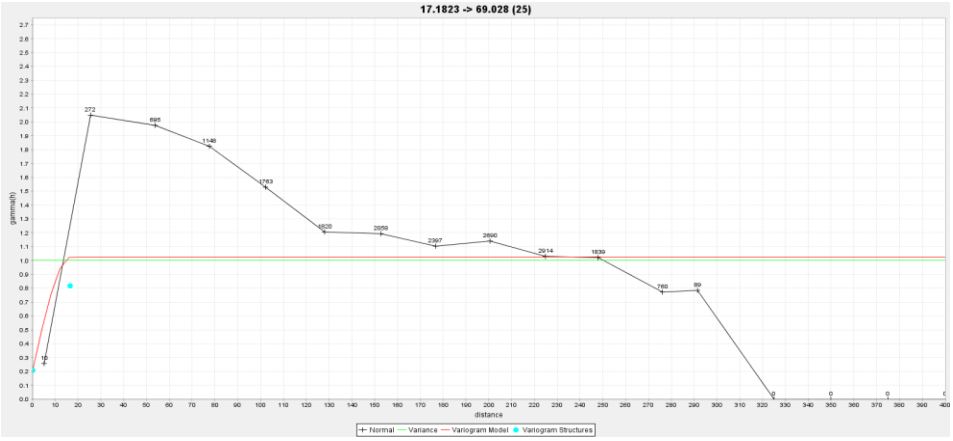
17.1823 -> 69.028 (25)
gamma(h)
distance
Normal
Variance
Variogram Model
Variogram Structures

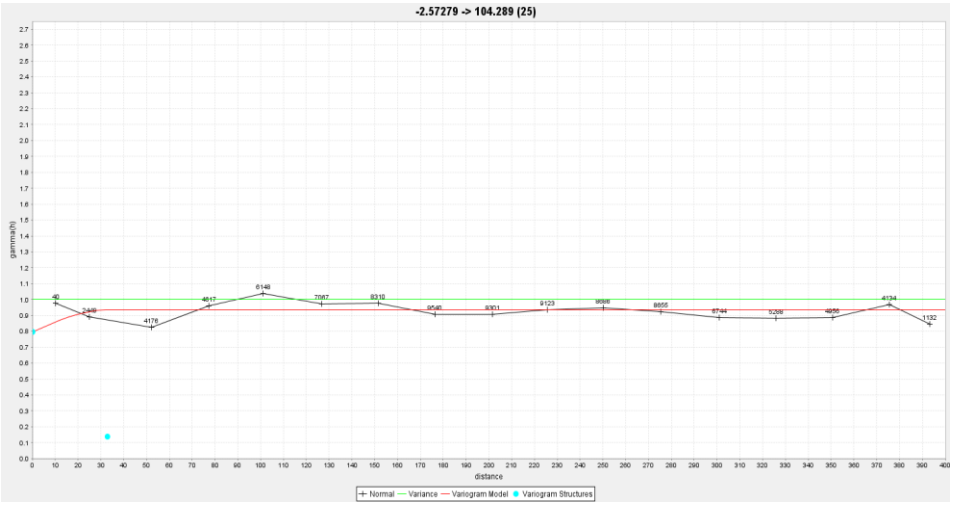
-2.57279 -> 104.289 (25)
gamma(h)
distance
Normal
Variance
Variogram Model
Variogram Structures

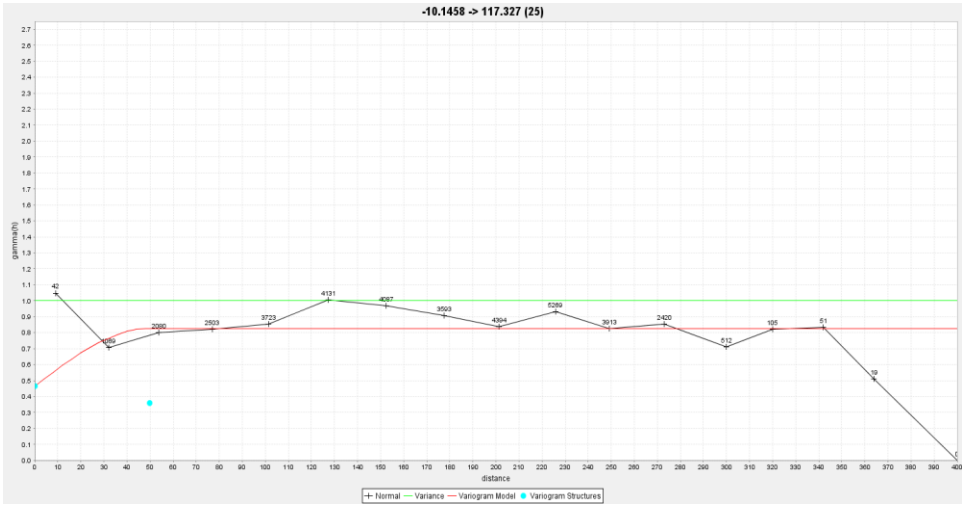
-10.1458 -> 117.327 (25)
gamma(h)
distance
Normal
Variance
Variogram Model
Variogram Structures

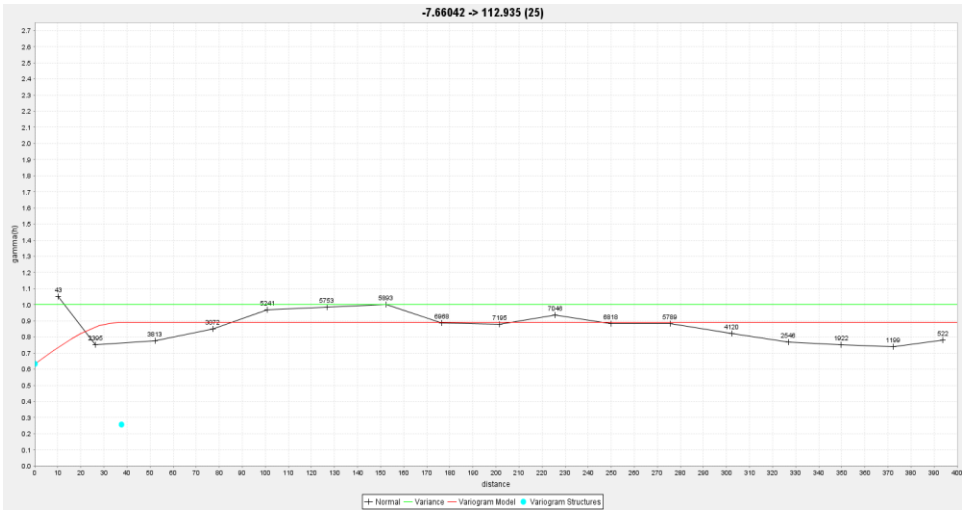
-7.66042 -> 112.935 (25)
gamma(h)
distance
Normal
Variance
Variogram Model
Variogram Structures

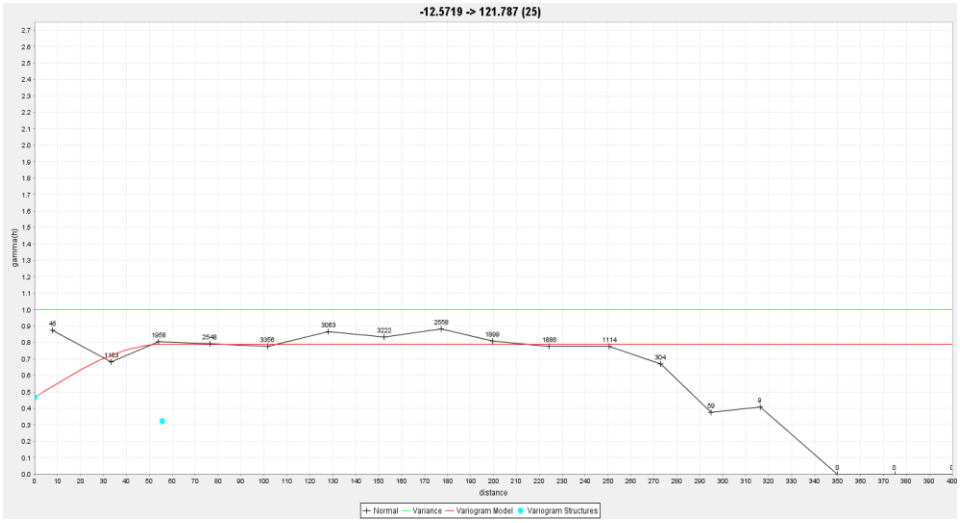
-12.5719 -> 121.787 (25)
gamma(h)
distance
Normal
Variance
Variogram Model
Variogram Structures

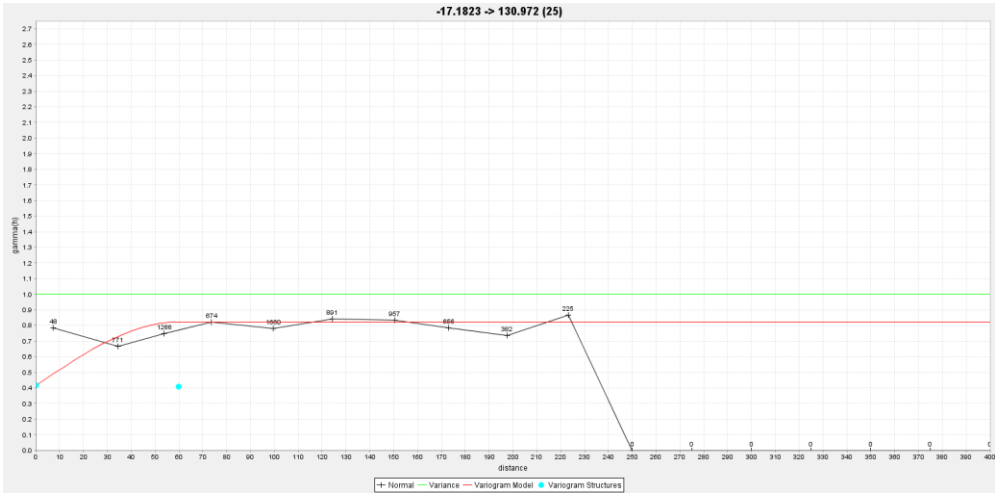
-17.1823 -> 130.972 (25)
semivariance (units)
distance
Normal
Variance
Variogram Model
Variogram Structures


-21.3576 -> 140.602 (25)
semivariance (units)
distance
Normal
Variance
Variogram Model
Variogram Structures


-19.3331 -> 135.726 (25)
semivariance (units)
distance
Normal
Variance
Variogram Model
Variogram Structures

D.2. 2D global semi-variogram maps with contoured nugget along several bearings (bearing marked in blackline)

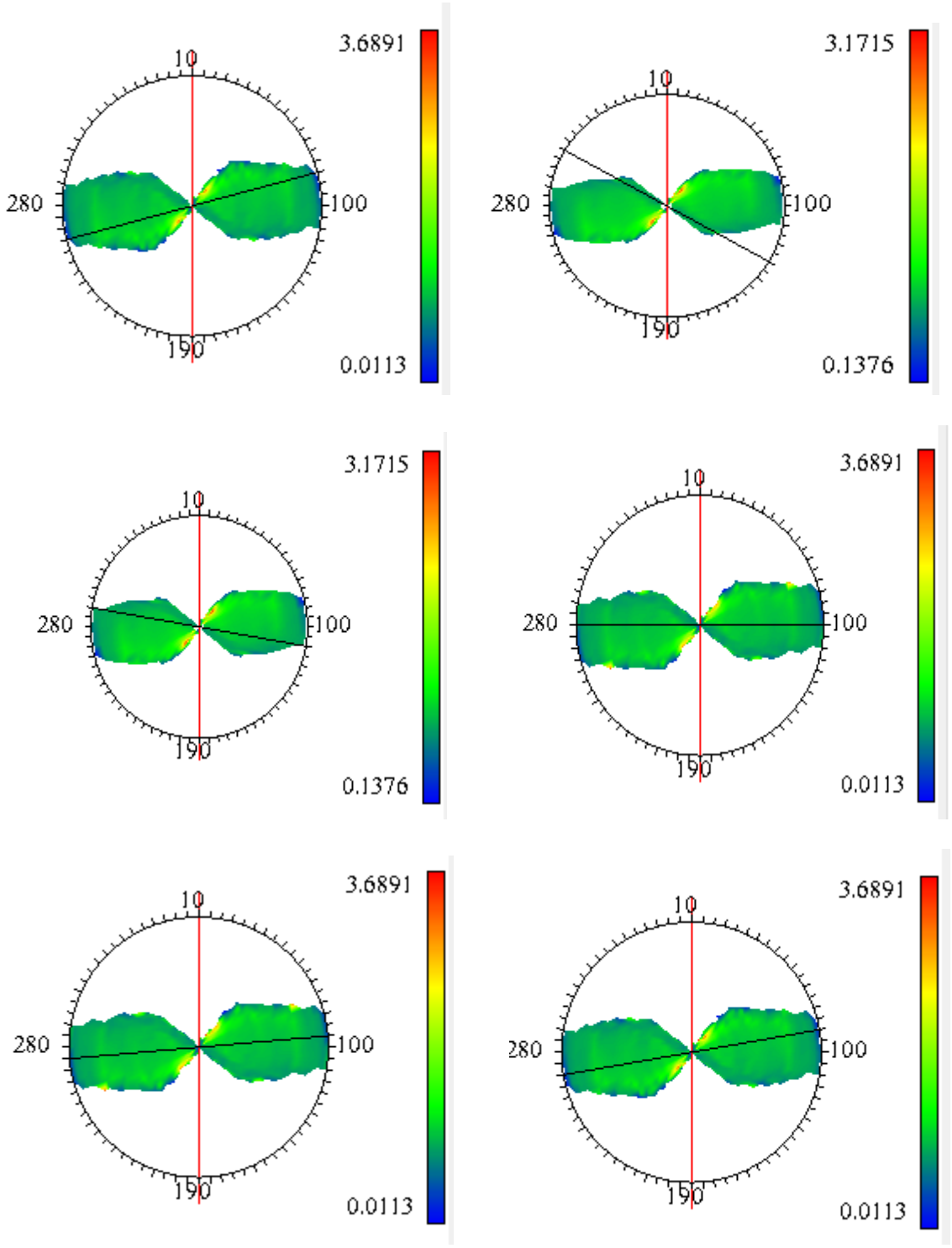

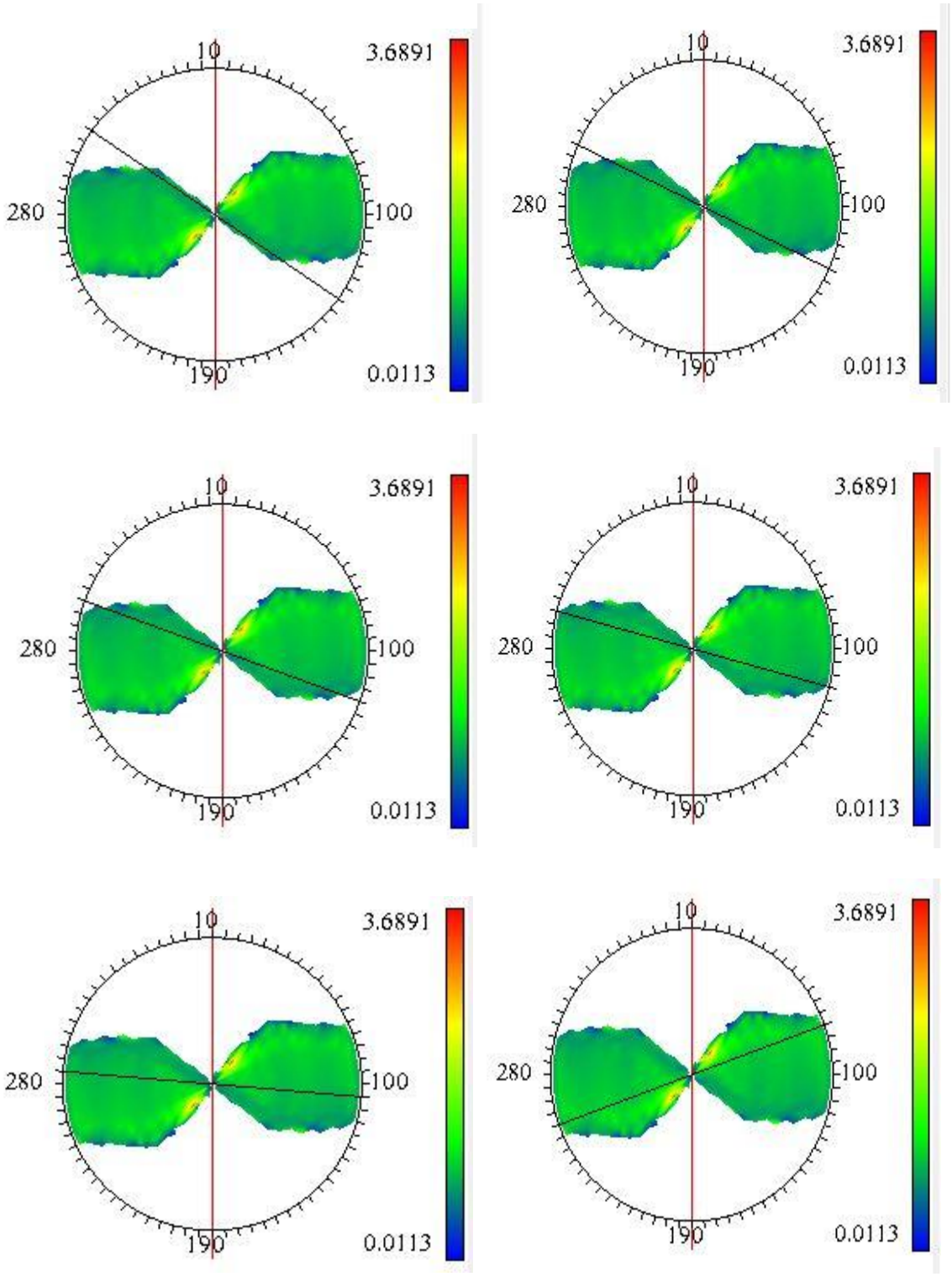
10
280
100
190
3.6891
0.0113

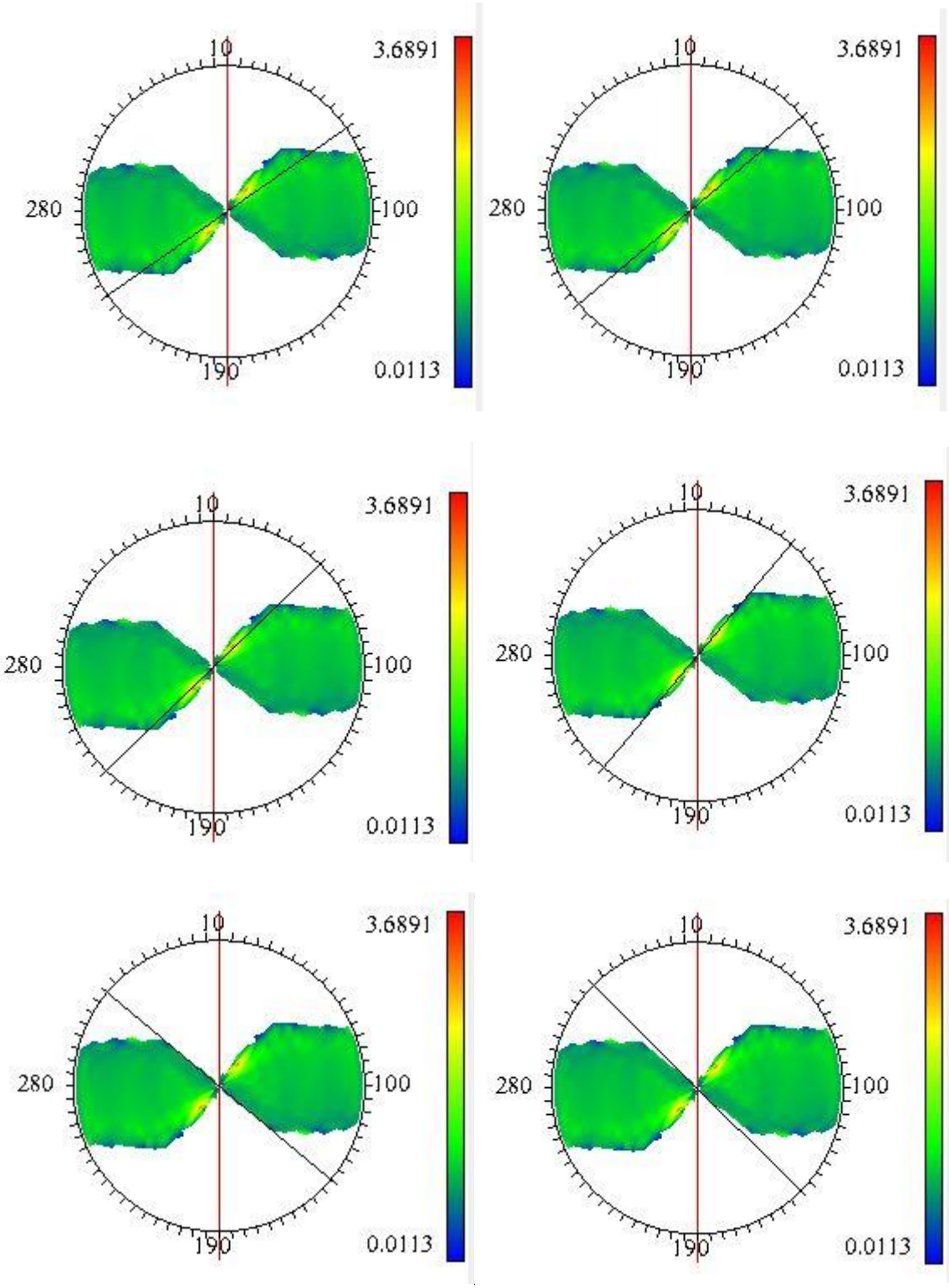
10
280
100
190
3.6891
0.0113